

See discussions, stats, and author profiles for this publication at: <http://www.researchgate.net/publication/238180331>

# PCB Volatilization from Sediments

ARTICLE *in* JOURNAL OF ENVIRONMENTAL ENGINEERING · JANUARY 2006

Impact Factor: 1.27 · DOI: 10.1061/(ASCE)0733-9372(2006)132:1(102)

---

CITATION

1

---

READS

30

## 4 AUTHORS, INCLUDING:



[Makram T Suidan](#)

American University of Beirut

389 PUBLICATIONS 7,149 CITATIONS

[SEE PROFILE](#)



[Gregory D. Sayles](#)

United States Environmental Protection Age...

42 PUBLICATIONS 854 CITATIONS

[SEE PROFILE](#)

# UNIVERSITY OF CINCINNATI

**DATE: February 19, 2003**

---

I, **Shuang Qi** \_\_\_\_\_ ,  
hereby submit this as part of the requirements for the degree of:

**Doctorate of Philosophy (Ph.D.)**

---

in:

**Environmental Engineering**

---

It is entitled:

**PCB Volatilization From Sediments**

---

---

---

---

**Approved by:**

---

**Makram Suidan**

---

**Gregory Sayles**

---

**George Sorial**

---

**Dionysios Dionysiou**

---

---

# **PCB VOLATILIZATION FROM SEDIMENTS**

A dissertation submitted to the

Division of Research and Graduate Studies of the University of Cincinnati

in partial fulfillment of the requirements for the degree of

**Doctorate of Philosophy (Ph.D.)**

in the Department of Civil and Environmental Engineering  
of the College of Engineering

2003

by

**Shuang Qi**

M.S. Environmental Engineering  
Harbin Institute of Technology  
Harbin, China, 1998

B.S. Environmental Engineering  
Harbin Institute of Technology  
Harbin, China, 1996

Committee Chair: Makram Suidan, Ph.D.

## Abstract

In this research, the volatility of PCB was investigated. A simple microcosm of sediment, water and air that allowed for (pseudo) one-dimensional transport of PCB was established to conduct PCB volatilization studies. First, the rate and extent of PCB volatilization from sediment and other substrates spiked with two PCB congeners, 4,4'-dichlorobiphenyl (DCB) and 2,2', 4, 4', 5, 5'-hexachlorobiphenyl (HCB) were determined experimentally. Second, the rate of PCB volatilization from two types of Lake Hartwell sediments, uniformly naturally contaminated with PCBs, was measured. A relationship between the rate of volatilization and the extent of substitution of the PCB with chlorine was accessed. A fundamental mathematical model of PCB transport in a sediment-water-air system was developed. The data obtained from volatilization experiments were applied to validate the one-dimensional mathematical model. The calibrated model was run to simulate various scenarios that led to better understanding of the transport mechanism of PCBs.

For all the scenarios investigated, experimental results revealed significant volatilization of DCB from all the different substrates studied. Important observations included: Volatilization of DCB from water was very fast, the higher the water level, the slower the volatilization rate; The rate of volatilization decreased when the sediment lost moisture; the rates of PCB volatilization from contaminated silica sand and bentonite clay were very similar and faster than the rate observed for natural sediments but still slower than the rate of volatilization from water; volatilization of PCB was positively correlated with sediment contamination level; volatilization of solid PCBs from glass surfaces was surprisingly fast; PCBs volatilized faster from surfaces

covered with a thin water layer than when no water was present; in all cases studied, the volatilization of HCB was dramatically lower than that of DCB. The data obtained from Lake Hartwell study showed significant volatilization of PCBs. PCBs volatilized faster from the deep layer sediment than from the top layer sediment. Results also indicated lower chlorinated congeners volatilized preferentially.



## Acknowledgements

The past four years in the Environmental Engineering Program at the University of Cincinnati have been quite a journey for me. I learned, I achieved and I matured.

I am deeply grateful to my advisor Dr. Makram Suidan, the person without whom my journey would not have been possible. I thank him for inspiring me and guiding me in this field. I am especially appreciative for his encouragement, support, and more important, belief in me. Without all these, I would not have gone so far. It is my pleasure to be his student.

My gratitude also extends to Dr. Gregory Sayles, Dr. George Sorial and Dr. Dionysios D. Dionysiou. Their insights and suggestions are greatly appreciated.

I wish to thank all members of Dr. Suidan's Research Group, who provided support and help through my Ph.D. study. Special thanks to Dr. Amid Khodadoust for his help and patience, which made my first year in the lab much easier. Many thanks to Dr. Cristina Alonso, she is a very good partner to work with.

I would like to dedicate this dissertation to my parents Guocai Qi, Xiufeng Liu, my brother Peter Qi, and my husband Pillar Zhang for their unconditional love and support through the years. No matter what degree I have, no matter where I am, I know they will always be there.

## TABLE OF CONTENTS

	<b>Page</b>
<b>Chapter 1 Introduction</b>	<b>9</b>
1.1 Background and Problem Statement	9
1.2 Literature Review	12
1.3 Research Objectives	13
1.4 Thesis Layout	15
<b>Chapter 2 Mathematical Model</b>	<b>16</b>
2.1 Introduction	16
2.2 Governing Model Equations	19
<b>Chapter 3 Materials and Methods</b>	<b>26</b>
3.1 Selection of PCB Congeners	26
3.2 Experimental Setup	27
3.3 Silylation of the Glass Columns	29
3.4 Substrates tested	30
3.5 PCB Extractions and Analysis	31
3.5.1 Extraction Methods	31
3.5.2 PCB Analysis	34
<b>Chapter 4 Volatilization Experiments</b>	<b>36</b>
4.1 Volatilization of DCB from Water	36
4.1.1 Introduction	36



4.1.2	Results and Discussion	37
4.2	Volatilization of PCB from Spiked Sediments	43
4.2.1	Introduction	43
4.2.2	Results and Discussion	46
4.3	Volatilization of PCB from Silica Sand and Bentonite Clay	54
4.3.1	Introduction	54
4.3.2	Results and Discussion	54
4.4	Volatilization of Solid PCB from Glass Surface	59
4.4.1	Introduction	59
4.4.2	Results and Discussion	60
4.5	Conclusions	64
<b>Chapter 5</b>	<b>Adsorption Studies</b>	<b>69</b>
5.1	Introduction	69
5.2	Materials and Methods	71
5.3	Results and Discussion	72
<b>Chapter 6</b>	<b>Parameter Estimation and Model Simulation</b>	<b>79</b>
6.1	Introduction	79
6.2	Parameter Estimations	80
6.2.1	Parameter estimation of volatilization of DCB from water	80
6.2.2	Parameter estimation of PCB volatilization from sediments	81
6.3	Model Simulations	84
6.3.1	Simulation of the effect of sediment depth on PCB volatilization	84
6.3.2	Simulation of the effect of the overlaying water level	90
6.4	Conclusions	90
<b>Chapter 7</b>	<b>Volatilization of PCB from Lake Hartwell Sediments</b>	<b>94</b>
7.1	Introduction	94

7.2	Materials and Methods	95
7.2.1	Sediments tested	95
7.2.2	Experimental setup	96
7.3	Results and Discussion	99
7.3.1	Experimental results	99
7.3.2	Comparison with field study	100
7.3.3	Comparison with Fundamental Study Results	102
<b>Chapter 8 Summary</b>		<b>106</b>
<b>Bibliography</b>		<b>109</b>
<b>Appendices</b>		<b>113</b>
1.	Preliminary Experiments	113
2.	Silylation	117
3.	Preparation of the PCB contaminated substrates	118
4.	Establishment of Sediment Extraction Method	120
5.	Moisture Content Analysis	123
6.	Volatile Organic Matter Content Analysis	124
7.	PCB Analysis by GC-ECD	125
8.	<sup>14</sup> C-labeled PCB Analysis by LSC	126
9.	Measurement of System Flow Rate	127
10.	Original Data for Figures in Chapter 4	128
11.	Original Data for Chapter 5	135
12.	Original Data for Chapter 7	136

## **List of Tables**

Table 3-1 Physical-chemical properties of PCB Congeners Studied

Table 3-2 Substrates Characterization

Table 3-3 Composition of the Solvents

Table 4-1 Fluxes of DCB volatilization from Sediment, sand and clay

Table 4-2 Fluxes of DCB volatilization from glass surface

Table 5-1 Experimental design for adsorption studies

Table 5-2 K and N values for DCB adsorption isotherms

Table 6-1 Estimated parameter values and known model variables

Table 7-1 Sediment Characterizations

Table 7-2 Monitored PCB Congeners

Table 7-3 Comparison of Field and Laboratory Results

## **List of Figures**

Figure 1-1 Chemical Structure of PCBs

Figure 2-1 Schematic of the System

Figure 2-2 Schematic of the sediment particle

Figure 3-1 Experimental Apparatus

Figure 4-1 Volatilization of DCB from Water for Three Water Levels

Figure 4-2 Experimental Schematics

Figure 4-3 Volatilization of DCB from Complete Mixed Water

Figure 4-4 Volatilization of PCBs from sediments with/without an overlaying water layer

Figure 4-5 Volatilization of DCB from sediments with a thin overlaying water layer

Figure 4-6 Volatilization of PCB from sediments with a thick overlaying water layer

Figure 4-7 Comparison of the effects of thick and thin overlaying water layer

Figure 4-8 PCB volatilization from sediments for different contamination levels

Figure 4-9 Volatilization of PCB from contaminated silica sand and bentonite clay

Figure 4-10 Comparison of DCB volatilization

Figure 4-11 Volatilization of solid PCB from treated glass surfaces

Figure 4-12 Comparison of DCB volatilization from treated and untreated glass surface

Figure 4-13 Comparison of HCB volatilization from treated and untreated glass surface

Figure 4-14 DCB volatilization from treated glass surface with different overlaying water levels

Figure 4-15 HCB volatilization from treated glass surface with different overlaying water levels

Figure 5-1 DCB adsorption isotherm, Marine Sediment

Figure 5-2 DCB adsorption isotherm, Silica Sand

Figure 5-3 DCB adsorption isotherm, Bentonite Clay

Figure 5-4 DCB adsorption isotherms

Figure 6-1 Parameter estimation and model simulation for DCB volatilization from water

Figure 6-2 Parameter estimation and model simulation for DCB volatilization from sediments for three contamination levels

Figure 6-3 Effect of the sediment heights on the rate of volatilization of PCB

Figure 6-4 Effect of the amount of sediment on PCB volatilization (constant initial concentration)

Figure 6-5 Effect of the amount of sediment on PCB volatilization (constant initial amount)

Figure 6-6 Effect of the water height on the rate of volatilization of PCB

Figure 7-1 Volatilization of PCB Congeners from Lake Hartwell Sediment in 80 days

Figure 7-2 Comparison of DCB Volatilization from Sediments

Figure 7-3 DCB Volatilization Rate versus Level of Sediment Contamination

Figure 7-4 DCB volatilization rate versus sediment organic content

## Nomenclature

$C_s^*$	water sediment concentration corresponding to the solid phase concentration at the particle surface
$C_w$	concentration of PCBs in the water phase
$C_s$	concentration of PCBs in the sediment water phase
$C_{w0}, C_{s0}$	initial concentration in the water and the sediment-water
$D_w$	hydrodynamic dispersion coefficient in the water phase
$D_s$	hydrodynamic dispersion coefficient in the sediments
$D_p$	diffusion coefficient in the sediment particle
$h_w, h_s$	depth of the water and sediments column
$H$	PCBs Henry's constant
$k_f$	external-film mass transfer coefficient in the sediments
$k_{fg}$	gas phase film mass transfer coefficient
$q_{ave}$	average volume solid phase concentration of PCBs given as a mass ratio: mass solute sorbed divided by mass of sorbent
$q_r$	solid phase concentration of PCBs in the sediment particle at radial position $r$
$r$	radial position
$R_p$	radius of the sediment particle
$t$	time
$v_z$	fluid phase pore velocity in the sediments
$z$	height of column

Greek letters

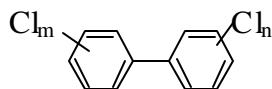
$\epsilon$  porosity of the sediments

$D_s$  density of the solid phase

# Chapter 1 Introduction

## 1.1 Background and Problem Statement

Polychlorinated biphenyls (PCBs) are a family of 209 distinct chemical compounds (congeners) consisting of two benzene rings and 1 to 10 chlorine atoms. PCBs have the following general structure (Figure 1). They range in texture from light, oily fluids to heavier, greasy or waxy substances.



where  $m + n = 1$  to  $10$   
and  $m, n = 1$  to  $5$

**Figure 1-1** Chemical Structure of PCBs

PCBs were discovered over 100 years ago. The production of PCBs started at Monsanto corporation (St. Louis, MO) in 1929. PCBs were commercially produced as complex mixtures of congeners (Aroclors). PCB's physical and chemical stability and their electrical insulating properties led to their commercial applications in transformers, capacitors, printing inks, paints, dust control agents, pesticides, etc (Erickson, 1997). PCBs replaced combustible insulating fluids and thus reduced the risk of fires in office building, hospitals, factories and schools. Not only did PCB make capacitors flame resistant, they also allowed capacitors to be made smaller, thereby lowering equipment cost. For many years, PCBs were routinely used in the production of a wide variety of common products such as plastic, adhesives, paints and pesticides. It is estimated that



$5.7 \times 10^{11}$  g (1.25 billion pounds) of PCBs were produced in the U.S., about  $5.5 \times 10^{11}$  g are thought to be in use, destroyed, or otherwise unavailable, leaving the rest widely distributed in the mobile environment (Durfee *et al.*, 1976). PCBs have been identified in at least 387 of the nation's 1416 Superfund sites.

PCBs have entered into water, soils and sediments through both legal and illegal uses and both accidental and intentional disposal. In the past, disposal of PCB-laden wastes into rivers, streams, and open landfills was considered an acceptable, legal, and hazard-free practice. Sometimes, PCBs were intentionally released into the environment to reduce dust emissions from dirt roads or as extenders in some agricultural pesticide formulations. These practices were inappropriate and potentially harmful to the environment. PCBs were accidentally released into the environment due to leaking of sealed fluid compartments during their use in commercial transformers and capacitors and as a result of improper disposal of PCB-containing equipment or chemical products. The contamination of food for animal and human beings has also resulted from PCBs leaking or leaching from malfunctioning heating coils into foods during manufacturing. Finally, the incomplete combustion products such as polychlorinated dibenzodioxins (PCDDs), polychlorinated dibenzofurans (PCDFs), and quaterphenyls (PCQs) caused by transformer and capacitor fire are considered more toxic than PCBs.

PCB's physical and chemical stability resulted in serious contamination problems. PCBs are persistent in the environment due to their resistance to chemical and biological degradation. PCBs are preferentially adsorbed on humic organics in soil and sediment. They enter the food

chain through benthic organisms and invertebrates living in PCB-contaminated sediment (Kleiman, 1997). Concern about the presence of PCBs in the environment started around 1966 when research in Sweden showed the presence of PCBs in soil and water samples being screened for DDT (Jensen, 1966). Animal studies with both commercial mixtures and individual congeners have been conducted and results showed a variety of chronic toxic effect (Erickson, 1997). It is believed that PCBs can mimic natural human hormones, thereby serving as endocrine-disruptors (Klein, 1997). Due to their toxic effects on both environment and humans, PCB's manufacture was banned in the late 1970's.

The transport of PCB's in the environment is complex and global. PCBs are considered as ubiquitous environmental contaminants (Atlas and Giam, 1981; Bacon *et al.* 1992; Ballschmitter, 1991). This is somewhat paradoxical since PCBs include some of the least soluble and volatile organic compounds; still they are found virtually everywhere on the surface of the earth (Bacci *et al.*, 1986). PCBs are transported by air, water, biota and various other routes. PCBs enter the atmosphere following volatilization from spills, landfills, road oils, and other sources. In the past few years, there is increasing attention regarding the volatility of PCB from contaminated soil and sediment. Knowledge of the mechanisms for the transport of PCBs in the environment is of great importance, because the disposal, management and remediation of existing contamination must be controlled based on sound prediction of their environmental impact. U. S. EPA National Risk Management Resource Laboratory (NRMRL) funded this investigation to evaluate the potential for PCB volatilization from sediments.

## 1.2 Literature Review

The atmosphere is believed to serve as an important pathway for the transport of PCBs. Activities that include landfilling, city dumping, incineration, and accidental spilling will contribute to enhanced PCB transport to the atmosphere. Haque *et al.* (1974) reported on the volatilization of PCBs from soils as early as 1974. The importance of PCB transport into and out of Sislwit Lake, a remote lake in the Isle Royale National Park in Lake Superior was studied by constructing a mass balance of PCB congeners (Swackhamer *et al.*, 1988). Results showed removal from the lake by volatilization was more important than sedimentation for most congeners. The volatilization of PCBs from Green Bay was estimated during sampling that covered the period from June through October 1989. Calculated total PCB volatilization rates ranged from 13 to 1300 ng/m<sup>2</sup>.day. The results supported the hypothesis that volatilization was an important pathway that affected the fate of hydrophobic organic chemicals (HOCs) in aquatic system (Achman *et al.*, 1993). Chiarenzelli *et al.* (1996, 1997, 1988) conducted laboratory studies on volatilization of PCBs from a Federal Superfund Site (St. Lawrence River near Massena, New York) sediment with averaged PCBs concentrations of 65 ppb. They found that air-drying of this sediment for 24 hours at ambient conditions resulted in PCB volatilization losses of 14-23%, with 80-90% of the total loss occurring within the first eight hours. They also found that PCB loss was positively correlated with water loss. Lower orthochlorinated congeners volatilized preferentially. With the complete evaporation of water or depletion of lower orthochlorinated congeners, the rate of volatilization slowed down dramatically. They observed the same trend from subaqueous sand (1998). Another investigation on aluminum foundry wastes revealed alteration in the Aroclor 1248 composition in the shallow portions, which they

attributed to volatilization (Chiarenzelli *et al.*, 1998). Bremle and Larsson (1998) investigated PCB concentration and composition of PCBs in the air during the build-up of a landfill of PCB-contaminated sediment. They found that air was enriched in the more volatile PCB congeners as compared to the composition of PCBs in the deposited sediment. This suggests that volatilization is a major transport pathway in addition to particle transport. Harner and Mackay (1995) modeled the long-term exchange of PCBs between the soil and atmosphere in the southern U.K. from 1942 to 1992 and revealed that soil and sediment served as a source of PCBs to the atmosphere instead of the sink they once were. Results from a mass balance study on PCBs in Lake Superior by Jeremiasson and his colleagues (1994) suggested the net transfer of PCBs from the sediments to the overlaying water and, subsequently to the atmosphere. The sampling results at a Native American reservation in upper New York State by the State University of New York showed that PCB ambient air concentrations were far higher than expected. It was surmised that the possible source of PCB in air might have been caused by volatilization from sediment. These studies have raised public concerns regarding the management, disposal and remediation of PCB-contaminated sediments. This investigation was undertaken to evaluate the potential for PCB volatilization from sediments.

### **1.3 Research Objectives**

The goal of this research is to investigate the importance of PCB volatilization from sediments. The primary objective of this study is to determine the rate and extent of PCB

volatilization from sediment to the overlaying air using a simple macrocosm consisting of sediment, water and air that allowed for (pseudo) one-dimensional transport of PCB from the sediment to the gas phase. A secondary objective is to use the experimental data obtained from these experiments to validate the one-dimensional mathematical model that can lead to better understanding of the transport mechanism of PCBs.

The specific objectives include:

1. To experimentally determine the rate and extent of PCB volatilization from sediments and other substrates spiked with two PCB congeners, 4,4'-dichlorobiphenyl (DCB) and 2,2', 4, 4', 5, 5'-hexachlorobiphenyl (HCB);
2. To experimentally determine the rate of PCB volatilization from two specimens of Lake Hartwell sediment uniformly contaminated with PCBs; assess if there is a relationship between the rate of volatilization and the extent of substitution of the PCB with chlorine;
3. To use experimental results to validate the mathematical model.

#### **1.4 Thesis Layout**

Dr. Cristina Alonso and Ms. Shuang Qi developed a mathematical model of PCB volatilization from sediments to provide the theoretical basis for the study of this process. The description of the sorption of PCB from sediments was based on the dual-resistance model. A detailed description of this mathematic model is depicted in Chapter 2.

Series of experiments were performed to study the volatility of PCBs using a macrocosm of sediment, water and air that allows for one-dimensional transport of PCB. Description of the experimental setup and the methods used in this study is presented in Chapter 3. Chapter 4 discusses the experimental results obtained from the following scenarios: volatilization of DCB from water; volatilization of the two PCBs from aged contaminated sediment with no overlaying water layer; volatilization when the sediment was covered with a thin or thick water layer; volatilization of PCBs from aged contaminated silica sand or bentonite clay; and volatilization of solid PCBs from treated and untreated glass surfaces. Adsorption studies are described in Chapter 5. Chapter 6 demonstrates the model calibration using the experimental results from Chapter 4. The results of simulating runs using the calibrated model are also presented in Chapter 6. Two experiments were performed using naturally contaminated Lake Hartwell sediment. One presented the top layer while the other presented the deep layer. Chapter 7 describes the detailed experimental setup. The results from this work provided a measure of the volatilization rate for various PCB congeners. The data were analyzed to assess any relationships that might exist between the rate of volatilization and the extent of chlorination of the various congeners. Results observed in this study were compared with those of a field study, which was conducted at Lake Hartwell.

## Chapter 2 Mathematical Model

### 2.1 Introduction

The mechanisms of sorption (adsorption/desorption) of organic chemicals to natural particles are not completely understood (Pignatello and Xing, 1996; Weber *et al.*, 1991). Kinetics of sorption is complex, involving not only non-equilibrium between the solid and the liquid phases but also limitations of the sorption process rate. Sorption has been reported to take weeks, months or even years to reach equilibrium. Wu and Gschwend, (1986) explained the slow intraparticle mass transfer using an intraparticle diffusion model or pore-diffusion model which assumes that diffusion occurs in water filled pores within homogeneous particles and that diffusion is retarded by equilibrium sorption within the pores. Miller and Pedit (1992) used a general dual-resistance surface model, in which sorption rates are represented as the result of resistance due to diffusion through a boundary layer and resistance due to diffusion radially along the solid surfaces within the spherical particle. Brusseau *et al* (1991) studied two mechanisms responsible for nonequilibrium sorption: retarded intraparticle diffusion, involving instantaneous sorption to pore walls, and intraorganic diffusion. They concluded that intraorganic matter diffusion was responsible for the nonequilibrium sorption exhibited by their system. Ball and Roberts (1991) presented a two-compartment sorption model assuming diffusion in the pores and diffusion in the sorbed phase. More complicated models, built on the basic diffusion models previously described, have been proposed. Gong and DePinto (1998) discussed the fact that desorption of hydrophobic organic compounds from soils and sediments

exhibits two-stage behavior: Initial fast release followed by a longer term of slow release. They explained their experimental data by employing a two-compartment model that assumes that one fraction of the PCBs in solid phase reaches instantaneous equilibrium with the surrounding aqueous phase while the remaining fraction encounters intraparticle diffusional resistance.

In this research a model of PCB volatilization from sediments covered with water into air is specifically developed to provide the theoretical basis for the study of this process. The description of the sorption of PCB from sediments is based in the dual-resistance model.

The model considered the following processes: sorption process (adsorption and desorption) of PCBs to and from the sediment particles; advection and dispersion of PCBs through the water in inter-sediment pores due to water flow in the vertical direction ( $z$ ); transport of PCBs from the sediments to the overlaying water above the sediments with dispersion in the water due to possible irregular mixing; transport of PCBs from the water column to the air through an air film. The maximum flux into the air is simulated by assuming that the air concentration of PCB is zero. Microbial biodegradation of PCBs in the sediment water and in the water is not included in the current model, but could be included in future versions if considered necessary. The overall system comprises three separate zones: sediments contaminated with PCBs, overlaying water above the sediments, and air above the water (Figure 2-1).

The main model assumptions in this system are: constant temperature throughout the system; uniform processes and variables are constant across the column cross-section; absence of



convective flow in the horizontal direction; homogeneous PCB-sediment mixture; constant height of the sediment and water columns; no flux of PCBs at the bottom of the sediments; uniform water flow in the vertical direction; and stagnant gas and water phases. The following processes are not considered: competitive processes amongst the PCB congeners, microbial activity, and resedimentation or resuspension of sediments. It is also assumed that sediment

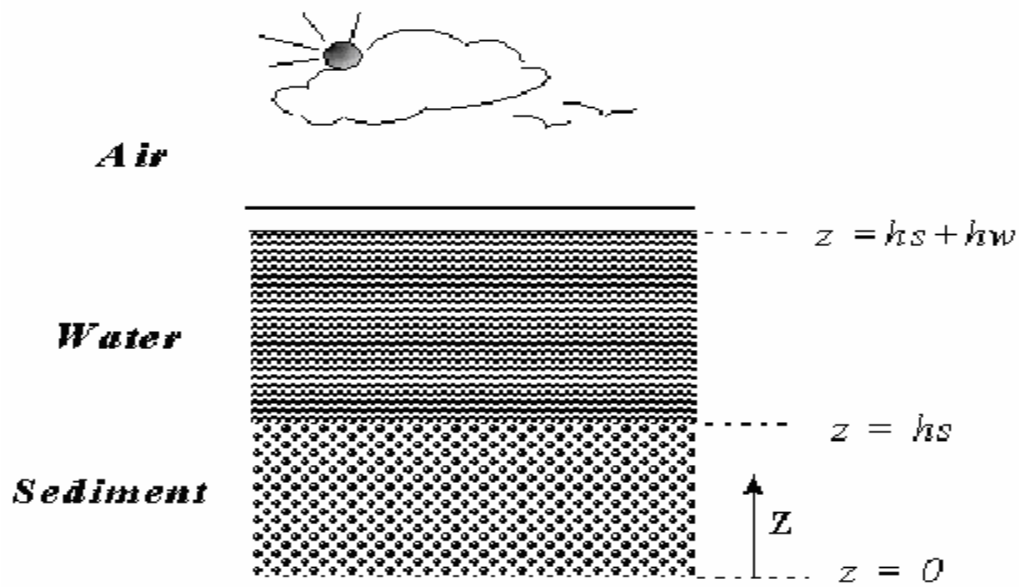


**Figure 2-1 Schematic of the System**

particles are the only source of PCBs; the initial concentration of PCB in the sediments is known; initially there is no PCB in the gas phase; PCB concentration and flux at the water-sediment interface are continuous - that is, the PCB concentration in water is the same as PCB concentration in sediment water, and the same is true for the PCB flux. PCB concentration in the water-gas interface is in equilibrium according to Henry's law. The PCB transport through the

water phase is considered to be by dispersion. A dispersion term is included to simulate various degrees of mixing. Mass transfer resistance offered by the gas phase is modeled using a film mass transfer coefficient.

## 2.2 Governing model equations

### Gas phase:

The transport of PCBs in the gas phase is modeled as mass transfer through a film characterized by a mass transfer coefficient,  $k_{fg}$ . Since in this case the concentration of PCBs in the air,  $C_g$ , is very small or null, it is neglected. Then, the flux of PCB into the gas phase per unit area,  $J$ , is given by:

$$J = k_{fg} (C_g^* - C_g), \quad C_g = 0 \quad (1)$$

where  $C_g^*$  is the concentration of PCB in the gas phase at the gas-water interface given by Henry's law:

$$C_g^* = H C_w(t, h_s + h_w) \quad @ \quad z = h_s + h_w \quad (2)$$

where  $h_s$  is the depth of the sediment column and  $h_w$  is the depth of the water column,  $H$  is the

solute Henry's law constant and  $C_w$  is the water phase PCB concentration.

Water phase:

Transport of PCB in the water phase is due to dispersion, and is described as:

$$\frac{\partial C_w}{\partial t} = D_w \frac{\partial^2 C_w}{\partial z^2} \quad (3)$$

where  $D_w$  is the water phase hydrodynamic dispersion coefficient. The initial and boundary conditions at the sediment-water and water-gas interfaces are given by equation 4. The boundary condition for the gas-water interface is obtained assuming that at the gas-water interface the flux of PCB from the water phase given by Fick's law, equals the flux into the gas film (equation 1).

$$\begin{aligned} \text{For } t \leq 0, \quad C_w(t \leq 0, z) &= C_{wo} \\ \text{For } t > 0, \quad C_w(t, h_s) &= C^* \quad @z = h_s \\ J = k_{g2} H C_w(t, h_s + h_w) &= -D_w \left. \frac{\partial C_w}{\partial z} \right|_{z=h_s+h_w} \quad @z = h_s + h_w \end{aligned} \quad (4)$$

where  $C^*$  is the concentration in the sediment-water interface.

Sediment phase:

The one-dimensional mass balance equation for the general advection-dispersion-sorption model is modified from Weber *et al.* (1991) and Miller and Weber (1988):

$$\frac{\partial C_s}{\partial t} = -v_z \frac{\partial C_s}{\partial z} + D_s \frac{\partial^2 C_s}{\partial z^2} + r_{sorption} + r_{reaction} + S(C)_{source} \quad (5)$$

where  $C_s$  is the concentration of PCBs in the water phase of the inter-particle pores in sediments,  $v_z$  is the fluid phase inter-particle pore velocity (considered positive when there is upflow in the  $z$  direction),  $D_s$  is the hydrodynamic dispersion coefficient (this is negative because  $z$  is negative in the sediments),  $r_{sorption}$  and  $r_{reaction}$  are the rate of sorption and reaction respectively. The *reaction* and *source* terms are neglected here as no reaction is assumed to occur, and there is no extraneous source of contaminant. The rate of sorption,  $r_{sorption}$ , represents the variation of the concentration associated with microscale sorption processes in the inter-particle pores of the sediment phase:

$$r_{sorption} = - \left( \frac{1-\epsilon}{\epsilon} \right) \rho_s \left( \frac{\partial q_{ave}}{\partial t} \right) \quad (6)$$

where  $\epsilon$  is the porosity of the sediments,  $\rho_s$  is the density of the solid sediment phase, and  $q_{ave}$  is the average volume solid phase concentration of PCBs given as a mass ratio: Mass solute sorbed divided by mass of sorbent. The mass balance equation for this case is then:

$$\frac{\partial C_s}{\partial t} = -v_z \frac{\partial C_s}{\partial z} + D_s \frac{\partial^2 C_s}{\partial z^2} - \left( \frac{1-\epsilon}{\epsilon} \right) \rho_s \left( \frac{\partial q_{ave}}{\partial t} \right) \quad (7)$$

The initial and boundary conditions are given by equation 8, with  $C_{so}$  being the initial concentration in the inter-sediment water:

$$\begin{aligned}
 & \text{For } t \leq 0 \quad C_s(t \leq 0, z) = C_{so} \\
 & \text{For } t > 0, \quad C_s(t, h_s) = C_w(t, h_s) \quad @ z = h_s \\
 & -D_w \frac{\partial C_s}{\partial z} \Big|_{z=h_s} = -D_s \frac{\partial C_s}{\partial z} \Big|_{z=h_s} + v_z C_s(t, h_s) \quad @ z = h_s \\
 & \frac{\partial C_s}{\partial z} \Big|_{z=0} = 0 \quad @ z = 0
 \end{aligned} \tag{8}$$

The expression for the variation of  $q_{ave}$  with time is related with the sorption model used and depends on the description of the aqueous-solid phase equilibrium, as well as, the rate at which equilibrium is approached. The next section outlines the description of the sorption model selected for this work.

#### Model for the Sorption Process:

The dual-resistance model (Miller and Weber, 1988 and Weber and Miller, 1988) has been used to describe the sorption (adsorption and desorption) of PCBs in sediments. PCBs are assumed to be transported by intraparticle surface diffusion into or from the porous sediment particle followed by mass transfer through a liquid film surrounding the solid particle (Figure 2-2). The sediment particle is assumed to be a sphere with radius  $R_p$ . The variation of  $q_r$ , the solid-phase concentration at the radial position  $r$ , inside the particle is given by the diffusion equation:

$$\frac{\partial q_r}{\partial t} = \left( \frac{D_p}{r^2} \right) \frac{\partial}{\partial r} \left( r^2 \frac{\partial q_r}{\partial r} \right) \quad 0 < r < R_p \quad (9)$$

where  $D_p$  is the intraparticle surface diffusion coefficient in the sediment particle. Initial conditions are needed for this equation. The boundary condition for symmetric concentration inside the sediment particle or null flux in the center of the particle is:

$$BC: \quad \left. \frac{\partial q_r}{\partial r} \right|_{r=0} = 0 \quad (10)$$

The external solute mass transfer across the film surrounding the solid particle is given by the flux through the film at the solid-phase boundary:

$$BC: \quad \left. \frac{\partial q_r}{\partial r} \right|_{r=R_p} D_p = \frac{k_f}{\rho_s} (C_s - C_s^*), \quad C_s^* = \text{function}(q_r(R_p)) \quad (11)$$

where  $k_f$  is the external-film mass transfer coefficient and  $C_s^*$  is the solution phase concentration corresponding to the solid phase external concentration at radius  $R_p$ . Both magnitudes are related by the equilibrium isotherm.  $D_s$  in this case is the density of the particle. Then  $q_{ave}$  is given by:

$$q_{ave} = \frac{3}{R_p^3} \left( \int_0^{R_p} q_r r^2 dr \right) \quad (12)$$

And:

$$\frac{\partial q_{ave}}{\partial t} = \frac{3}{R_p} \frac{k_f}{\rho_s} (C_s - C_s^*) \quad (13)$$

and the mass balance equation in the sediments is:

$$\frac{\partial C_s}{\partial t} = -v_z \frac{\partial C_s}{\partial z} + D_s \frac{\partial^2 C_s}{\partial z^2} - \left( \frac{1-\epsilon}{\epsilon} \right) \left( \frac{3}{R_p} \right) k_f (C_s - C_s^*) \quad (14)$$

### Solution Methodology

With this formulation, the mathematical model consists of a system of coupled partial differential equations, where variables are functions of three dimensions, height ( $z$ ), radius ( $r$ ) and time ( $t$ ). The numerical solution of the model is obtained with a computer program written in C++ language.

The non-linear parameter estimation technique used was normalized least squared errors and the method of Lavengerg-Maquardt.

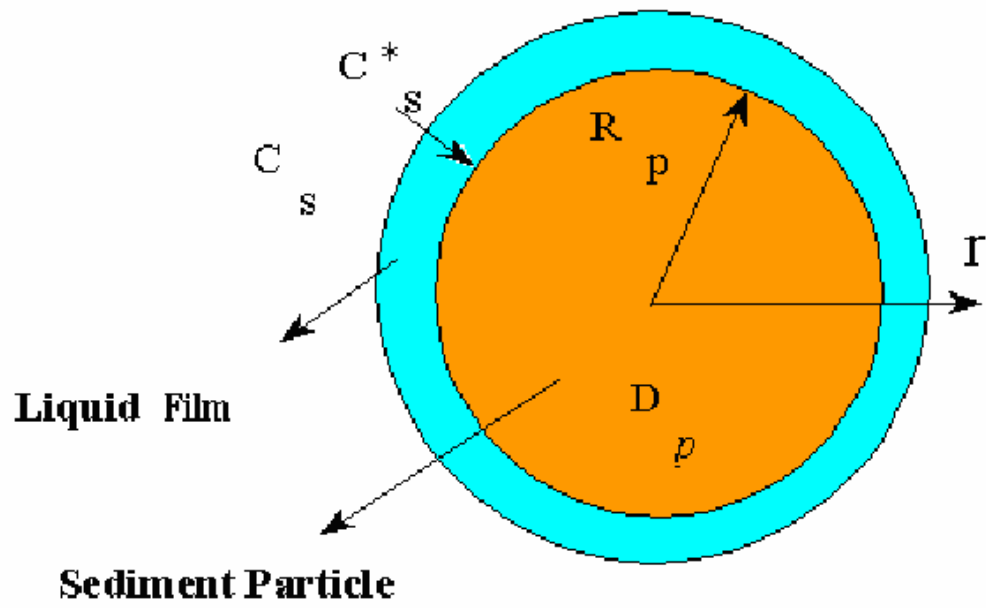


Figure 2-2 Schematic of the sediment particle



## Chapter 3 Materials and Methods

### 3.1 Selection of PCB Congeners

PCBs have a wide range of solubility, volatility, and other physical and chemical properties. For this study, the volatilization of a PCB with few chlorines and a PCB with many chlorines was considered. Two PCB congeners, 4,4'-dichlorobiphenyl (DCB) and 2,2', 4, 4', 5, 5'-hexachlorobiphenyl (HCB) (Ultra Scientific, North Kingstown, RI) were selected as representative PCBs. These two congeners have substantially different physical and chemical properties such as water solubility and Henry's Law Constant. Furthermore, both congeners were frequently observed in contaminated sediment and studied by other researchers (Larsson, 1983; Gong *et al.*, 1998). Their principal physical chemical properties are listed in Table 3-1. <sup>14</sup>C-labeled DCB from Sigma Chemical Co. (St. Louis, MO.) was also used in experiments and adsorption/desorption study with the following radioactivity: DCB, 11.3mCi/mM.

**Table 3-1** Physical and Chemical Properties of PCB Congeners Studied

PCB Congeners	Molecular Weight (g/mol)	Density (g/cm <sup>3</sup> )	Solubility (µg/l)	Log Kow	Henry's Law Constant (Pa.m <sup>3</sup> /mol)
4,4'-DCB	223.1	1.05	50-80	4.92-5.58	9.66-20.16
2,2',4,4',5,5'-HCB	360.9	1.3	1-9	6.34-8.35	2.33-13.37

- Data used for this table are from Mackay, D. (10)

There are some advantages in using radiolabeled material. These include the lower detection limit of the liquid scintillation counter that is used to determine radioactivity as

compared to the detection limit of the GC-ECD. The other is that liquid samples can be analyzed directly without the need for extraction. The cost of  $^{14}\text{C}$  labeled PCB, however, is much higher than unlabeled PCB. Hence, it was used only in some of the volatilization experiments and the preliminary adsorption study.

### **3.2 Experimental Setup**

The schematic of the experimental system is shown in Figure 3-1. The system consisted of four parts: a glass column, a water trap, a PCB trap and a 100 rpm fixed speed pump. The column was a glass gas-washing bottle, which was 20 cm high with an inside diameter of 5.5 cm. Prior to use, the columns were silylated and baked at 250°C for 2 hours. To minimize adsorption loss of PCB by the system, all connections were made using stainless steel tubing and fittings to the extent possible. Viton tubing (chosen for minimal adsorption of PCBs) was used in the peristaltic pump. Air was recirculated around the system at a rate of 5.76 l/h. The direction of the airflow caused the volatilized PCBs and moisture to pass through stainless steel tubing into a moisture trap. Such a flow rate was shown in preliminary experiments (see Appendix 1) to provide a sufficient turn over rate that will not retard volatilization. The moisture trap consisted of a stainless steel tube packed with 5 g of anhydrous sodium sulfate. The air exiting the moisture trap was conducted through stainless steel tubing to another stainless steel trap packed with 10 g of florisil (60x100 mesh, Sigma Chemical Co.) where volatilized PCB was absorbed. The dry and decontaminated air was then pumped back into the headspace of the gas-washing bottle.

Tested substrates were placed at the bottom of each gas-washing bottle. Prior to placement into the gas-washing bottle, all substrates were thoroughly homogenized by rigorous mixing. The substrates were either covered with overlying natural water or left without any water cover. The purpose of the water was to prevent the drying of the surface of the sediment that would cause mechanistic changes in the volatilization of PCBs. About three quarters of the column height was maintained as headspace to reduce aerosol facilitated transport.

All experiments were conducted at room temperature. Sodium azide and sodium molybdate were added to the sediment during the contamination step to insure abiotic conditions during the course of the experiment (0.2 ml/g sediment of a solution; 0.38 M sodium azide and 0.5 M sodium molybdate). The rate of transport of PCBs from the sediment to the air phase was quantified by measuring the mass of PCB entering the air with time (PCB accumulated in the florisil trap) and by closing the mass balance by extraction of the sediment and water for the PCB congeners at the end of each test.

The optimum operational parameters of the system such as the speed of the pump, the amount of florisil and sodium sulfate in the stainless steel traps were determined after several preliminary experiments. These experiments are described in Appendix 1.

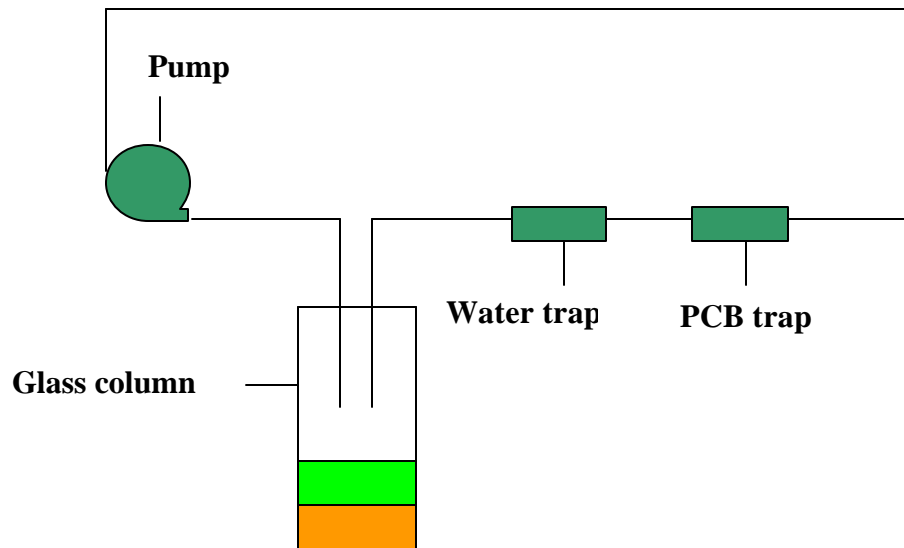


**Figure 3-1** Experimental Apparatus

### 3.3 Silylation of the Glass Columns

As mentioned earlier, to prevent PCB adsorption onto the glass column, all the columns were treated with a technique called Silylation. Silylation is a process of deactivating glass surface; minimizing nonspecific binding and sample loss; reducing adsorption of polar compounds, including proteins and trace metals, onto glass surface; protecting delicate samples against the possible reactive effects of  $-OH$  sites present on all types of glassware using 5% DMDCS (dimethyldichlorosilane) in toluene (Supelco). The detailed procedure is described in Appendix 2.

### 3.4 Substrates Tested

PCB volatilization from different substrates was investigated. The substrates included spiked sediments, silica sand, bentonite clay and naturally contaminated Lake Hartwell sediments.

PCB-free sediment collected at New York Harbor by U.S. EPA personnel as well as sand and clay were spiked with the two PCB congeners, mixed with natural overlaying water using a rotating tumbler at room temperature. The sediment thus contaminated was aged for three months prior to use in the volatilization experiments. The preparation of the aged contaminated substrates is described in details in Appendix 3.

Characterization of the substrates was tested to identify the physical and chemical properties of the substrates that can impact adsorption/desorption and volatilization characteristic. The substrates were characterized by Agvise Laboratories (North Dakota) and the results are summarized in Table 3-2.

Moisture content of the sediment was determined using a modified procedure of the American Society for Testing and Materials (ASTM). See Appendix 5 for details.

**Table 3-2 Substrates Characterization**

		E.R. Sediments	Silica Sand	Bentonite Clay
Density (g/cm <sup>3</sup> )		2.53	2.59	2.54
pH (water)		7.6	6.5	8.7
% Organic matter <sup>1</sup>		5.4	0.1	0.7
% Volatile organic matter <sup>3</sup>		6.8	0.09	1.2
Particle Size Distribution ( $\mu\text{m}$ ) <sup>2</sup>	<4	46	49	85
	4-63	39	40	0
	63-2000	15	11	15
Heavy Metal Content (ppm)	Zinc	17.32	0.31	8.46
	Iron	196.5	1.5	8.1
	Copper	15.49	0.13	0.21
	Manganese	46.3	1.6	1.7

Note: 1. Walkley-Black method;

2. hydrometer method;

3. This measurement was conducted at UC lab.

### 3.5 PCB Extractions and Analysis

#### 3.5.1 Extraction Methods

Hexane and an acetone/hexane mixture (1:1) were used to recover PCBs from glass columns, florisil and sodium sulfate traps, as well as from stainless steel tubing. A rotating

tumbler was used to facilitate the extraction process. 3,4,4'-trichlorobiphenyl (Ultra Scientific) was added as surrogate congener to monitor the extraction efficiency. The composition of the solvents is listed in Table 3-3.

Preliminary experiments were conducted with different proportions of the solvents acetone and hexane, different mixing methods and different mixing periods. A detailed description of these experiments is presented in Appendix 4. A solvent proportion of 75% hexane and 25% acetone with 2 days of tumbling time were selected to be used in sediment extraction in this research.

**Table 3-3 Composition of the Solvents**

Substrates	Solvents proportion
water	hexane
Sediment(clay and sand)	Acetone/hexane(25%:75%)
Florisil	Hexane
sodium sulfate	Hexane
tubing	Acetone/hexane(1:1)

Method to extract PCBs from the glass column

The method used for the extraction of PCB from the contaminated sediments is summarized as following:

- Add appropriate amount of surrogate internal standard to the substrates in the glass column. The mass of surrogate added is one that results in a final concentration of the surrogate in the final extract solution to be analyzed in the range of 80-120 µg/l. This will be calculated based on the results of preliminary extractions of the substrates.
- Pour as much of the substrates as possible from the glass column into a wide mouth 60 ml brown glass bottle. Add 5 ml of acetone into the glass column and shake and pour contents into the wide mouth brown glass bottle. Repeat this procedure once more. Add 30 ml of hexane and activated copper to the wide mouth brown glass bottle.
- Seal the wide mouth brown glass bottle and tumble for 24 hours
- Transport the contents of the wide mouth brown glass bottle to a 50 ml centrifuge tube. Centrifuge tube contents for 25 minutes at 5,000 rpm.
- Decant the hexane into a graduated cylinder and bring the volume of hexane back to 25 mls.

Method to extract PCBs from the florisil, sodium sulfate

The procedures of PCBs extraction are as follows:

- Transfer florisil and sodium sulfate from metal traps to a wide mouth 60 ml brown glass bottle.
- Add surrogate internal standard and 40 ml hexane to the wide mouth brown glass bottle.
- Seal the wide mouth brown glass bottle and tumble for 24 hours.
- Transport the solvent from the wide mouth brown glass bottle to a pre-cleaned, labeled 120 ml brown glass bottle.



- Add 25 ml fresh hexane to the wide mouth brown glass bottle and tumble it for at least an hour and remove the solvent.
- Repeat the extraction procedure one additional time and combine the solvent.

#### Method to extract PCB from the tubing and metal tubes

The tubing including stainless steel, glass and viton (connected to the pump) and metal tubes were eluted with about 10ml of Hexane.

#### 3.5.2 Analytical methods

PCB analysis was performed on an HP 5890 gas chromatograph (GC) (Hewlett-Packard Co. Palo Alto, C.A) using an electron capture detector and a DB-5 capillary column. Helium and P5 (argon/methane) were used as carrier and makeup gases, respectively. Trichlorobiphenyl (2,4,4') (Ultra Scientific) was used as internal standard for GC analysis. See Appendix 7 for detailed method.

The concentration of  $^{14}\text{C}$  labeled DCB was measured via a TRI-CARB 2300 TR liquid scintillation counter (Packard Instrument CO., Downers Grove, IL). Refer Appendix 8 for details.

All the experiments were run in duplicate sets. For each experiment, twelve glass columns were initially loaded with water or contaminated substrate depending on the

experimental design. At each sampling time, two columns were sacrificed and the distribution of PCB within the system was analyzed; hence six time data points were generated for each experiment. The initial amount of PCB in the water or contaminated substrates was determined by extracting the same amount of material loaded to the glass column before each experiment. The percentage of PCB volatilized was determined by dividing the amount recovered from the florisil trap, traps and tubing by the initial mass.

## **Chapter 4 Volatilization Experiments**

Experiments were performed to study the volatility of PCBs (DCB and HCB) using a macrocosm consisting of sediment, water and air that allows for one-dimensional transport of PCB. Experimental results and a discussion of these results will be presented in this Chapter. The experimental setup and methods used were described in Chapter 3. Any deviation from these procedures will be noted in the respective sections. Scenarios investigated were as follows:

1. volatilization of DCB from water for three water depths;
2. volatilization of the two PCBs from aged contaminated sediment with no overlaying water layer;
3. volatilization when the sediment was covered with a thin or thick water layer;
4. volatilization of PCBs from sediments contaminated at three different levels;
5. volatilization of PCBs from aged contaminated silica sand or bentonite clay;
6. volatilization of solid PCBs from treated and untreated glass surfaces.

### **4.1 Volatilization of DCB from Water**

#### 4.1.1 Introduction

To study the rate of volatilization of DCB from water with time, the glass columns were loaded only with water containing dissolved DCB (under 60% saturation). No substrate was present. DCB in acetone was spiked into water contained in a volumetric flask by syringe injection. The water was vigorously mixed by hand-shaking several times and then left still for

overnight to make the DCB dissolve completely and distribute evenly. Triplicate extractions were performed on the same volume of water that would be applied to the glass column to determine the initial DCB quantity. The percentage of volatilization was based on this initial amount. At the time of sampling, the whole system was extracted and analyzed.

Three different heights of water (2.8, 5.5, 8.3 cm corresponding to 50, 100, 150 ml) were studied in order to obtain sufficient data for estimating values for the unknown parameters of the mathematical model that correspond to volatilization from water. Each water depth experiment was performed twice thus resulting in six independent experiments. All the experiments were run in a similar manner.

The solubility of HCB in water (less than 1  $\mu\text{g/l}$ ) at room temperature was below the detection limit of both GC and LSC; hence the volatilization of HCB from water was not evaluated.

#### 4.1.2 Results and Discussion

At the beginning of each experiment, twelve columns were loaded with DCB dissolved in water and were run for varying periods of time prior to sampling. At each sampling event, two glass columns were sacrificed, thus six sampling events were obtained for each experiment. These experiments will be referred as Experiment 1 and 1' (2.8 cm), Experiment 2 and 2' (5.5 cm), and Experiment 3 and 3' (8.3 cm). Duplicate columns are named with capital letters, i.e., A and A'.

For the 2.8 cm water depth experiments (Experiment 1 and 1'), the columns were loaded with 1.073 (Experiment 1') and 1.290  $\mu\text{g}$  (Experiment 1) of DCB, respectively. Six systems were run for 8, 16, 24, 48, 72 and 96 hours, respectively.  $^{14}\text{C}$ -labeled DCB was used in Experiment 1'. The original data from these experiments are shown in Table A4-1 and Table A4-2 in Appendix 10. The amount of DCB recovered is reported in  $\mu\text{g}$ .

For the 5.5 cm water depth experiments, the columns were loaded with 2.022 (Experiment 2) and 3.674  $\mu\text{g}$  (Experiment 2') of DCB, respectively. The original data from these experiments are shown in Table A4-3 and Table A4-4 in Appendix 10. The amount of DCB recovered is reported in  $\mu\text{g}$ .

For the 8.3 cm water depth experiments, 2.807 (Experiment 3) and 3.225  $\mu\text{g}$  (Experiment 3') of DCB were added, respectively. Six systems were run for 12, 24, 48, 72, 96 and 120 days, respectively.  $^{14}\text{C}$ -labeled DCB was used in both experiments. The original data from these experiments are shown in Table A4-5 and Table A4-6 in Appendix 10. The amount of DCB recovered is reported in  $\mu\text{g}$ .

Results of the experiments in which  $^{14}\text{C}$ -labeled DCB was used (Experiments 1', 3 and 3') showed overall better PCB recovery than similar experiments when none  $^{14}\text{C}$ -labeled DCB was used. This may be due to the fact that in cases when  $^{14}\text{C}$ -labeled DCB was used, direct analysis was possible.

The only difference between each pair of experiments with the same water depth (1 and 1', 2 and 2' and 3 and 3') is the initial amount of DCB in the glass column. According to the mathematical model the amount of DCB remaining in water at time  $t$  ( $C$ ) relative to the initial amount of DCB ( $C_0$ ) is only a function of the water depth in the glass column, it does not depend on the initial amount of DCB present. Therefore the percentage of DCB volatilized in both experiments should be the same. The results of volatilization of DCB from three different water levels (2.8, 5.5 and 8.3 cm) are summarized in Figure 4-1 a, b and c. The percentage of DCB volatilized is presented versus time.

As can be seen from Figure 4-1, DCB volatilized from water very rapidly, and within 120 hours, essentially all the dissolved DCB disappeared. The data in Figure 4-1 suggest that the rate of volatilization decreased as a function of water depth. The results also illustrate comparable measurement by GC and liquid scintillation counter as well.

The effect of completely mixing the water phase was simulated by the bubbling of air into the water. An experiment designed for this purpose was used to investigate this effect. The system was the same as the one used for the other experiments except that this time the return air was directed into the water phase as shown in Figure 4-2. The experiment was running in the same way, with twelve glass columns and using duplicate columns for each time data point. Initially, each column was loaded with  $2.416 \mu\text{g}$  of DCB dissolved in 100 ml water.

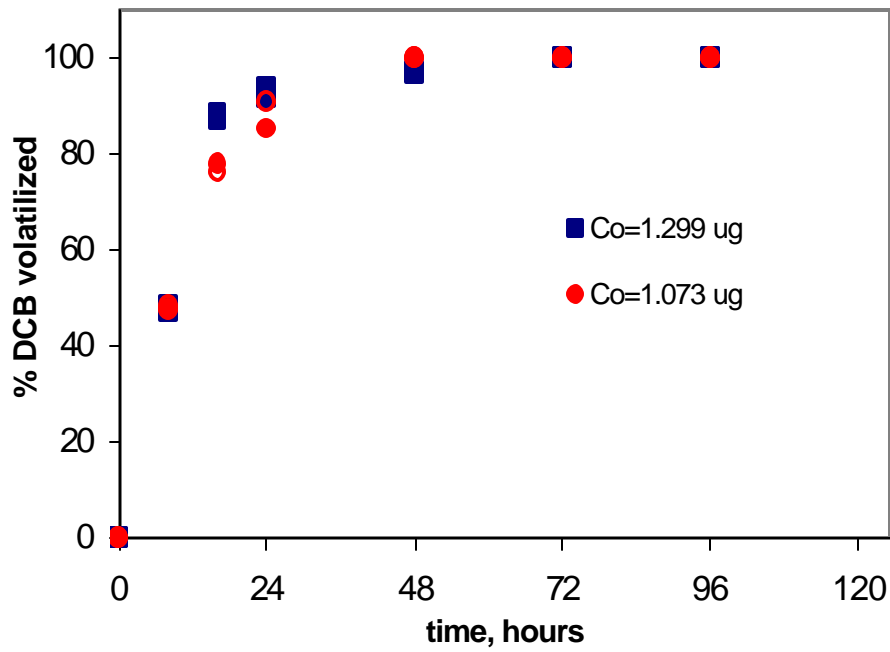


**Figure 4-1 (a)** Volatilization of DCB from Water (2.8 cm)

Full and empty symbols represent duplicate values for each data point

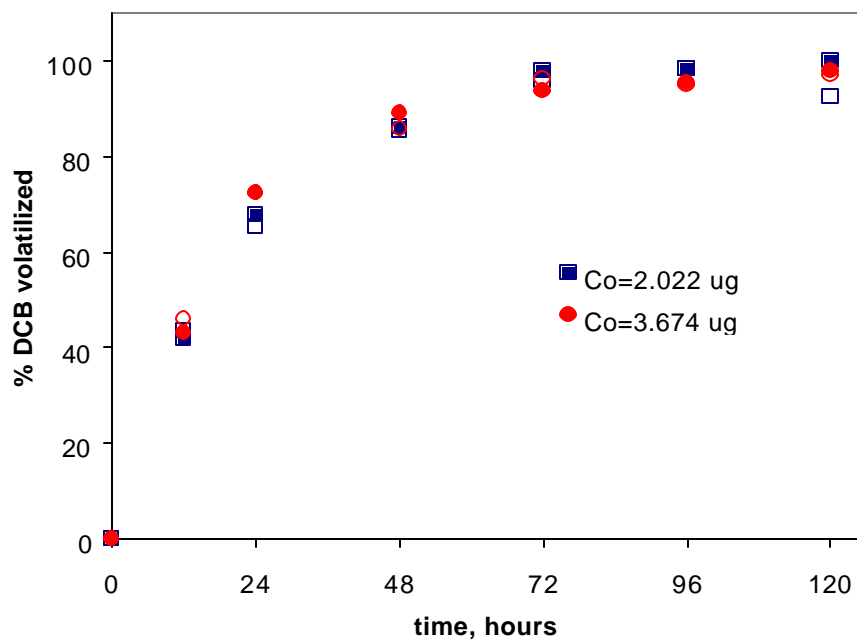


**Figure 4-1 (b)** Volatilization of DCB from Water (5.5 cm)

Full and empty symbols represent duplicate values for each data point



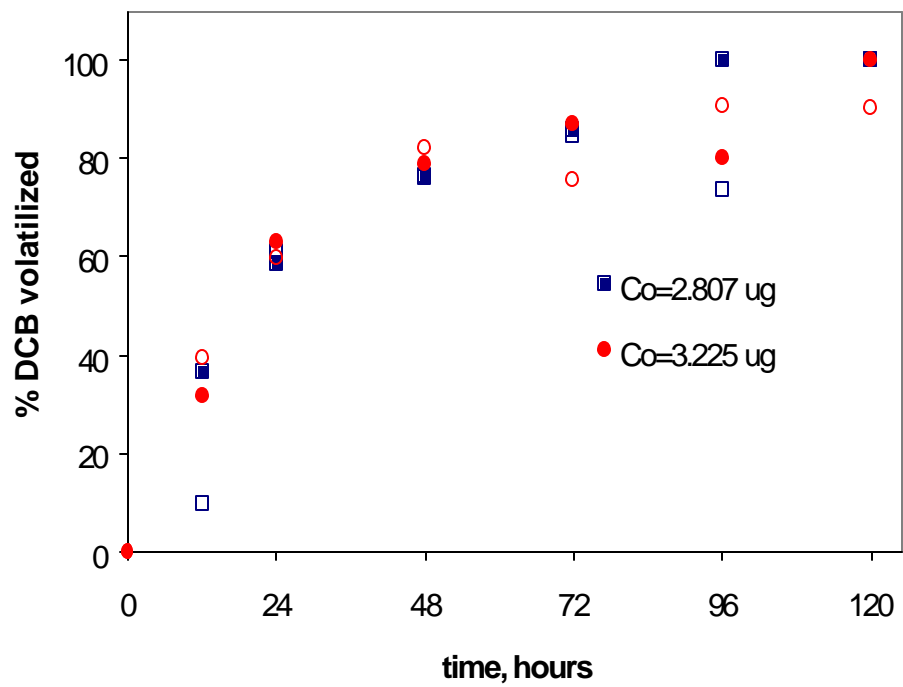


**Figure 4-1 (c)** Volatilization of DCB from Water (8.3 cm)

Full and empty symbols represent duplicate values for each data point

The original data from these experiments are shown in Table A4-7 in Appendix 10. Results are plotted in Figure 4-3. It can be observed that, as expected, the volatilization from completely mixed water was faster than from still water. This finding suggests that DCB volatilized faster when the aqueous phase is mixed or when the interfacial area is increased.

## **4.2 Volatilization of PCB from Contaminated Sediments**

### **4.2.1 Introduction**

The volatilization of DCB and HCB from the sediment was studied in the second set of experiments. Five grams of contaminated sediment were loaded into the columns with 47 ppm of DCB and 42 ppm of HCB in the sediment expressed as dry weight. Prior to placement into the gas-washing bottles, the sediment was thoroughly homogenized by rigorous mixing. When each column was sacrificed, the amount of DCB and HCB in each part of the system was analyzed and the data were used to determine the rate of volatilization of both congeners. These two rates were considered independent since it was assumed that the volatilization of DCB did not interfere with the volatilization of HCB. Four experiments were conducted: in the first experiment the sediment was either uncovered or had a thin overlaying water layer (0.5 cm). The second experiment was run for a longer time to achieve more volatilization using only DCB contaminated sediment (DCB showed more volatilization than HCB) and a thin layer of water (0.5 cm) covering the sediment. The third experiment was conducted with 100 ml water (5.5 cm) covering the sediment to see how the water level above the sediment affected the volatilization

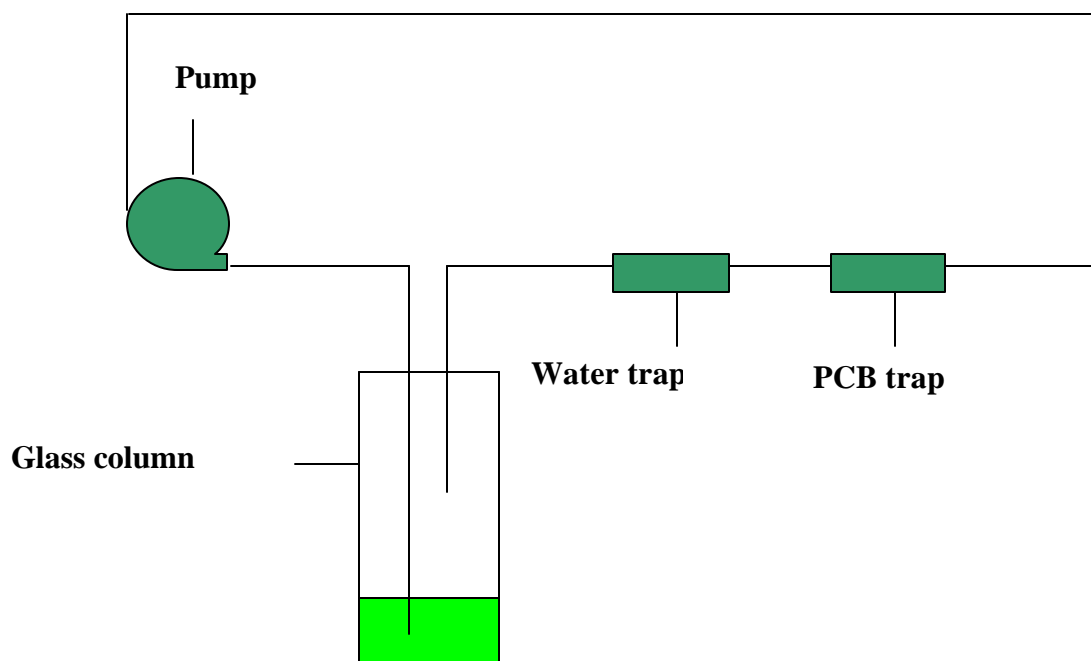


**Figure 4-2** Experimental Schematic

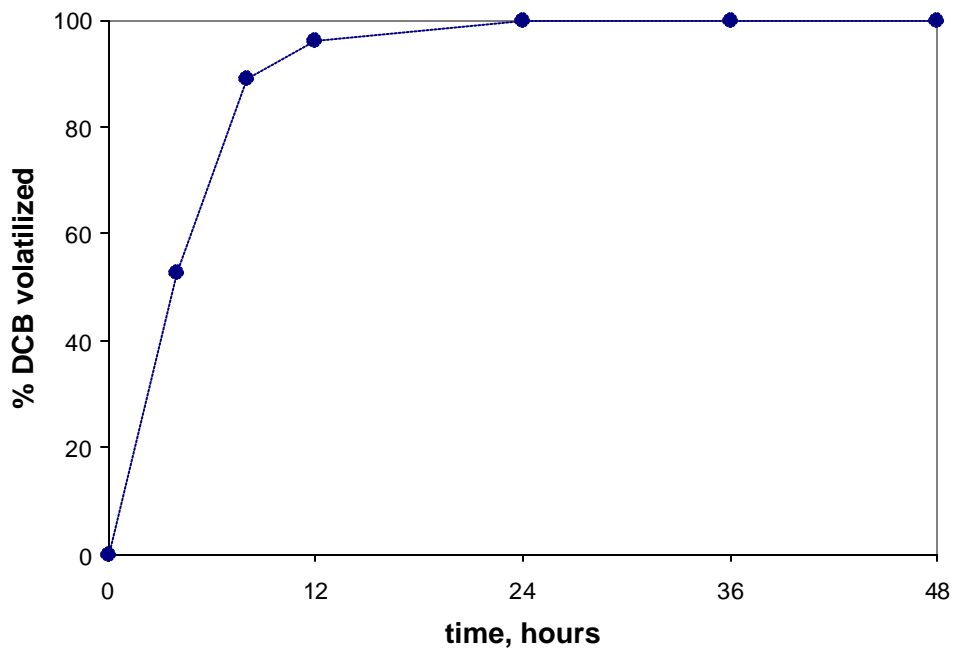


**Figure 4-3** Volatilization of DCB from Completely Mixed Water

rate. In the fourth experiment, the PCB volatilization rate was determined for two other contamination levels, which were 24 ppm (middle) and 14 ppm (low), respectively. Experimental results using these two sediments will be compared with the first contamination level 47 ppm (high) to explore if any relationship exists between contamination level and volatilization rate.

#### 4.2.2 Results and Discussion

Mass balance was established at the end of each experiment. Overall the recovery rates of PCBs from each system were within 85% and 110%. The volatilization rate was calculated by dividing the amount collected on the florisil trap by the initial amount that was determined by extracting the same amount of sediment (in triplicates) loaded to the glass column at the beginning of each experiment.

In the first experiment, the volatilization of both PCB congeners, DCB and HCB directly from the sediment, without any amount of water covering it, or when the sediment was covered by a thin overlaying water layer was studied. Twelve columns were each loaded with 5 g of the sediment. The initial amount of DCB and HCB was determined to be 64.54mg for DCB and 67.31mg for HCB. Six systems with two columns each were run for 2, 4, 6, 8, 10 and 12 days, respectively. The original data of these experiments are shown in Table A4-8 and A4-9 in Appendix 10. TCB (3,4,4'- trichlorobiphenyl) was applied as a surrogate to monitor the extraction efficiency. The data in the row labeled with TCB (%) represent the extent of recovery of TCB.

Figure 4-4 summarizes the results from the 12-day experiment for the volatilization of DCB and HCB from saturated sediment either without an overlaying water layer, or sediment covered with a thin water layer (0.5 cm). The percentage of PCB collected in the florisil trap is presented as a function of time. The experimental data suggest that there was no volatilization of HCB. The rate of volatilization of DCB from sediments was much slower than that observed from water. DCB volatilized faster from the sediment that had no water cover than from the sediment covered by a thin water layer. However, after 8 days the sediment that had no water cover started drying and the rate of DCB volatilization decreased markedly. A classic “steam distillation” process where water functions as a carrier medium can explain this phenomenon (Chiarenzelli *et al.*, 1996). First the congener that volatilized faster (which is DCB in this case) is much more water-soluble than the other congener (which is HCB); and secondly the PCB volatilization rate decreased as the sediment lost its water. Hence, in all subsequent experiments, the sediment was covered with a thin water layer to prevent the drying of the surface of the sediment that would cause mechanistic changes in the volatilization of PCBs.

Since the volatilization of PCB was still low after 12 days, a longer-term experiment on the volatilization of DCB from sediment was conducted with a thin overlaying layer of water (0.5 cm). Twelve columns were each loaded with 2.5g of DCB contaminated sediment. The initial amount of DCB was determined to be 59.02 $\mu$ g. Duplicate columns were used for each time point. The experiment was run for 55 days, and samples were analyzed at 2, 6, 13,

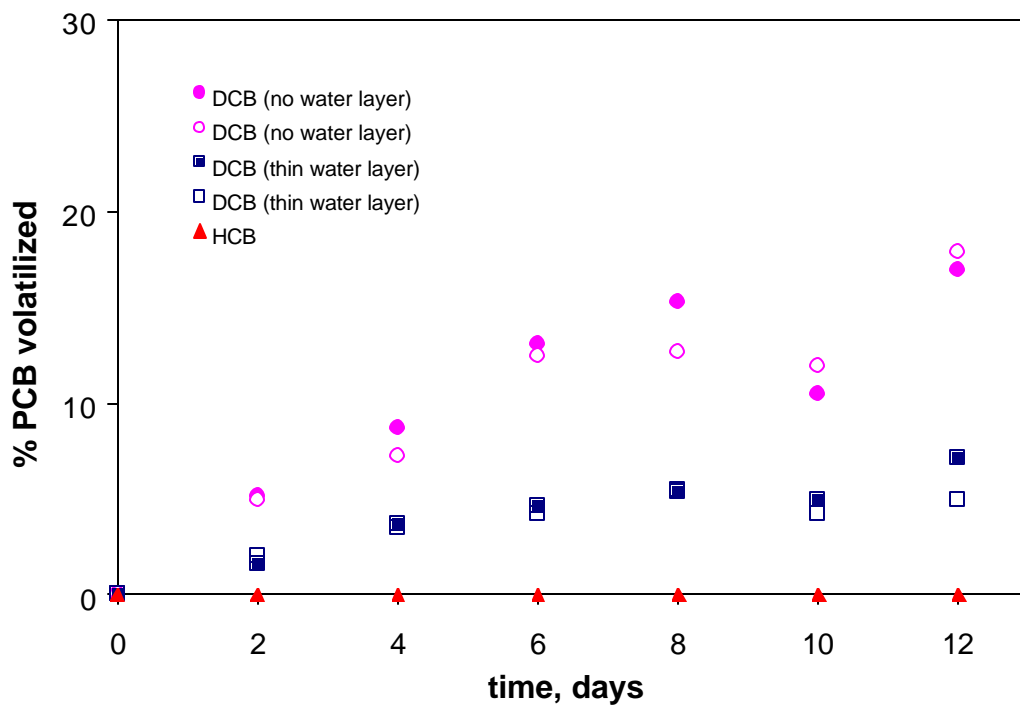


**Figure 4-4** Volatilization of PCBs from sediments with/without overlaying water layer

26, 40 and 55 days. Each sampling time was selected based on the preceding results. For example, since the amount of DCB remaining in the sediment after 6 and 13 days was not significantly different, it was decided that the next sampling time would be 26 days, 13 days after. The original data for this experiment are shown in Table A4-10 in Appendix 10. Results are plotted in Figure 4-5. After 55 days, about 30% of the initially loaded DCB has volatilized from the sediment phase.

Another experiment was performed using a higher water level (5.5cm) on top of the sediment. Sampling events were carried out on days 5, 20, 35, 50, 65 and 80. The initial amounts of DCB and HCB were determined to be 56.76 $\mu$ g and 53.34 $\mu$ g, respectively. The original data of this experiment are shown in Table A4-11 in Appendix 10. Figure 4-6 shows the results of volatilization of DCB and HCB from sediments with a thick overlaying water layer (5.5 cm). In this case, the rate of DCB volatilization from the sediment was slower than from sediment covered with a thin layer of water. Consistent with previous observations, the rate of HCB volatilization was very slow (less than 2%).

A comparison of DCB volatilization from sediment with 0.5 and 5.5 cm thick overlaying water layers is illustrated in Figure 4-7. Each data point represents the average of the duplicate values. The data in Figure 4-7 show that DCB volatilized faster from sediment covered with a thin water layer, but the difference is not dramatic. Another interesting observation from Figure 4-7 is that the volatilization process for both cases investigated appeared to be linear, with the best-fit linear equations shown on the figure. DCB volatilized at a rate of 0.55% and 0.35% per



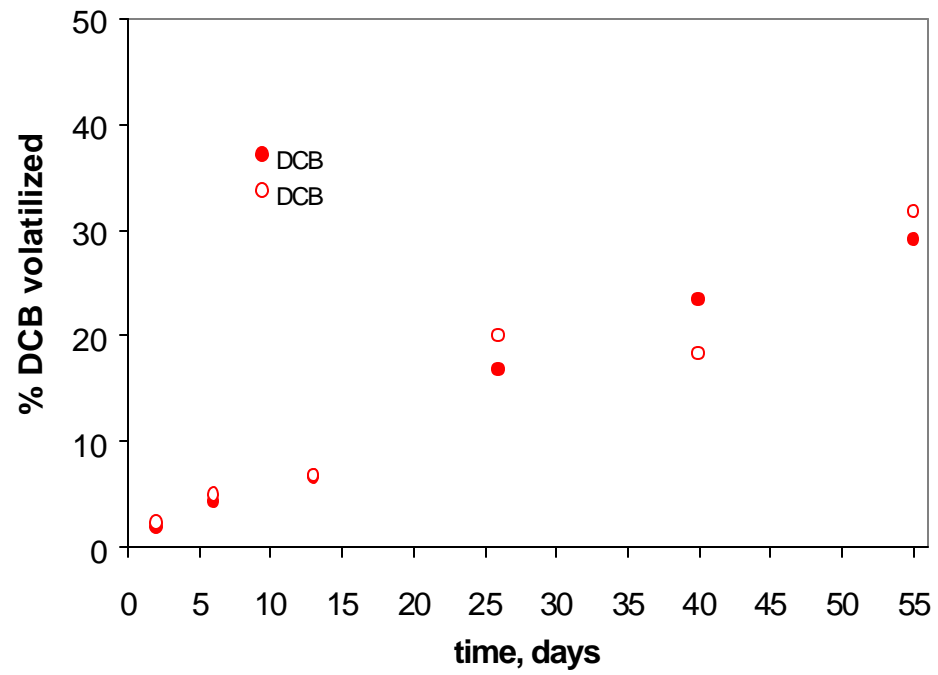


**Figure 4-5** Volatilization of DCB from sediments with a thin overlaying water layer

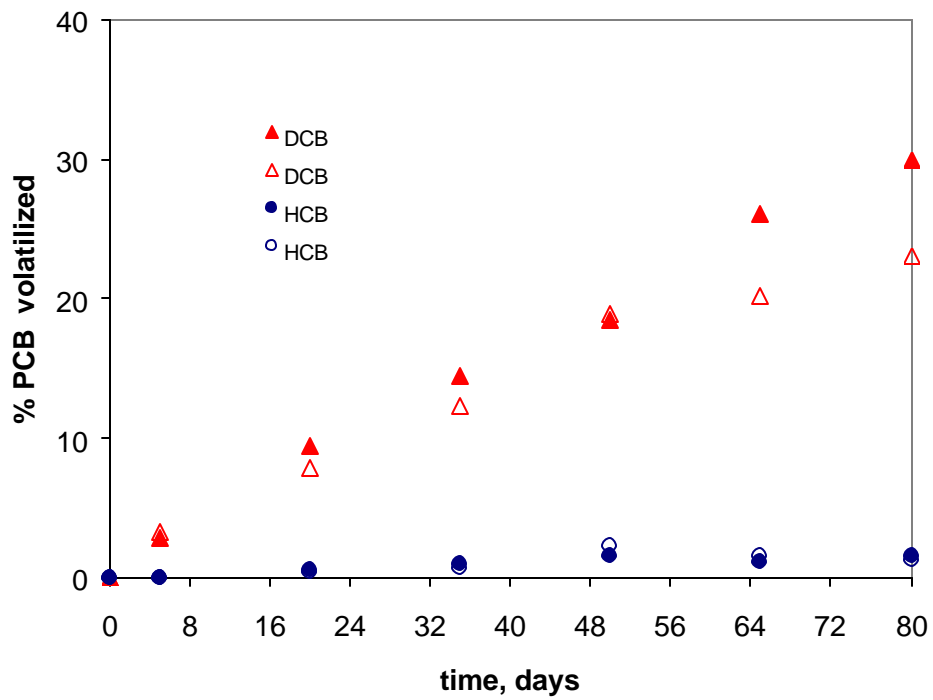


**Figure 4-6** Volatilization of PCB from sediments with a thick overlaying water layer

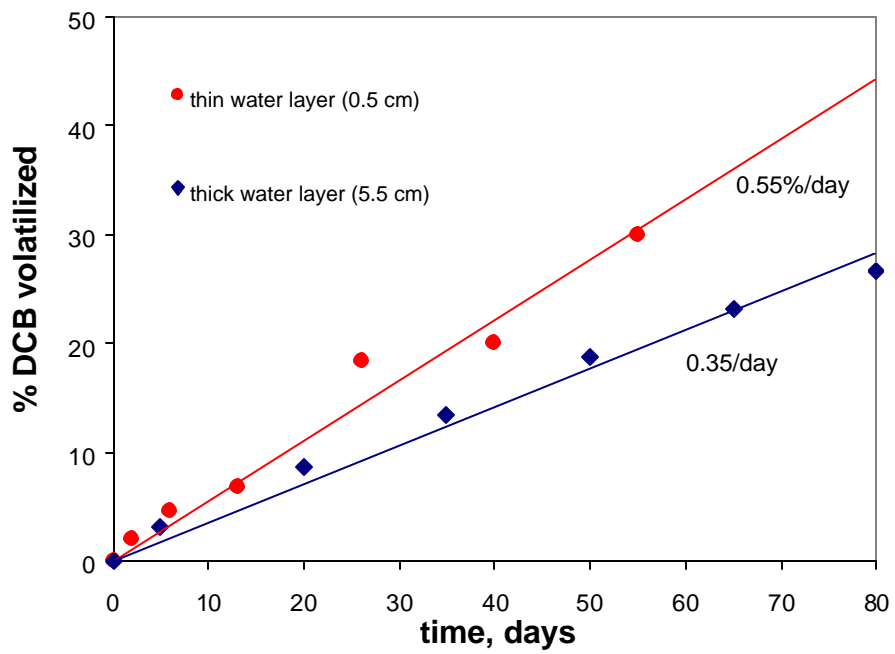


**Figure 4-7** Comparison of the effects of thick and thin overlaying water layer

day from sediment covered with 0.5 and 5.5 cm water layers, respectively.

The relationship between sediment contamination level and the volatilization rate was explored by conducting experiments using sediment contaminated with three different concentrations of the two PCB congeners; these were 47ppm (high), 24ppm (middle) and 14ppm (low), respectively. All these sediments were spiked with PCB congeners and aged over three months before use in the experiments. The experiments were run in a manner similar to the previous studies except for the sampling procedure. Only the PCB and the water traps were sampled with time for the experiments using the lower two levels of contamination. The percentage of volatilization was calculated by adding up the amount of PCB accumulated on the traps. In this way, fewer samples were generated. The PCB recovery rates were from 95.2% to 102.3%, which indicated that the majority of volatilized PCBs were adsorbed on the florasil and sodium sulfate traps. The original data of this experiment are shown in Table A4-12 in Appendix 10. Results from these experiments and the ones obtained for the higher contaminated sediment are presented in Figure 4-8. These results suggest that the DCB volatilization rate correlated with contamination level, that is, the higher contamination level the faster the volatilization rate. As can be seen from this figure, the rate of volatilization was highest for sediment contaminated with 47ppm DCB, with the slowest rate obtained from the sediment contaminated with 14ppm DCB. The volatilization rate of HCB was very low with less than 2% loss occurring during the 80-day course of the experiment. Its rate was significantly slower than that of DCB.

### **4.3 Volatilization of PCB from Silica Sand and Bentonite Clay**

#### 4.3.1 Introduction

To study how fast PCBs volatilize from inorganic materials, the third set of experiments was performed using aged contaminated silica sand and bentonite clay that contained mostly inorganic components (see Table 3-2). The clean silica sand and bentonite clay were spiked and aged with the two congeners following a procedure similar to that used for the sediments. The experimental sampling schedules were different than those of the sediment experiments since faster volatilization was expected from the sand and clay. In this set of experiments, contaminated silica sand and bentonite clay were covered with a thin water layer (0.5 cm).

#### 4.3.2 Results and Discussion

The initial amounts of PCB in the glass column were determined by extracting three 2.5g of silica sand and three 2g of bentonite clay. The DCB and HCB masses were 49.33 $\mu$ g and 52.02 $\mu$ g in silica sand and 20.60 $\mu$ g and 20.80 $\mu$ g in bentonite clay. The moisture contents for these two substrates were 36.9% and 71.3%, respectively. Hence the initial DCB concentrations were about 31 $\mu$ g/g and 36 $\mu$ g/g by dry weight. It needs to be pointed out that one pump broke down during the course of the experiment for silica sand, so only five data points were generated in that experiment.

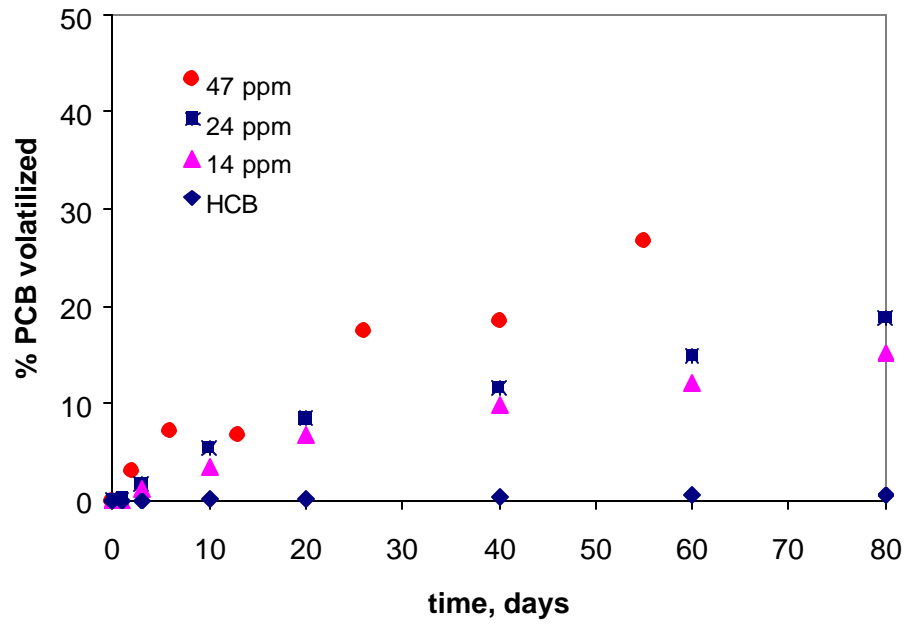
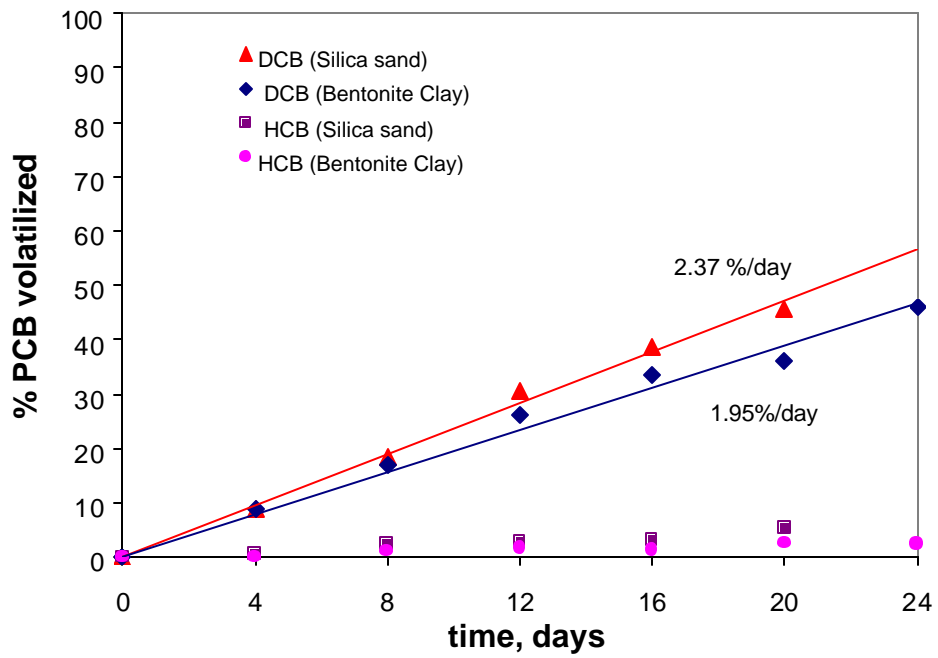


**Figure 4-8 PCB volatilization from sediments for three contamination levels**

The original data of these experiments are shown in Table A4-13 and A4-14 in Appendix 10. Data show decent PCB and surrogate recovery. Results of these experiments are plotted in Figure 4-9. Comparison of the results illustrates that the rates of DCB volatilization from silica sand and clay were very close. They both were much faster than from the sediment. Approximately 50% of the DCB originally loaded was released from the substrates. HCB showed increased volatilization as compared to the rates obtained for the sediments. The overall volatilization of HCB was about 6% keeping it much lower than that of the DCB.

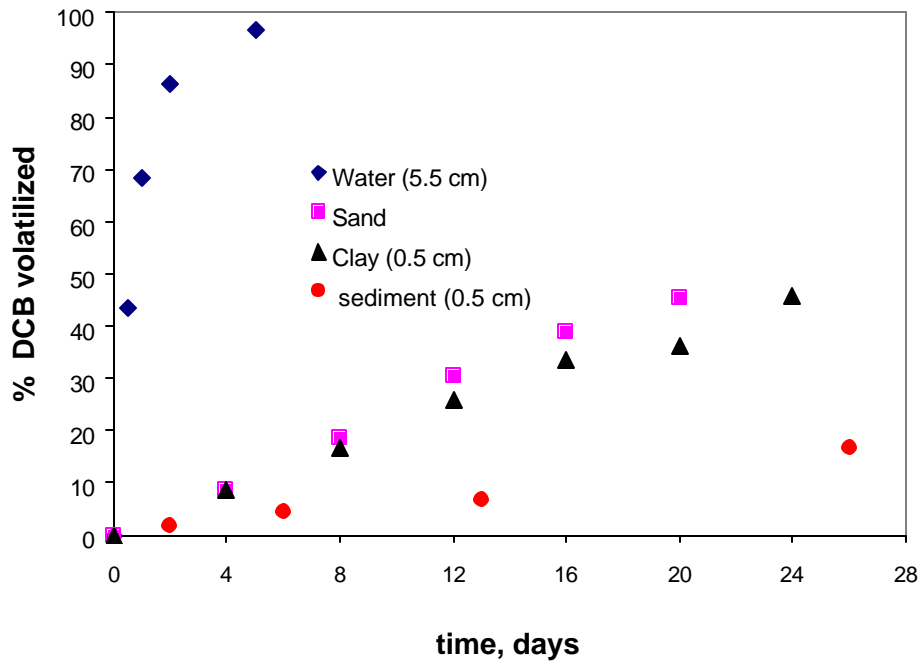
Like what has been observed from the results with the sediment, the data of the experiments using silica sand and bentonite clay indicate a linear volatilization rate. DCB volatilized with a rate of 2.37% and 1.95% per day from the sand and clay respectively. The silica sand and bentonite clay used in this research had similar characteristics in terms of density, porosity and heavy metal contents (see Table 3-2). But silica sand contained only 0.1% organic matter that was much less than that of bentonite clay (0.7).

Figure 4-10 summarizes the experimental results of DCB volatilization rates from different substrates studied: water, sediment, sand and clay. The data reveal that DCB volatilized faster from water (Qi et al., 2000) than it did from either silica sand or bentonite clay and was slowest from the natural sediment. Flux of DCB volatilization from these substrates was also calculated based on the linear volatilization fraction. The results are shown in Table 4-1.



**Figure 4-9 Volatilization of PCB from contaminated silica sand and bentonite clay**





**Figure 4-10 Comparison of DCB volatilization**

**Table 4-1 Fluxes of PCB volatilization from Sediment, sand and clay**

	% of volatilization	Flux (mg/m <sup>2</sup> -day)
Sediment (0.5 cm)	0.55	0.18
Sediment (5.5 cm)	0.35	0.11
Sand (0.5 cm)	2.37	0.64
Clay (0.5 cm)	1.95	0.22

## 4.4 Volatilization of Solid PCB from Glass Surface

### 4.4.1 Introduction

After conducting the experiments of PCB volatilization from different substrates, it was thought to be very interesting to determine how fast PCB would volatilize from the glass surface if there was no substrates present. The fourth set of experiments was carried out without using any substrates to fulfill this purpose. Several scenarios were investigated: volatilization of solid PCB from treated glass surfaces when there was a thin (0.5 cm) overlaying water layer and when there was no overlaying water layer present; volatilization of solid PCB from untreated glass surfaces when there was a thin (0.5 cm) overlaying water layer and when no water cover was present; volatilization of solid PCBs from treated glass surfaces when the surfaces were covered by different water levels of 0.5 cm, 4.1 cm and 8.3 cm corresponding to 10ml, 75ml and 150 ml water, respectively.

The difference between treated and untreated glass surfaces was limited to whether the glass surfaces were silylated or not. As mentioned in Chapter 3, all the previous experiments used the silylated glass column to prevent PCB adsorption to the glass surface thus interfering with the volatilization process. The silylation procedure is described in details in Appendix 2.

The experimental apparatus and the procedures followed were similar to those of the previous experiments. PCBs were dissolved in acetone and the solution was loaded into the glass column (20  $\mu$ g). Subsequently, the acetone was permitted to evaporate and the glass surfaces

were coated with a layer of solid PCB. All the experiments were performed in duplicate sets. At each sampling time, the PCB trap and moisture trap were removed and vacated. The contents were extracted and analyzed. Then traps were refilled with fresh florasil and sodium sulfate and the experiment continued. The quantity of PCB volatilized was determined by summing the amounts of PCB accumulated on the traps.

#### 4.4.2 Results and Discussion

The original data of these experiments are summarized in Table A4-15 in Appendix 10. Shown in Figure 4-11 are the results of solid PCB volatilization from treated glass surface, when the PCB was covered with or without a thin water layer (0.5cm). Two important findings are observed from the experimental results: one is that PCB was released very rapidly from glass surfaces; even HCB exhibited significant volatilization. Another interesting finding from these experiments is that solid PCB volatilized surprisingly faster from the surfaces covered by a thin water layer than from the surfaces that not covered by a thin water layer. The results suggest that moisture favored the PCB transport, in other words, the process of volatilization was enhanced by the evaporation of water.

Figures 4-12 and 4-13 summarize the results of DCB and HCB volatilization from treated and untreated glass surface, respectively. What these results show is that the treatment of glass surfaces did have impact on the volatilization process and thus yield different volatilization rates. Apparently, PCB volatilized faster from treated glass surface than from untreated glass surface

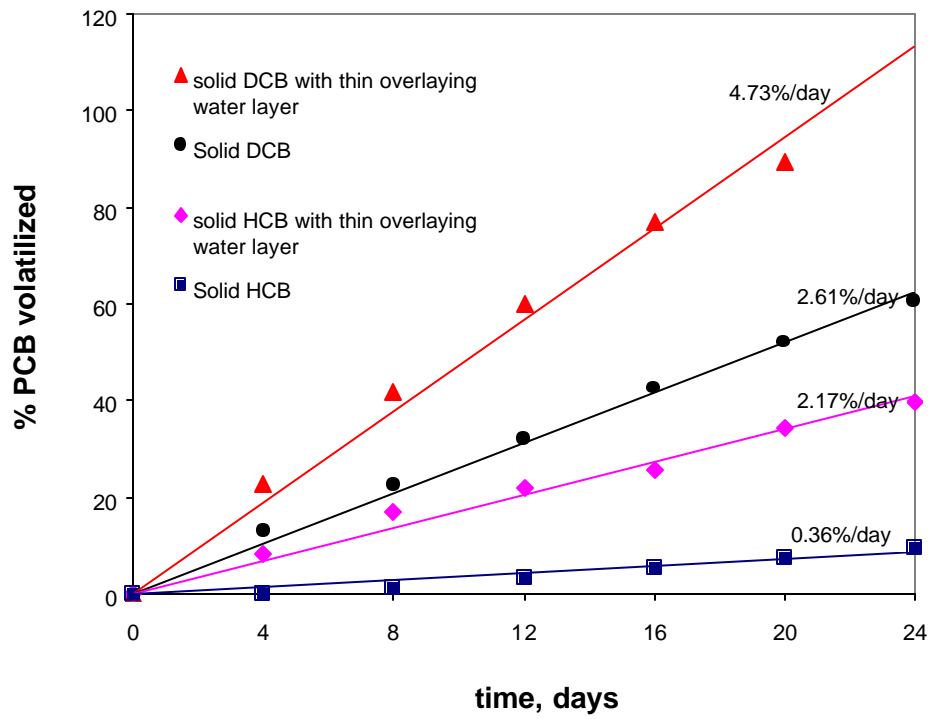


**Figure 4-11** Volatilization of solid PCB from treated glass surfaces

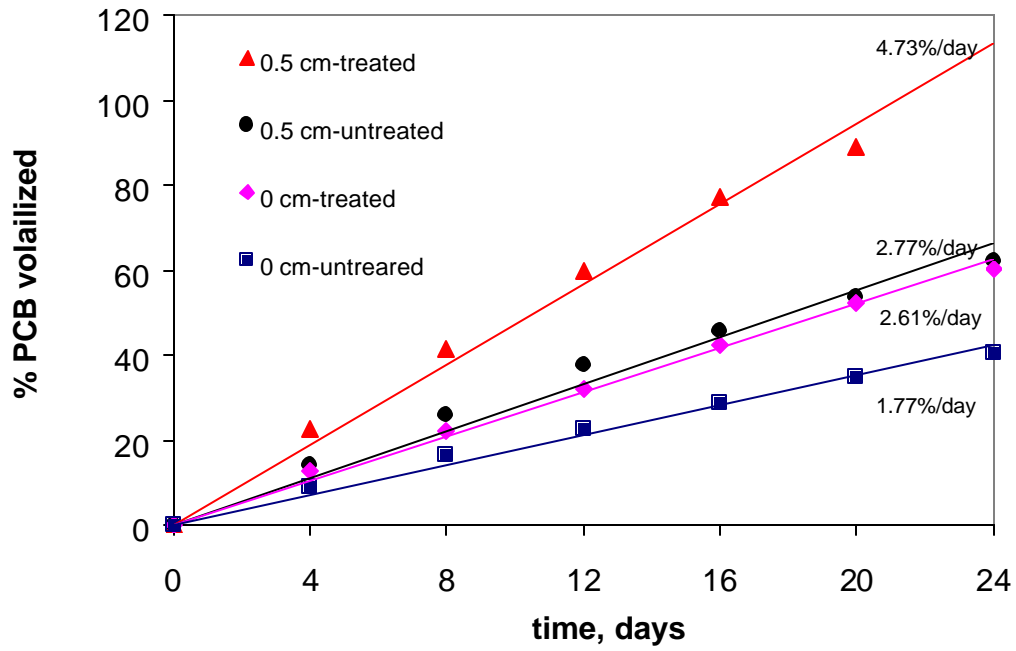


**Figure 4-12** Comparison of DCB volatilization from treated and untreated glass surface

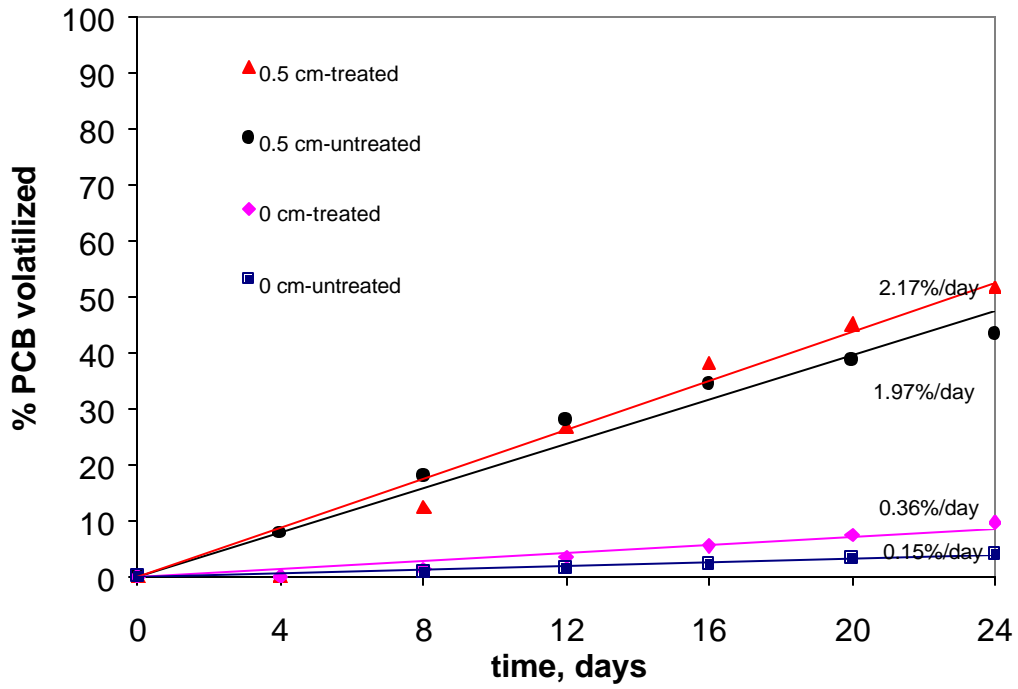


**Figure 4-13** Comparison of HCB volatilization from treated and untreated glass surface

for both cases regardless of whether the solid PCB was covered with or without a thin water layer. The discrepancy caused by the treatment of the glass surface was more significant for DCB than for HCB. This observation proves that silylation helped preventing PCB adsorption to the glass surface. To put it in another way, if the glass surface was not silylated, it would retard the volatilization process. The results also show that solid PCB volatilized faster from the surfaces covered by a thin water layer than from the surfaces that not covered by any water layer.

Figures 4-14 and 4-15 show the effect of water levels above the solid PCB on the volatilization rate from the treated glass surfaces. As expected, PCB transported faster from glass surfaces covered with lower water layer: fastest from the surface covered with 0.5 cm depth water, and slowest from the surface covered with 8.3 cm depth water.

The results of PCB volatilization from glass surface appeared linear. The volatilization rates were determined by the regression and they are shown on the graphics. The fluxes of PCB volatilization from glass surface were also calculated based on these fractions. They are summarized in Table 4-2.

#### **4.5 Conclusions**

In this fundamental study, volatilization of PCB was investigated using a simple microcosm of sediment, water and air that allows for (pseudo) one-dimensional transport of PCBs. Several scenarios were investigated: volatilization of DCB from water; volatilization of

PCB from aged contaminated sediments with no overlaying water layer; volatilization when the sediment was covered with a thin or thick water layer; volatilization of PCBs from sediments at three contamination levels; volatilization of PCBs from aged contaminated silica sand or bentonite clay; and volatilization of solid PCBs from treated and untreated glass surfaces. For all the scenarios investigated, experimental results showed significant volatilization of DCB. Important findings were:

- Volatilization of DCB from water was very fast, the higher the water level, the slower the volatilization rate;
- The rate of volatilization decreased when the sediment lost moisture;
- When sediment was covered with an overlaying water layer, either by a thin layer or thick layer, the rate of volatilization was slower than when the saturated sediment was not covered with water;
- The thicker the water layer, the slower the rate of volatilization;
- The rates of PCB volatilization from contaminated silica sand and bentonite clay were very similar and faster than the rates observed for natural sediments but still slower than the rate of volatilization from water;
- The higher the contamination level, the faster the rate of the volatilization;
- Volatilization of solid PCBs from treated glass surfaces was surprisingly fast. More interestingly, PCBs volatilized faster from surfaces covered with a thin water layer than when no water was present;
- PCB was released faster from treated glass surfaces than from untreated glass surfaces;



- PCB volatilized more quickly from glass surfaces that covered with a thinner water layer than when covered with a thicker water layer;
- In all cases studied, the volatilization of HCB was dramatically lower than that of DCB.

**Table 4-2** Fluxes of PCB volatilization from glass surface

	% of volatilization	Flux (mg/m <sup>2</sup> -day)
Solid DCB (0.5 cm)	4.73	0.52
Solid DCB (0 cm)	2.61	0.29
Solid DCB (0.5 cm-untreated)	2.77	0.3
Solid DCB (0 cm-untreated)	1.77	0.19
Solid DCB (4.1 cm)	3.22	0.35
Solid DCB (8.3 cm)	2.43	0.23
Solid HCB (0.5 cm)	2.17	0.24
Solid HCB (0 cm)	0.36	0.04
Solid HCB (0.5 cm-untreated)	1.97	0.22
Solid HCB (0 cm-untreated)	0.15	0.02
Solid HCB (4.1 cm)	1.71	0.19
Solid HCB (8.3 cm)	1.62	0.18

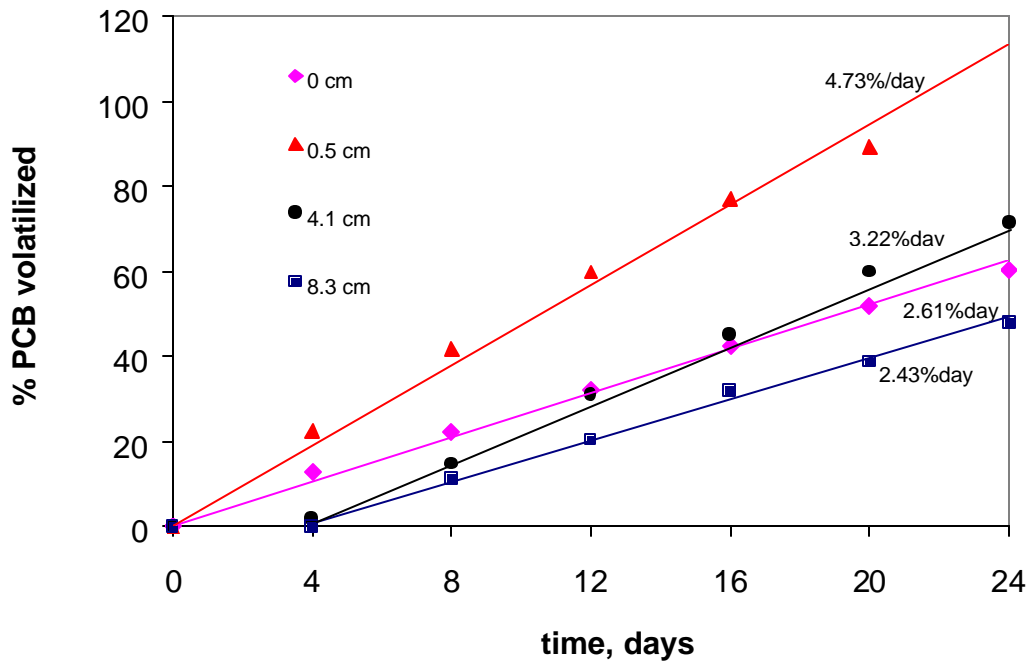
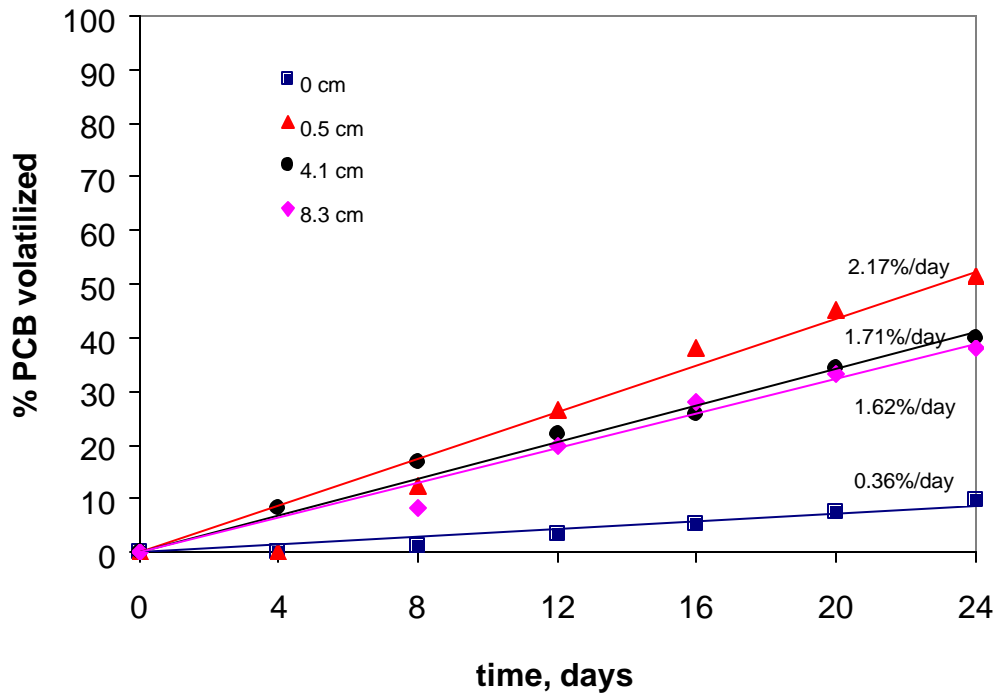


Figure 4-14 DCB volatilization from treated glass surface with different overlaying water levels



**Figure 4-15** HCB volatilization from treated glass surface with different overlying water layers

## Chapter 5 Adsorption Studies

### 5.1 Introduction

Since the manufacture and application of PCBs have been restricted due to stricter environmental regulation, PCB input to natural waters was reduced tremendously. PCB aqueous concentration may be increasingly affected by water-sediment interaction. As a first step in understanding of sediments contaminated with PCBs, it is necessary to quantify the amounts of PCBs that are adsorbed and desorbed by sediments under abiotic equilibrium conditions with the surrounding aqueous phase. A number of literature studies focused on characterizing PCB adsorption to soils and sediments (Haque et al., 1974; Hiraizumi et al., 1979; Steen et al., 1978; Lee et al., 1979; Haque & Schmedding, 1976; Horzempa et al., 1983). Several factors were shown to influence the magnitude of adsorption including sediment surface area, sediment organic carbon content and the degree of chlorination. Results compiled from adsorption/desorption isotherm data are used in models for determining diffusion and mass transfer coefficients, as well as, predicting PCB adsorption/desorption rates in sediments. In turn, knowledge of these mass transfer parameters is necessary in developing strategies for treating contaminated sediments.

An adsorption isotherm is defined as an equilibrium relationship, at a constant temperature, between the mass of an adsorbate on an adsorbent,  $q_s$ , and its concentration in solution,  $C_e$ . Equations commonly used to describe this equilibrium relationship for single-solute adsorption are the Freundlich and the Langmuir equations.

The Freundlich equation, which is a semi-empirical relationship, has been often found to accurately describe adsorption data over a wide concentration range. One form of this equation is:

$$q_e = K C_e^{1/n} \quad (5-1)$$

where K and n are experimental constants.

This equation can also be linearized as follows:

$$\log q_e = \log K + 1/n \log C_e \quad (5-2)$$

K and 1/n are constants for a given system; 1/n is unitless, and the units of K depend on the units of  $q_e$  and  $C_e$ . The parameter K is related primarily to the capacity of the adsorbent for the adsorbate, and 1/n is a function of the strength of adsorption. For fixed values of  $C_e$  and 1/n, the smaller the value of K, the smaller is the capacity,  $q_e$ . For fixed values of  $C_e$  and K, the smaller the value of 1/n, the stronger is the adsorption bond.

The Langmuir equation has the following form:

$$q_e = q_{\max} b C_e / (1 + b C_e) \quad (5-3)$$

where b and  $q_{\max}$  are constants.

In general, the Langmuir equation does not describe the adsorption data as accurately as the Freundlich equation.

In this chapter, studies of DCB adsorption to sediment, silica sand and bentonite clay will be described and discussed. Adsorption isotherms were constructed based on the data compiled from the adsorption experiments. Parameters of the isotherms were determined as well. They will be applied to the mathematical model of the volatilization process. Again, the solubility of HCB in water (less than 1  $\mu\text{g/l}$ ) at room temperature was below the detection limit of both GC/ECD and LSC; hence adsorption isotherms for HCB were not constructed.

## **5.2 Materials and Methods**

Adsorption experiments were performed using uncontaminated dry sediment, silica sand, bentonite clay and natural water. Substrates main physical and chemical characteristics are presented in Table 3-2. Amber brown glass bottles with a volume of 120 ml were sterilized and used in the experiments. Each bottle received 4 g of dry uncontaminated substrates, 2 ml of biocide, and 120 ml natural water – taking care to keep the headspace to a minimum. DCB was dissolved in acetone and introduced by injection. Experimental design is summarized in Table 5-1. The bottles were sealed and then equilibrated on a rotating tumbler. Samples were taken on monthly basis. Aqueous samples were filtered through 1  $\mu\text{m}$  Teflon filter paper. The filtrates were extracted and analyzed on the GC-ECD. Equilibrium was assumed achieved when the variation between two consecutive samples was less than 10%. All samples whose aqueous PCBs concentrations were above 80% of their solubility were discarded because either the system had not reached equilibrium or the system was oversaturated.

**Table 5-1** Experimental design for adsorption studies

Contents	PCB quantity introduced in bottles (× solubility)
Sediment + natural water + DCB + biocide	20×, 60×, 100×, 150×, 200×, 250×, 300×
Silica sand + natural water + DCB + biocide	10×, 20×, 60×, 100×, 150×, 200×
Bentonite clay +natural water +DCB + biocide	10×, 20×, 60×, 100×, 150×, 200×

It should be noted that the DCB concentration in the sediment phase was estimated indirectly by subtracting the measured final DCB concentration in the aqueous phase from the initial added DCB concentration. This difference yielded the amount of DCB adsorbed on the sediment ( $DCB_{\text{substrate}} = DCB_{\text{initial}} - DCB_{\text{aqueous}}$ ). This approach is commonly used in this field ((Horzempa et al., 1983; Larsson, 1983).

### 5.3 Results and Discussion

Equilibrium data for the adsorption of DCB onto the sediment were measured after an equilibration period of three-month. All aqueous phase concentrations of DCB that exceeded 80% of solubility were rejected, thus insuring that all the DCB was either in solution or adsorbed onto the sediment. Data collected at equilibrium conditions for the three substrates are summarized in Table A5-1 and Table A5-2 in Appendix 11.

The adsorption isotherms of DCB on marine sediment, silica sand and bentonite clay were constructed, which are shown in Figure 5-1, 5-2 and 5-3, respectively. Different isotherm

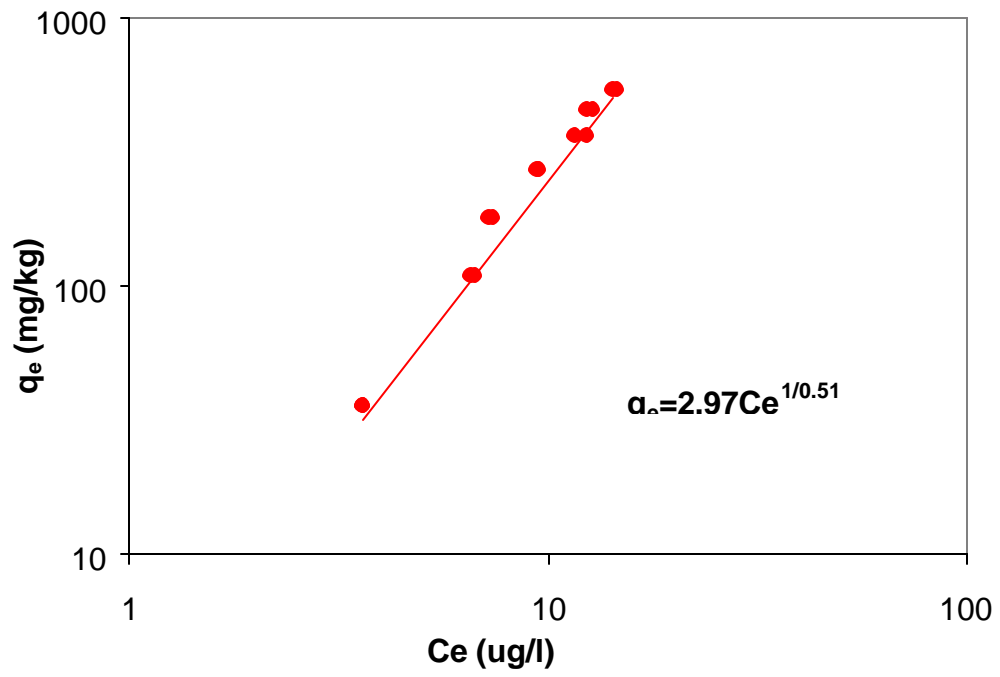


**Figure 5-1** DCB adsorption isotherm, Marine Sediment



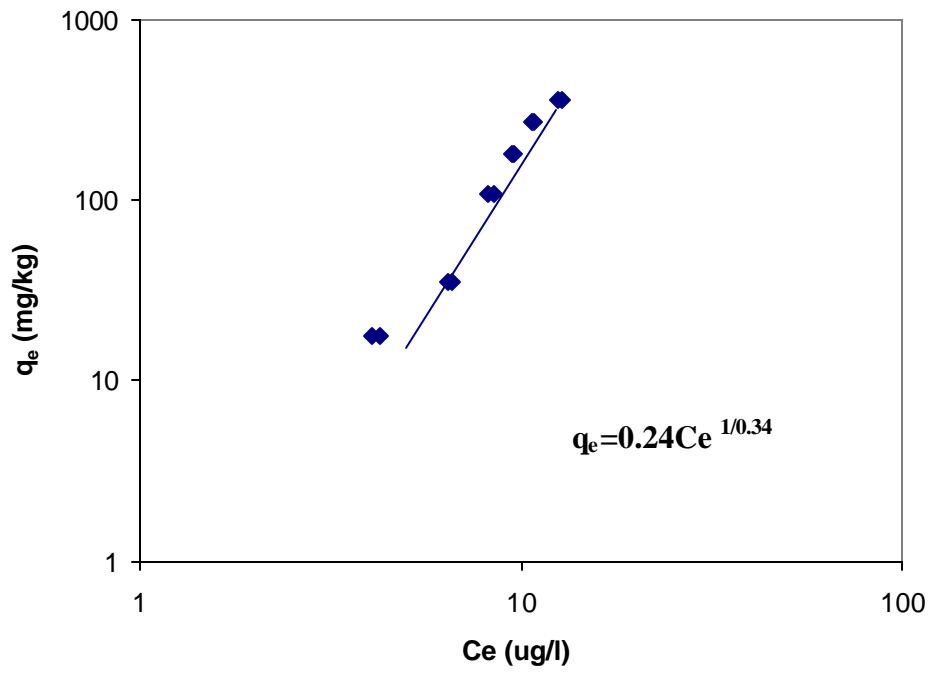


**Figure 5-2** DCB adsorption isotherm, Silica Sand

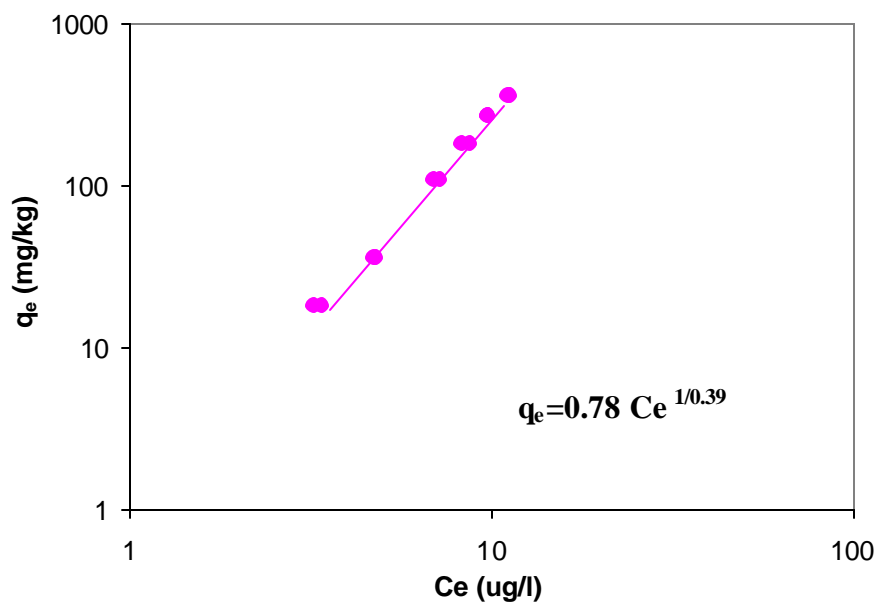


**Figure 5-3** DCB adsorption isotherm, Bentonite Clay

types including Langmuir, Freundlich and linear were used to fit the data. The best fits for the data were Freundlich isotherms which are typically described in the form of  $q_e = K C_e^{1/n}$ . Adsorption isotherms were constructed from these measurements that relate the solid phase concentrations that are in equilibrium with the measured aqueous phase measurements. The data were best linearized using the Freundlich isotherm equation.

The best-fit Freundlich equations are shown as following Equation 5-4, 5-5, 5-6. The values of K and n for the isotherms are summarized in Table 5-2.

$$q_e = 2.97 C_e^{1/0.51} \quad (5-4)$$

$$q_e = 0.24 C_e^{1/0.34} \quad (5-5)$$

$$q_e = 0.78 C_e^{1/0.39} \quad (5-6)$$

where  $q_e$  and  $C_e$  are the concentrations of PCB in the sediment particle and in the water, respectively.

**Table 5-2** K and n values for DCB adsorption isotherms

	K	n
sediment	2.97	0.51
sand	0.24	0.34
clay	0.78	0.39

Figure 5-4 summarizes the DCB adsorption isotherms for the three different substrates. As it can be observed, the DCB adsorption isotherm for the sediment is the highest followed by that for bentonite clay and is lowest for the silica sand. As mentioned earlier, the parameter K is

related mainly to the capacity of the adsorbent for the adsorbate, and  $1/n$  is a function of the strength of adsorption. In this case, sediment has the largest adsorption capacity, while the silica sand has the lowest. Sediment also has a stronger strength of adsorption bond than the clay and sand. It is mainly because sediment has higher organic content and higher heavy metal content (see Table 3-2).

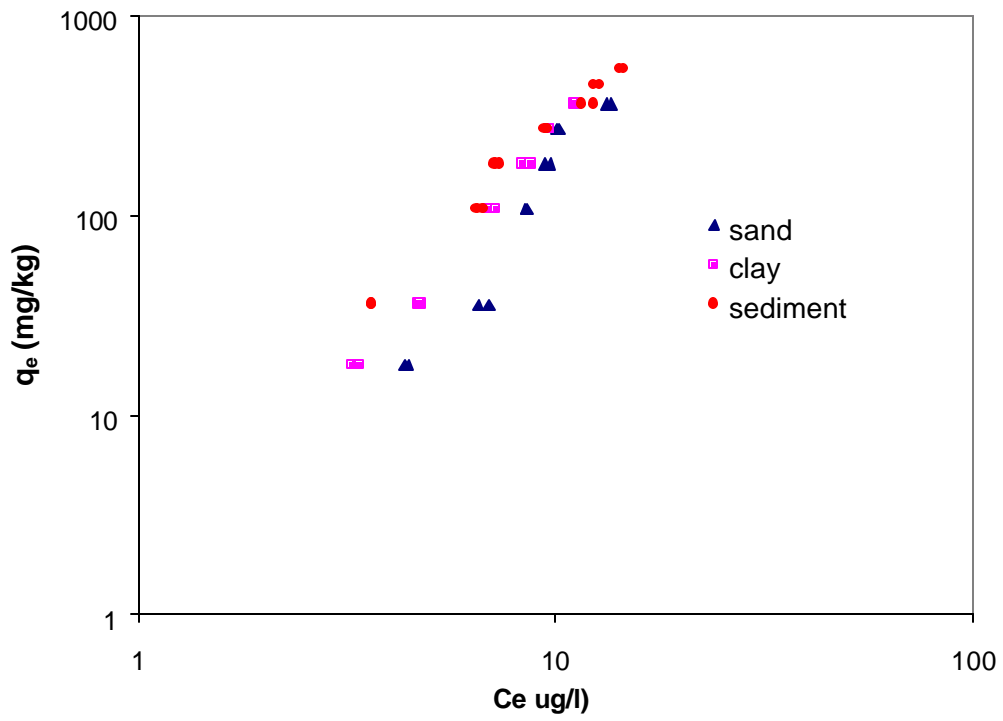


Figure 5-4 DCB adsorption isotherms

## Chapter 6 Parameter Estimation and Model Simulation

### 6.1 Introduction

A fundamental mathematical model of PCB transport in a sediment-water-air system was developed. Some of the parameters that appear in the mathematical model of the volatilization of PCBs from sediment are unknown and need to be estimated using experimental results specifically designed for this purpose and nonlinear parameter estimation techniques, while others are physical constants or compound properties that can be measured or taken from published results. The values of Henry's constant for DCB used in this research were obtained from Mackey *et al.*, 1992. The parameters that can be measured directly or indirectly in the system are: porosity of the sediments, radius and density of the sediment particle, and fluid phase pore velocity in the sediments, although this last variable will be neglected in this study. The parameters that need to be estimated using experimental results and nonlinear parameter estimation techniques are the following:  $D_w$ , hydrodynamic dispersion coefficient in the water phase,  $D_s$ , hydrodynamic dispersion coefficient in the sediments,  $k_{fg}$ , gas phase film mass transfer coefficient,  $k_f$ , external-film mass transfer coefficient in the sediments, and  $D_p$ , diffusion coefficient in the sediment particle. Experimental results from the system previously presented were used to calibrate and validate the mathematical model for the volatilization of PCBs. Two sets of experiments were conducted with the objective of performing a separate estimation of the parameters corresponding to the volatilization of PCBs from water, and the parameters corresponding to the volatilization of PCBs from sediments.

The expression for the equilibrium isotherm for DCB was obtained by conducting a set of experiments to study the adsorption of DCB to sediment. Uncontaminated dry sediment and natural water were used as explained in Chapter 5. The expression is:  $q_e = 2.97 C_e^{1/0.51}$ , where  $q_e$  and  $C_e$  is the concentration of PCB in the sediment particle and in the water at the solid-water interface, respectively.

## 6.2 Parameter Estimations

### 6.2.1 Volatilization of DCB from water

The unknown parameters corresponding to the volatilization of DCB from the water phase that were estimated included:  $D_w$ , hydrodynamic dispersion coefficient in the water phase and  $k_{fg}$ , gas phase film mass transfer coefficient. A study was conducted to analyze the rate of volatilization of DCB from water with time. Three different water depths (2.8, 5.5 and 8.3 cm corresponding to 50, 100 and 150 ml) were used in order to obtain enough data for the parameter estimation. The twelve columns were loaded with DCB dissolved in water and were run for specific amounts of time. For each water level duplicate experiments were conducted, some with regular DCB and some with  $^{14}\text{C}$ -labeled DCB. The columns were loaded with 1.29 and 1.073 g of DCB in the first experiment; 2.022 and 3.674  $\mu\text{g}$  of DCB in the second one; and 2.807 and 3.225 g of DCB in the third experiment.

The parameters  $D_w$ , hydrodynamic dispersion coefficient in the water phase and  $k_{fg}$ , gas phase film mass transfer coefficient were estimated using the data corresponding to 2.8 cm and

8.3 cm, while the other set of data, 5.5 cm, was used to test the calibrated model. Figure 6-1 shows the amount of PCB remaining in the water with time for the three cases. Experimental and model values are presented, model fittings for the 2.8 and 8.3 cm sets and model predictions for the 5.5 cm sets. Error bars correspond to the standard deviation of the data. It can be observed that the model fits the experimental data reasonably well.

### 6.2.2 Volatilization of DCB from sediment

The parameters corresponding to the volatilization of PCBs from sediment were estimated:  $D_s$ , hydrodynamic dispersion coefficient in the sediment,  $k_f$ , external-film mass transfer coefficient in the sediment, and  $D_p$ , diffusion coefficient in the sediment particle. Experimental results of the PCB volatilization from sediment for three contamination levels were used to estimate the unknown parameters. The parameters were estimated using the experimental data corresponding to 47ppm and 24ppm, while the other set of data, 14ppm was used to test the calibrated model. Figure 6-2 shows the experimental results and the fitted values of the amount of DCB remaining in the sediment with time. Experimental and model values are presented along with the model fit for the 47ppm and 24ppm sets and model predictions for the 14ppm set. Estimates of the parameters of the model for diffusion in water ( $D_w$  and  $k_{fg}$ ) were previously obtained and were assumed known here. The values of all the estimated parameters and other values used in the model are summarized in Table 6-1. The initial conditions for three sets of experiments are also presented in Table 6-1.



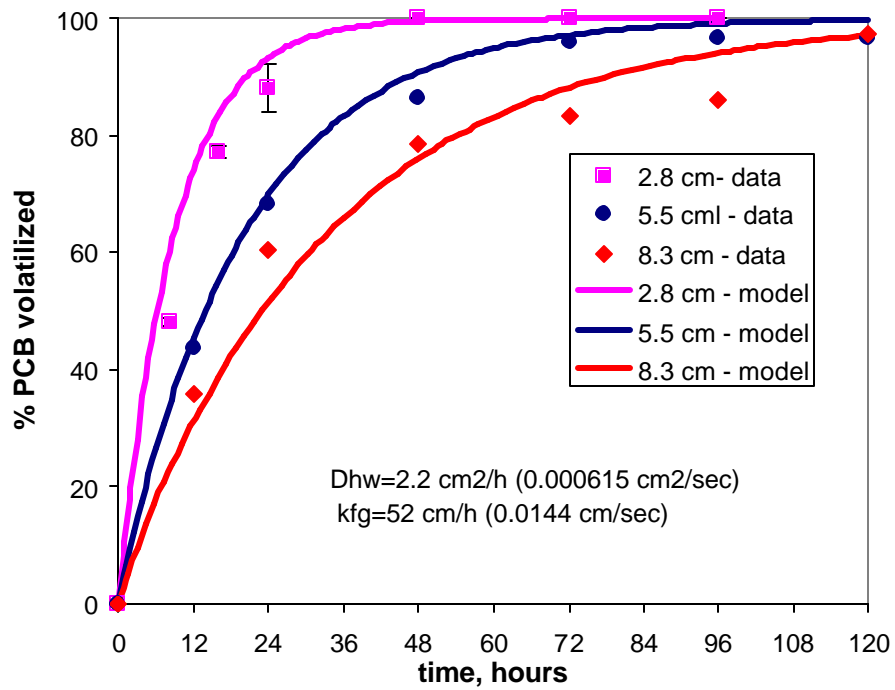


**Figure 6-1** Parameter estimation and model simulation for DCB volatilization from water

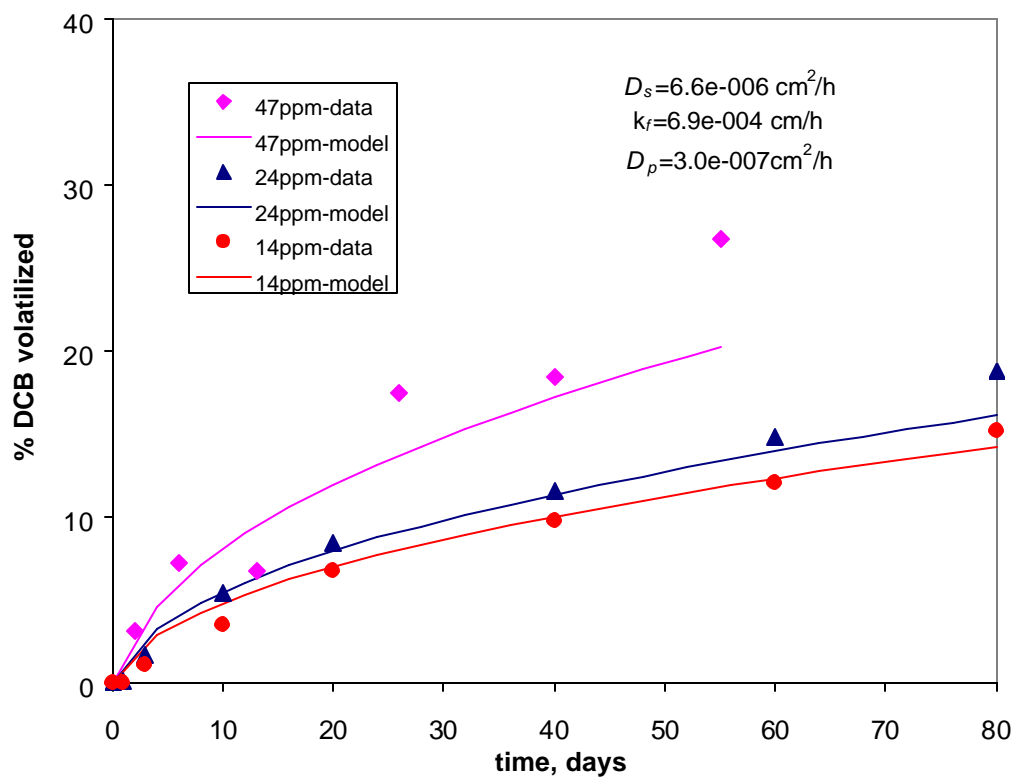


**Figure 6-2** Parameter estimation and model simulation for DCB volatilization from sediment contaminated at three different levels

In order to determine the most critical dynamic parameters in the estimation process a sensitivity analysis of the model was performed. The impact of each parameter was measured as the percentile variation of SSE when each parameter is modified 10% while keeping the others constant. The results of this study are presented in Table 1 as  $\%SSE$ . The most influential parameters are the ones with the highest impact values, in this case, the gas phase film mass transfer coefficient  $k_{fg}$  and PCB dispersion coefficient in sediment  $D_s$ . The low values of  $\%SSE$  for the intraparticle diffusion coefficient  $D_p$ , PCB dispersion coefficient in water  $D_w$  and sediment external film mass transfer coefficient  $k_f$  indicate that the model is not very sensitive to variations of these parameters. This analysis indicates which parameters should be more accurately evaluated. These results have also a physical interpretation: they indicate that the mass transfer of PCB from the sediments is limited by the dispersion of PCB in sediment, not by diffusion inside the particle nor by the resistance of the liquid film that covers the sediment particle, and that the volatilization of DCB from the water is limited by transport to the gas phase.

## 6.3 Model Simulations

### 6.3.1 Simulation of the effect of sediment depth on PCB volatilization

Using the model parameters estimated from the experimental data, the mathematical model was solved to simulate the effect of the depth of sediment on the rate of volatilization of PCBs. In the first set of runs, the sediment depth was varied from 0.01 cm to 0.05 cm, while the initial concentration of DCB in the sediments,  $C_0$ , was assumed to be  $1.15 \times 10^{-2}$  mg/g of

**Table 6-1 Estimated parameter values and known model variables**

Estimated parameter values			Known model values	
Name and symbol	Estimated Value	$\Delta$ SSE		
PCB Dispersion coeff in water, $D_w$	2.2 cm <sup>2</sup> /h	7.74	Column cross sectional area, $A$	18.18 cm <sup>2</sup>
Gas phase film mass transfer coeff, $k_{fg}$	52.0 cm/h	25.46	DCB Henry's constant, $H$	0.00687 (mg/l) <sub>gas</sub> /(mg/l) <sub>water</sub>
PCB Dispersion coeff in sediment, $D_s$	6.6 10 <sup>-6</sup> cm <sup>2</sup> /h	25.06	Porosity of the sediments, $e$	0.45
Intraparticle diffusion coeff, $D_p$	3.0 10 <sup>-7</sup> cm <sup>2</sup> /h	0	Sediments solid phase density, $\rho$	2300 mg/cm <sup>3</sup>
Sediment external-film mass transfer coeff, $k_f$	6.9 10 <sup>-4</sup> cm/h	0.67	Radius of the sediment particle, $R_p$	0.005 cm
<b>Initial Values</b>				
DCB volatilization (in itially there was no DCB in the water above the sediments)				
Initial conc. in sediments (dry weight), $q_0$		Sediment height, $h_s$		Initial amount
47ppm		0.11 cm		59 $\mu$ g
24ppm		0.22 cm		63 $\mu$ g
14ppm		0.22 cm		35 $\mu$ g

Note1: The water velocity in the sediments was assumed to be null for all the experiments.

Note2: Being SSE the sum of squared errors for each separate parameter estimation (volatilization from water only and volatilization from sediments),  $\%SSE = (SSE_j - SSE_0) / SSE_0 \times 100$ , where  $SSE_0$  corresponds to the estimated parameters and  $SSE_j$  is obtained when parameter  $j$  is increased by 10%.

sediment. The overlying water depth,  $h_w$ , was set at 1.0 cm. The amount of DCB volatilized to the air was calculated for a period of 20 days. The data in Figure 6-3 summarize the results of the simulation. The fraction of DCB that volatilized during the first 20 days decreases sharply with sediment depth.

To quantify the volatilization of DCB, the total mass of DCB and the corresponding fraction of DCB transported to the air were calculated after simulated runs of 20, 40 and 80 days for different values of sediment depth. This was done while keeping the overlying water cover constant at 1.0 cm. Two different conditions were investigated: constant initial concentration of DCB in the sediments (the initial amount of DCB increases when the height increases) and constant total mass of DCB (the initial concentration of PCB in the sediments decreases when the height increases). Figures 6-4 and 6-5 present the results of these simulated runs. Each figure has two plots; the plot on top shows the total amount of DCB volatilized while the other presents the same values as a fraction of the amount initially present. It can be observed that for the first case where the DCB concentration is kept constant, the mass of DCB volatilized increases with sediment height while ultimately reaching a plateau value that is insensitive to contamination depth. This observation suggests that over reasonable observation periods of 20 to 80 days, the rate of release of DCB to the air is affected by the contamination present in only the top 0.04 cm of sediment. Or in other words, volatilization of DCB takes place from the surface layers of the sediment, and after DCB is depleted from the top layers, further release is going to be very slow. For the second case where the total mass of DCB is distributed over varying depths of sediment,

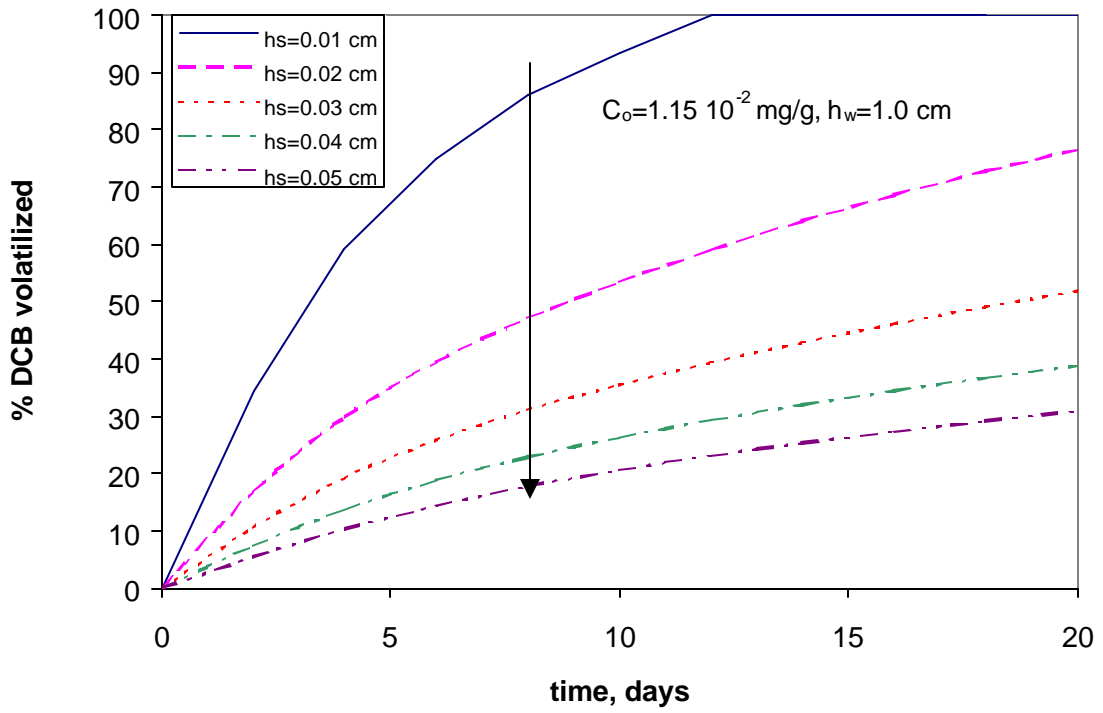


**Figure 6-3** Effect of the sediment heights on the rate of volatilization of DCB

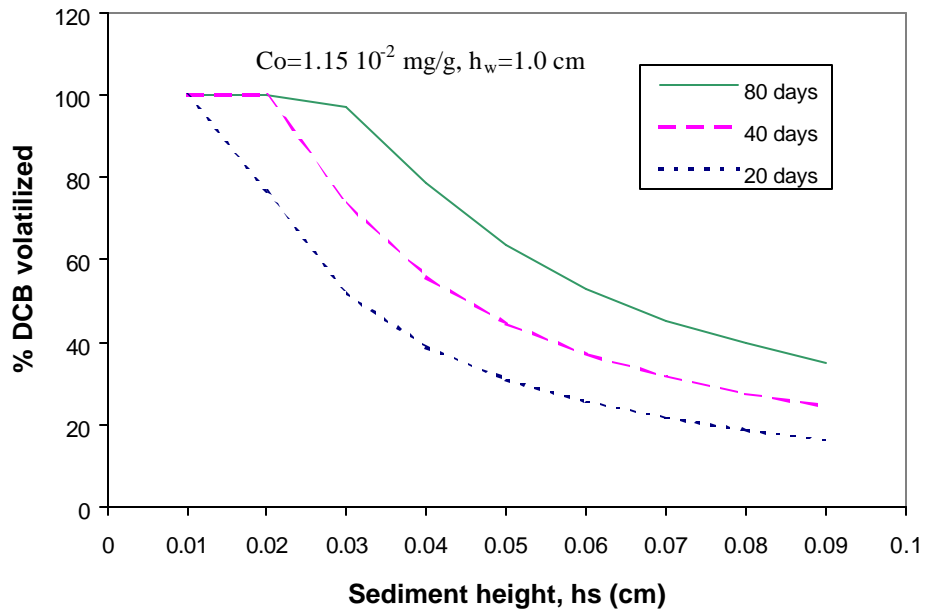
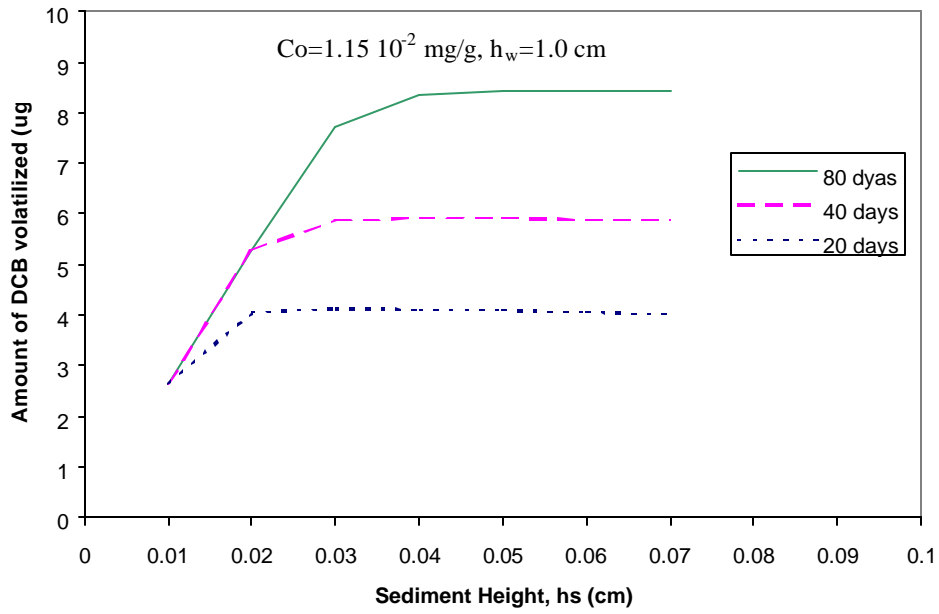


**Figure 6-4** The effect of sediment depth on DCB volatilization (constant initial concentration)

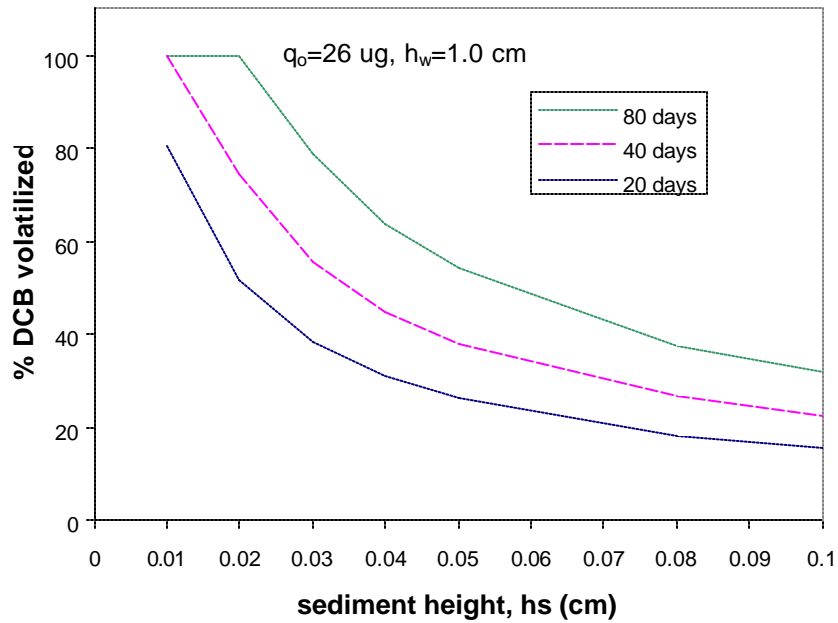
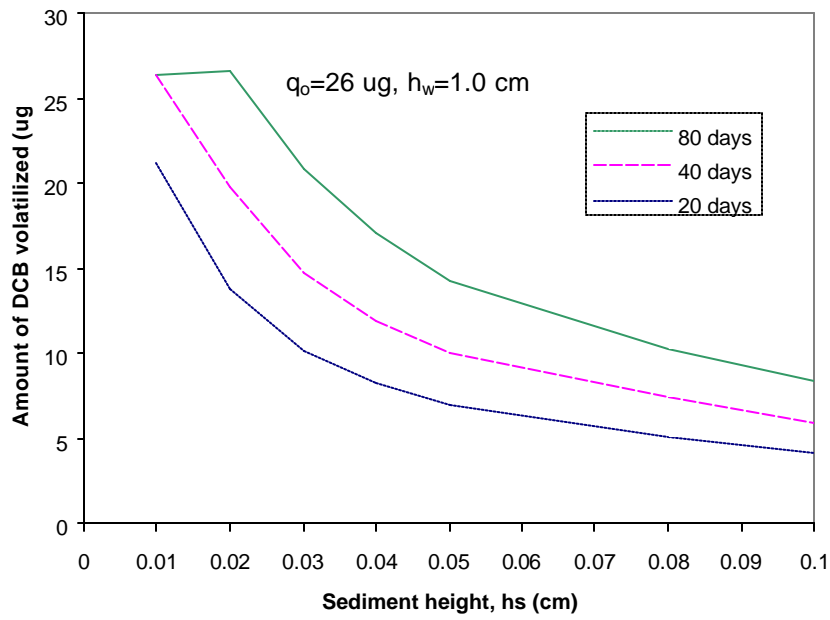


**Figure 6-5** The effect of sediment depth on DCB volatilization (constant initial amount)



Simulation results show that less DCB is volatilized as the sediment depth increases. This is true when expressed as a total mass and as a fraction. It is interesting to note, however, that the rate of decrease is a declining one suggesting contributions to the total release from the deeper layers.

### 6.3.2 Simulation of the effect of the overlaying water level

The calibrated mathematical model was used to evaluate the effect of the depth of the overlaying water cover on the rate of volatilization of DCB by varying the water levels above the sediment while maintaining the initial concentration of DCB in the sediments,  $C_0$ , and the sediment depth,  $h_s$ , constant at  $1.15 \times 10^{-2}$  mg/g of sediment and 0.1 cm, respectively. Figure 6-6 shows the results for the case of changing the water height from 1.0 cm to 80 cm when  $h_s=0.1$  cm. It was observed that the change in the rate of volatilization was negligible when the water level varied from 0.1cm to 1.0 cm. When the water level changed from 1.0 cm to 80 cm, the percentage of DCB volatilized decreased when the water height increased. But the impact was not significant when the water level varied from 1.0 cm to 20 cm. These simulations indicated that the water level above the sediment plays a more important role in the transport process when the level is high because DCB transport in the water phase becomes a limiting step after DCB leaves sediment particles.

## 6.4 Conclusions

A one-dimensional mathematical model describing the transport of DCB in a three-phase (sediment-water-air) system was developed and calibrated with the estimation of the unknown

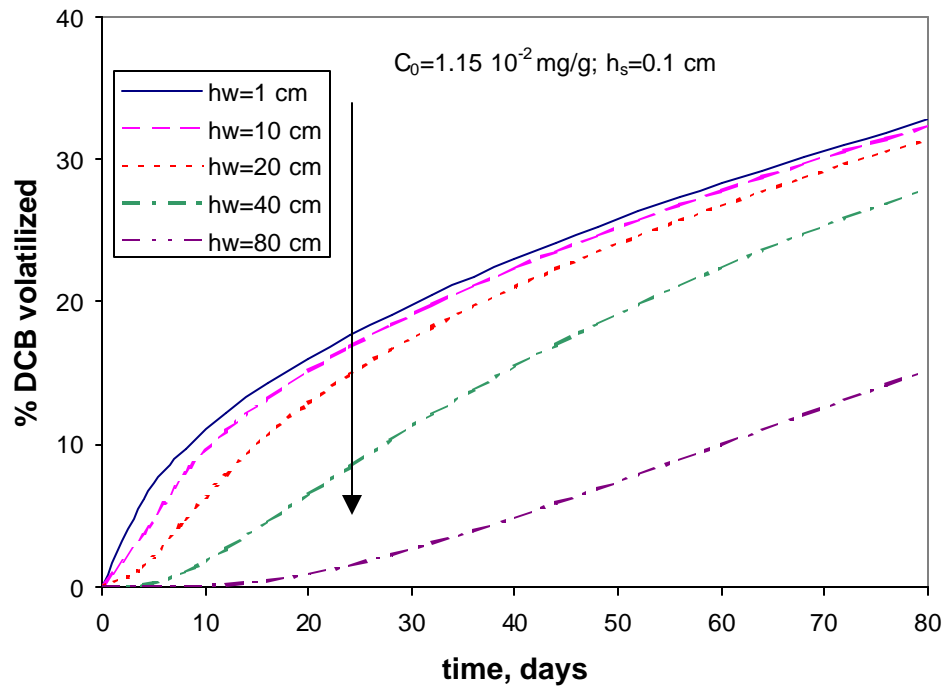


**Figure 6-6** Effect of the water height on the rate of volatilization of DCB

parameters. The parameters that play a role in the volatilization from water in the absence of sediments were estimated first, followed by the parameters for the volatilization of DCB from sediments. The reliability of the estimates is increased when the estimation is performed in two steps, as opposed to determining all the parameters at the same time, because a lower number of parameters are estimated simultaneously, and therefore, the interactions between parameters that are correlated decrease. Results from experiments conducted using a system with sediment, water and air were used in the parameter estimation. It was shown that model simulations were able to fit experimental results under these conditions.

A sensitivity analysis of the model parameters showed that the most influencing parameters are the gas phase film mass transfer coefficient and DCB dispersion coefficient in sediment. It indicates that the mass transfer of PCB from the sediments is limited by the dispersion, not by the resistance of liquid film that covers the sediment particle, and that the volatilization of DCB from the water is limited in the transport to the gas phase.

The model allowed for various parameters to be varied, such as water layer and sediment thickness, and initial concentration of DCB in the sediments and in the water, to simulate various scenarios. The effect of the depth of sediment on the rate of volatilization of DCB was studied. It was observed that for the case of constant initial concentration of DCB in the sediment, the amount of DCB volatilized first increases, and then after certain point it reaches a plateau. This suggests that more sediment with the same DCB concentration does not mean more volatilization. If the initial amount of DCB in the sediment is the same, less DCB is volatilized when the sediment height increases. The effect of water level above sediments was also

investigated. It was shown that the percentage of DCB volatilized decreases when the water height increases.

The experimental data collected on HCB revealed that the rate of volatilization of this congener is much slower than that of DCB. Consequently, a very important conclusion of this study is that DCB can define an upper limit of the rate of release of PCBs from contaminated sediments. For example, within 80 days of observation, DCB was shown released from only the upper 0.04 cm of sediment depth. It is proposed that for a more highly chlorinated congener, such as HCB, this statement is even more of a truism.

# Chapter 7 Volatilization of PCB from Lake Hartwell Sediments

## 7.1 Introduction

The rate of PCB volatilization from fully homogenized, uniformly contaminated, and naturally aged sediments was studied. In this chapter, experiments using Lake Hartwell sediments will be described and results of volatilization experiments will be presented and discussed.

The sediments and water were collected from Lake Hartwell superfund site. The Lake Hartwell area consists of 730 acres that were used for capacitor manufacturing from 1955 to 1978. The plant used various dielectric fluids in its manufacturing processes, including ones containing PCBs. Waste disposal practices at that facility included land-burial of off-specification capacitors and wastewater treatment sludge at the plant site and at six satellite disposal areas. PCBs were also discharged with plant effluent directly into Town Creek, which is a tributary of Twelve-Mile Creek. Twelve-Mile Creek is a major tributary of Lake Hartwell. Between 1955 and 1977, approximately 400,000 lbs of PCBs were discharged into Tom Creek and an unspecified amount was buried in six off-site disposal areas.

There are two parts to the project. The 3-day field study assessed the overall rate of release of PCBs under natural conditions. The bench-scale experiment determined the rate of PCB volatilization from fully homogenized, uniformly contaminated, and naturally aged field sediment.

The primary objective of the bench-scale study was to experimentally quantify the rate at which the various PCB congeners are transported from sediment uniformly contaminated with PCBs to overlying air in a controlled environment. A second objective was to assess any relationships that might exist between the rate of volatilization and the extent of chlorination of the various congeners. Results of these bench-scale experiments will also be compared with the results of the field study.

## **7.2 Materials and Methods**

### **7.2.1 Sediments tested**

All experiments were performed on two naturally occurring contaminated sediment and overlying water samples collected from the Lake Hartwell Superfund Site. One of the two samples from Lake Hartwell was collected to represent the top or “native” layer occurring at depths of between 0 and 6 inches from the surface. The second sample represents the deeper, and therefore, older contamination occurring at depths between 7 and 12 inches from the surface. The native or top layer was lighter in color than the deeper layer suggesting differences in organic content and possibly different redox conditions.

Characterization of the sediment was performed to identify the physical and chemical properties of the sediment that can impact adsorption/desorption and volatilization

characteristics. The moisture content of the sediment was determined using a modified version of American Society for Testing and Materials (ASTM).

The moisture content of the top and deep layer sediment is 47.66% and 47.92%, respectively. The sediment characterization was performed by Agvise Laboratories (North Dakota). The results are summarized in Table 1.

The results indicate that top layer sediment and deep layer sediment have very similar characteristics except for the pH and organic matter content. The pH of deeper sediment is lower than that of top layer. It is likely because the anaerobic condition in the deep layer caused dechlorination of the PCBs; therefore, the resulting hydrochloride acid causes a decrease in pH. The results from Agvise Laboratories show that the top layer sediment has a slightly higher organic matter content than the deeper layer. But the results obtained from our lab test suggest that the deep layer sediment contains a higher volatile organic matter content than that of the top layer.

### 7.2.2 Experimental setup

The experimental apparatus was the same as the one used in the fundamental studies (Refer to Chapter 3 for details). Hexane and an acetone/hexane mixture (1:1) were used to recover PCBs from glass columns, PCB and water traps, as well as from tubing connecting the system. A rotating tumbler was used to facilitate the extraction process. The appropriate concentrations of surrogate internal standards (SIS) were added to the sample prior extraction to

allow accurate measurement of target organic compounds. The SIS compounds added were PCB 14, PCB 34, PCB 112 and PCB 104. Activated copper was added to sediment samples to complex any sulfur that may be present in the samples.

**Table 7-1 Sediment Characterization**

	Top Layer (LH)	Deep Layer (LH)	
Bulk Density (g/cm <sup>3</sup> )	0.76	0.71	
Particle Density (g/cm <sup>3</sup> )	2.53	2.54	
pH ( water)	5.3	4.9	
Porosity (%)	69.8	72.2	
% organic matter (Walkley-Black)	3.0	3.7	
% Volatile organic matter <sup>1</sup>	10.6	13.8	
Particle Size Distribution (µm)	<4	13	41
	4-63	48	50
	63-2000	39	9
Heavy Metal Content (ppm)	Zinc	2.77	2.96
	Iron	269.3	250.2
	Copper	1.54	1.50
	Manganese	129.9	129.1

Note: 1. % Volatile organic matter was measured at UC lab.

Every volatilization experiment was conducted for a total period of 80 days. The content of the gas washing bottles was analyzed on day 0 and again on day 80. Sampling and analysis for the volatilized PCB was carried out on days 1, 3, 10, 20, 40, 60, and 80 in order to be consistent with the sampling schedule of the previous fundamental studies. On those days, the tubing, the florisil trap, and the moisture trap from every reactor system were removed and



extracted. The percentage of PCB volatilized was determined by dividing the amount recovered by the amount initially present.

One each of a laboratory control sample (LCS), blank spike (BS), procedural blank (PB), and matrix spikes (MS) were processed along with the sediment samples on day 0 and 80. One procedural blank (PB) was processed along with the air samples on day 3, 60 and 80.

Extracts were sent to the Battelle-Duxbury laboratory for sample cleanup and analysis. Fifty-one PCB congeners were identified and quantified using gas chromatographic/mass spectroscopic analyses.

**Table 7-2 Monitored PCB Congeners**

	PCB Congeners
Di	PCB8/5
Tri	PCB18, PCB28, PCB31, PCB33/20
Tetra	PCB41/64/71, PCB42, PCB44, PCB49, PCB52, PCB56/60, PCB66, PCB70/76, PCB74
Penta	PCB84, PCB85, PCB87/115, PCB92, PCB95, PCB97, PCB99, PCB101/90, PCB105, PCB110, PCB118
Hexa	PCB128, PCB132, PCB135/144, PCB136, PCB137, PCB138/160/163, PCB141, PCB146, PCB149, PCB151, PCB 153, PCB156, PCB158, PCB167
Hepta	PCB170/190, PCB174, PCB177
Octa	PCB180, PCB183, PCB184, PCB187/182, PCB194, PCB195
Nona	PCB203/196, PCB206, PCB209

## 7.3 Results and Discussion

### 7.3.1 Experimental Results

Table A7-1 and A7-2 in Appendix 12 summarize the mean values of the duplicate results of the volatilization experiments. The data are not corrected for surrogate recovery. The mass balance and percentage of volatilization of individual PCB congener and the total PCBs (SPCB) volatilized are calculated and shown in the last two columns in the table.

Figure 7-1 presents volatilization rates of various PCB congeners in this 80-day study. A strong correlation between degree of chlorination and volatilization rate is observed: the higher chlorinated congeners have lower volatilization rates. It is important to note that congener PCB 153 is excluded from hexachlobiphenyl, because the GC-analysis data of PCB 153 collected on the florisil trap is dramatically higher than the original content of the sediment.

The volatilization process is dependent on the organic compounds' water solubility, vapor pressure and Henry's law constant. Generally speaking, lower and ortho substituted chlorinated biphenyls have higher water solubility and Henry's law constant, thus they are more volatile. The 51 PCB congeners investigated under this project have varied properties: low to high degrees of chlorination, low to high ortho chlorine substitution, low to high air-water partitioning coefficients. All these factors affect the rate of PCB released from sediment.

Figure 7-1 also demonstrates that PCB volatilized faster from deep layer sediment than from top layer sediment. The overall volatilization rates are 2.52% and 6.54% for the upper and lower layers, respectively.

### 7.3.2 Comparison with Field Study Results

A comparison of the bench-scale experiment outputs with the results of fieldwork is shown in Table 7-3. The sediment concentration was calculated on a dry weight basis. As can be seen from Table 7-3, data from the laboratory study are very compatible with field data. The fieldwork experiment was performed over a three-day duration while the bench-scale experiments were run for eighty days. Consequently, the total flux was normalized to three days and eighty days, respectively. When the flux is normalized to PCB concentration, the results become even closer.

**Table 7-3 Comparison of Field and Laboratory Results**

	Sediment Concentration (ng/g)		Flux (ng/m <sup>2</sup> -day)		Flux Normalized to PCB Concentration	
	Field	Lab	Field	Lab	Field	Lab
Top Layer	1046	1340	652	608	0.62	0.45
Deep Layer	6106	7008	6489	8211	1.06	1.17

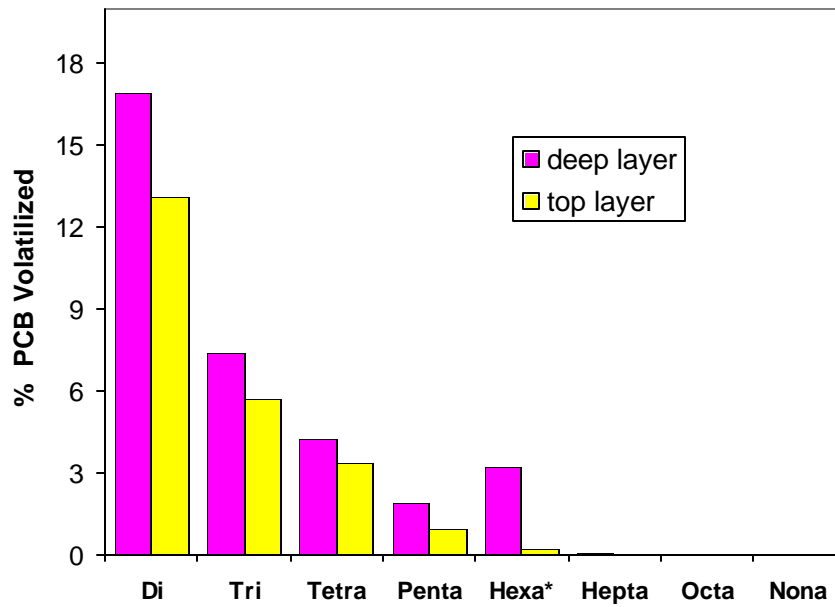


**Figure 7-1** Volatilization of PCB Congeners from Lake Hartwell Sediment in 80 days

\*: PCB 153 is excluded from Hexachlorobiphenyl

### 7.3.3 Comparison with Laboratory Fundamental Study Results

To further evaluate the experimental results, the volatilization rate of dichlorobiphenyl (DCB) observed from the Lake Hartwell sediment was compared to the rate of volatilization of DCB observed in controlled laboratory experiments. In the controlled laboratory experiments, a marine sediment (East River, NY) was spiked with DCB and aged for three months prior to use. Figure 7-2 shows the two observed results: DCB volatilized fastest from marine sediment, while the volatilization rate from the deeper sediment was faster than that observed for the upper layer sediment. This phenomenon is interpreted from the perspective of contamination level. The higher the sediment contamination level, the faster the volatilization rate. This is demonstrated in Figure 7-3. Apparently, DCB was released more rapidly from the marine sediment that the concentration of DCB was the highest. Figure 7-4 suggests a relationship between the volatilization rate of DCB and the sediment organic matter content. The data suggest that the volatilization rate of DCB increases as the sediment organic matter content increases.

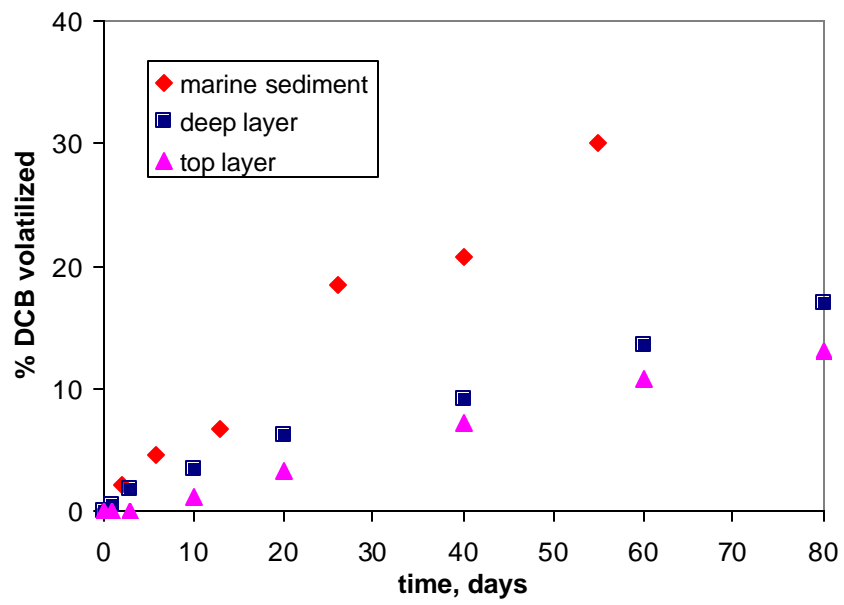


**Figure 7-2** Comparison of DCB Volatilization from Sediments

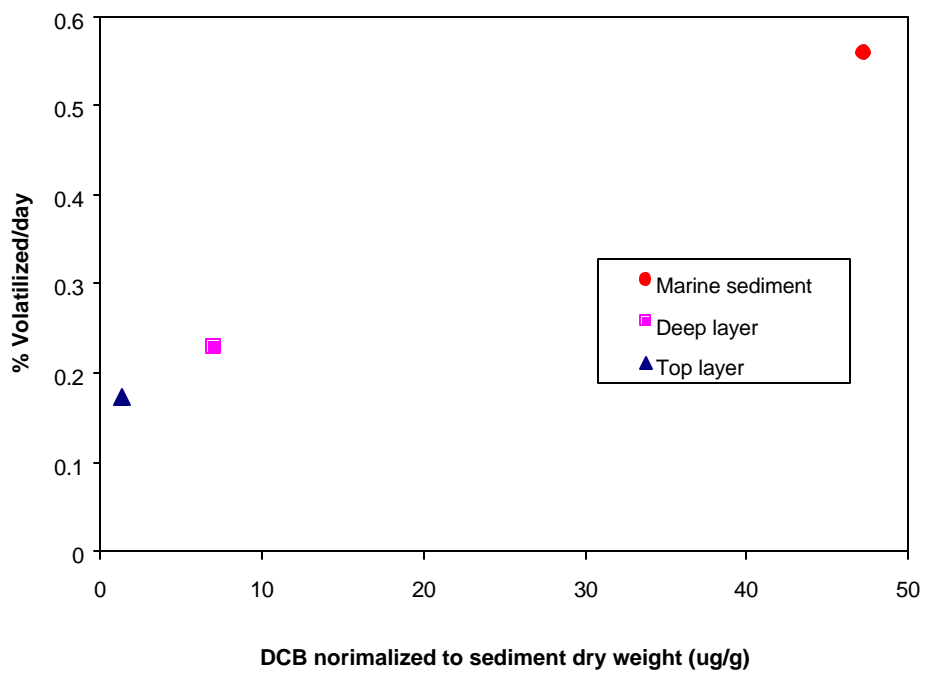


**Figure 7-3** DCB Volatilization Rate versus Level of Sediment Contamination

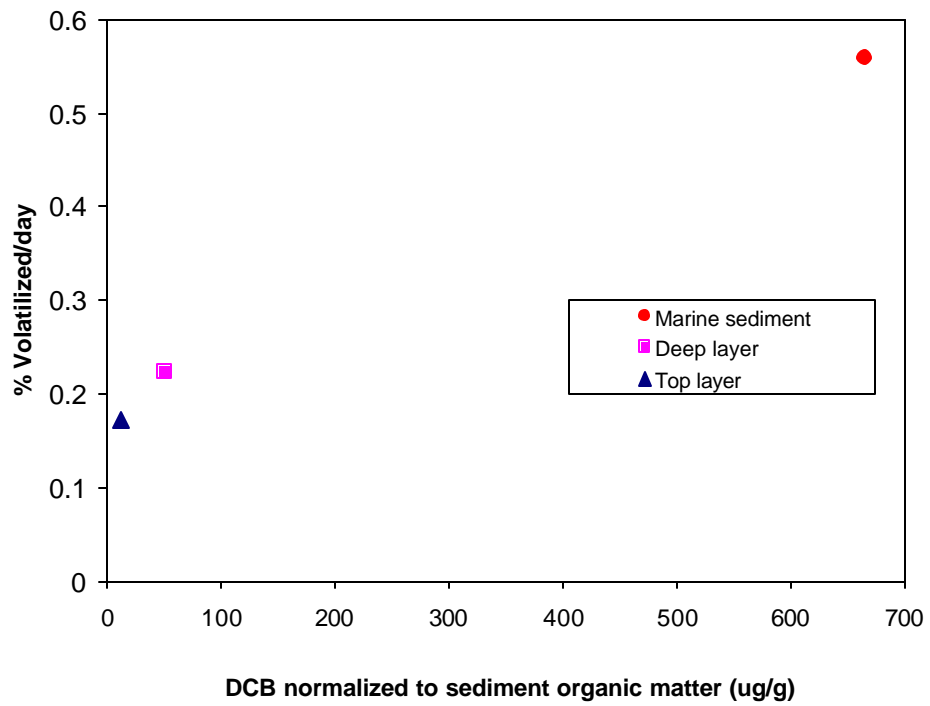


**Figure 7-4** DCB volatilization rate versus sediment organic content



## Chapter 8 Summary

In this research, the volatility of PCB was investigated. First, the rate and extent of PCB volatilization from sediment and other substrates spiked with two PCB congeners, 4,4'-dichlorobiphenyl (DCB) and 2,2', 4, 4', 5, 5'-hexachlorobiphenyl (HCB) were determined experimentally. Second, the rate of PCB volatilization from two types of Lake Hartwell sediments, uniformly naturally contaminated with PCBs, was measured. A relationship between the rate of volatilization and the extent of substitution of the PCB with chlorine was accessed. A fundamental mathematical model of PCB transport in a sediment-water-air system was developed. The data obtained from volatilization experiments were applied to validate the one-dimensional mathematical model. The calibrated model was run to simulate various scenarios that led to better understanding of the transport mechanism of PCBs.

In the fundamental study, volatilization experiments were run using a simple microcosm of sediment, water and air that allows for (pseudo) one-dimensional transport of PCBs. Two PCB congeners, 4,4'-dichlorobiphenyl (DCB) and 2,2', 4,4', 5,5'-hexachlorobiphenyl (HCB) were studied in the experiments. The scenarios investigated included: volatilization of DCB from water; volatilization of PCB from aged contaminated sediments with no overlaying water layer; volatilization when the sediment was covered with a thin or thick water layer; volatilization of PCBs from sediments for three contamination levels; volatilization of PCBs from aged contaminated silica sand or bentonite clay; and volatilization of solid PCBs from treated and untreated glass surfaces. For all the scenarios investigated, experimental results revealed significant volatilization of DCB from all the different substrates studied. Important observations

included: Volatilization of DCB from water was very fast, the higher the water level, the slower the volatilization rate; The rate of volatilization decreased when the sediment lost moisture; the rates of PCB volatilization from contaminated silica sand and bentonite clay were very similar and faster than the rate observed for natural sediments but still slower than the rate of volatilization from water; volatilization of PCB was positively correlated with sediment contamination level; volatilization of solid PCBs from glass surfaces was surprisingly fast; PCBs volatilized faster from surfaces covered with a thin water layer than when no water was present; in all cases studied, the volatilization of HCB was dramatically lower than that of DCB.

Volatilization experiments were performed using two specimens of Lake Hartwell sediments: one from lightly contaminated top layer and another from highly contaminated deep layer were performed. The results from these experiments provided a measure of the rate of volatilization for the various PCB congeners. The data showed significant volatilization of PCBs. The overall volatilization rates of this 80-day study were 2.52% and 6.54% for top layer sediments and deep layer sediments, respectively. Results also indicated lower chlorinated congeners volatilized preferentially. Results of this study were compared with data from a field study. The laboratory microcosm data were very comparable with field study results in terms of sediment concentration, flux and flux normalized to sediment concentration. Comparison of volatilization of DCB with data from the fundamental study revealed that DCB was transported faster from highly contaminated sediment than from lightly contaminated sediment.

A one-dimensional mathematical model describing the fate of PCB in a three-phase (sediment-water-air) system was developed and calibrated after the estimation of the unknown

parameters. The parameters in the mathematical model were estimated in two steps so that the reliability of the estimates is increased since a fewer number of parameters are estimated simultaneously, and therefore, the interactions between parameters that are correlated decrease. The sensitivity analysis of the model parameters showed that the most critical parameters are the gas phase film mass transfer coefficient  $k_{fg}$  and PCB dispersion coefficient in sediment  $D_s$ . This indicates that the mass transfer of PCB from the sediments is limited by dispersion and not by the resistance of liquid film that covers the sediment particle, and that the volatilization of DCB from water is limited by transport to the gas phase. A very important conclusion of the model simulation is that DCB can define an upper limit of the rate of release of PCBs from contaminated sediments, that is, volatilization of DCB takes place from the surface layers of the sediment, and after DCB is depleted from the top layers, further release is going to be very slow.

The results of this study demonstrate that PCBs could indeed volatilize from sediments. In particular, the lower chlorinated PCB congeners such as dichlorobiphenyl and trichlorobiphenyl have great propensity for loss through volatilization. The moisture condition of sediment is also critical to the rate and extent of volatilization. In other words, enrichment in lower chlorinated congeners and high water content would enhance the rate of PCB volatilization. So it is recommend that the volatility of PCB be considered in decision making regarding the management and remediation of the existing PCB contaminated sediments, which might involve activities such as dredging, land farming and land filling.

## Bibliography

- Achman, D.R., K.C. Hornbuckle, and S.J. Elsenreich. 1993. Volatilization of Polychlorinated Biphenyls from Green Bay, Lake Michigan. *Environ. Sci. Technol.* 27: 75-87.
- Atlas, E., and C. S. Giam. 1981. Global transport of organic pollutants: Ambient concentrations in remote marine atmosphere. *Science* 211: 163.
- Bacon, C. E., W. M. Jarman, and D. P. Costa. 1992. Organochlorine and chlorinate biphenyl levels in pinniped milk from the Arctic, the Antarctic, California and Australia. *Chemosphere* 24: 779.
- Bacci, M., D. Calamari, C. Gaggi, R. Ranelli, S. Focardi and M. Morosini. 1986. *Chemosphere* 15: 745-754.
- Ball, W.P. and Roberts, P.V. (1991). Long-Term Sorption of Halogenated Organic Chemicals by Aquifer Material. 2. Intraparticle Diffusion, *Environ. Sci. Technol.* 25 (7): 1237-1249.
- Ballschmitter, K. 1991. Global distribution of organic compounds. *Environ. Carcinog. Rev.* 9: 1.
- Bremle, G., and P. Larsson. 1998. PCB in the Air During Landfilling of A Contaminated Lake sediment. *Atmosphere Environment* 32(6): 1011-1019.
- Brusseau, M.L., Jessup, R.E. and Rao, P.S.C., (1991). Nonequilibrium Sorption of Organic Chemicals: Elucidation of Rate-Limiting Processes, *Environ. Sci. Technol.* 25 (1): 134-142.
- Chiarenzelli, J., R. Scudato, M. Wunderlich, and D. Rafferty. 1996. Volatilization of Polychlorinated Biphenyls from Sediment during Drying at Ambient Conditions. *Chemosphere* 33(5): 899-911.
- Chiarenzelli, J.R., R. J. Scudato, and M. L. Wunderlich. 1997. Volatile Loss of PCB Aroclors from Subaqueous Soils. *Environ.Sci.Technol.* 31(2): 597-602.

Chiarenzelli, J.R., R. J. Scudato, M. L. Wunderlich, G. N. Onega, and O. P. Lashko, 1997. PCB Volatile Loss and Moisture Content of Sediment during Drying. *Chemosphere* 34(11), 2429-2436.

Chiarenzelli, J., R. Scudato, B. Bush, D. Carpenter, and S. Bushart. 1998. Do large-scale Remedial and Dredging events have the Potential to Release Significant Amounts of Semivolatile Compounds to the Atmosphere. *Environ. Health Perspectives*, 106(2), 47-49.

Chiarenzelli, J, R. Scudato, K. Jensen, T. Maloney, M. Wunderlich, J. Pagano, and J. Schneider. 1998. Alteration of Aroclor 1248 in Foundry Waste by Volatilization. *Water, Air and Soil Pollution* 104:113-124.

Durfee, R. L., G. Contos, F. C. Whitmore, J. D. Barden, E. E. Hackman, III and R. A. Westin. 1976. "PCB in the United States-industrial Use and Environmental Distributions," Prepared for the Office of Toxic Substances, U.S. Environmental Protection Agency, EPA 560/6-76-005; NTIS No. PB-252 012, 488.

Erickson, M.D. 1997. *Analytical Chemistry of PCBs*. Lewis Publishers, New York.

Formica, S.J., Baron, J.A., Thibodeaux, L.J. and Valsaraj, K.T. 1988. PCB Transport into Lake Sediments. Conceptual Model and Laboratory Simulation. *Environ. Sci. Technol.* 22(12): 1435-1440.

Gong, Y., J. V. DePinto, G. Y. Rhee, and X. Liu. 1998. Desorption rates of Two PCB Congeners from Suspended sediments - I. Experimental Results. *Wat. Res.* 32 (8): 2507-2517.

Gong, Y., DePinto, J.V., Rhee, G.Y. and Liu, X. (1998). Desorption rates of Two PCB Congeners from Suspended sediments - II. Model Simulations, *Wat. Res.* 32 (8): 2518-2532.

Haque, R.. 1974. Aqueous Solubility, Adsorption, and Vapor Behavior of Polychlorinated Biphenyl Aroclor 1254. *Environ. Sci. Technol.* 8: 139-142.

Harner, T., D. Mackay, and K. C. Jonea. 1995. Model of the Long-Term Exchange of PCBs between Soil and the Atmosphere in the Southern U.K. *Environ. Sci. Technol.* 29: 1200-1209.

Horzempa, L. M. and Di Toro, D.M.; (1983); The Extent of Reversibility of Polychlorinated Biphenyl Adsorption; *Wat.Res.*; 17(8); 851-859.

Jeremiason, J. D., K. C. Hornbuckle, and S. J. Eisenreich. 1994. Decreases in Water Concentrations Reflect Loss by Volatilization. *Environ. Sci. Technol.* 28: 903-914.

Kleiman, C.F. 1997. Position Paper of the American Council on Science and Health: Public Health Concerns about Environmental Polychlorinated Biphenyls (PCBs). *Ecotoxicol. Environ.Safety* 38: 71-84.

Larsson, P. 1983. Transport of <sup>14</sup>C-labelled PCB compounds from sediment to water and from water to air in laboratory model systems. *Wat. Res.* 17 (10): 1317-1326.

Mackay, D., W. Y. Shui, and C. M. Ma. 1992. *Illustrated handbook of physical-chemical properties and environmental fate for organic chemicals*, Volume I, Lewis Publishers, Michigan.

Magar, V., J. Icker, J. Abbott, R. Brenner, G. Durell, G. Johoson, E. Crecelius, C. McCarthy, and L. Bingler. 2001. "Natural Recovery of PCB-Contaminated Sediments at the Sangamo-Weston/Lake Hartwell Superfund Site." *The Sixth International In Situ and On-Site Bioremediation Symposium*, pp. 231-236. San Diego, CA.

Miller, C.T. and Weber W.J. (1988). Modeling the Sorption of Hydrophobic Contaminants by Aquifer Materials-II. Column Reactor Systems, *Wat. Res.* 22 (4): 457-464.

Miller, C. T., and Pedit, J. A. (1992). Use of a Reactive Surface-Diffusion Model to Describe Apparent Sorption-Desorption Hysteresis and Abiotic Degradation of Lindane in a Subsurface Material, *Environ. Sci. Technol.* 26 (7): 1417-1427.

- Pignatello, J.J. and Xing, B. (1996). Mechanisms of slow Sorption of Organic Chemicals to Natural Particles, *Environ. Sci. Technol.* 30 (1): 1-11.
- Qi, S., C. Alonso, M. Suidan, and G. Sayles. 2000. "Investigation of PCB Volatilization from Sediment." 73rd WEF Annual Conference Proceedings.
- Swackhamer, D. L., B. D. McVeety, and R. A. Hites. 1988. Deposition and Evaporation of Polychlorobiphenyl Congeners to and from Siskiwit Lake, Isle Royale, Lake Superior. *Environ. Sci. Technol.* 22: 664-672.
- Weber, W.J. and Miller, C.T. (1988). Modeling the Sorption of Hydrophobic Contaminants by Aquifer Materials-I. Rates and Equilibria, *Wat. Res.* 22 (4): 457-464.
- Weber, W.J.Jr., McGinley, P.M. and Katz, L.E. (1991). Sorption Phenomena in Subsurface Systems: Concepts, Models and Effects on Contaminant fate and Transport, *Wat. Res.* 25 (5): 499-528.
- Wu, S. C. and Gschwend, P. M. (1986). Sorption Kinetics of Hydrophobic Organic Compounds to natural Sediments and Soils, *Environ. Sci. Technol.* 20 (7): 717-725.

## Appendix 1 Preliminary Experiments

At the beginning of this study, series of preliminary experiments were performed with the objective of obtaining results that would allow the optimum design of the volatilization studies. These experiments intended to get an initial idea of the rate of volatilization of the two PCB congeners, and the behavior of the system, so the main experiments can be design to achieve optimum performance. One set of experiments was performed to locate the distribution of PCB in the system. The second set of experiments was conducted to select the optimum operational parameter including speed of pump head and number of necessary PCB and water traps. The schematic of the experimental system is in Figure 3.1 in Chapter 3.

In the first experiment, two conditions were analyzed, volatilization from solid PCBs and volatilization from PCBs covered with water. For each condition, the experiment was run simultaneously in two identical systems. Systems A and B, were run for one condition. Initially the glass columns were loaded with pure solid DCB with neither liquid nor sediment present. Five milliliters of DCB stock solution (100mg/l in acetone) was added to the glass column. Acetone was allowed to evaporate for 18 hours, before the experiment was started. The system was then operated for 5 days. Systems C and D were used for the other condition. Initially the glass columns were loaded with DCB in water at 83% saturation (the solubility of DCB in water is 60  $\mu\text{g/l}$ ). The system was run for 5 days without bubbling of air. Certified acetone and acetone/hexane (1:1) were used as solvents to do the extractions. Extractions were performed until no PCB was observed in the analysis. The results from these experiments are shown in Table A1. From these results it can be concluded that DCB did volatilize from the glass column and that the florisil trap worked well to absorb PCB. The DCB recovery in Table A1 is identified



with the closure of the PCB mass balance, since there was no contaminant degradation, the amount of PCB in all the parts of the system had to account for the initial mass of PCB. The total PCB recovered after the extraction of all the system elements is given here as percentage of the initial amount of PCB. The PCB recovery is good in systems A and B, but it is poorer in systems C and D.

Table A1 Amount of PCB Recovered after 5-day Volatilization.

	A Pure DCB (500 µg)	B Pure DCB (500 µg)	C DCB in water (50 µg/l, 5 µg)	D DCB in water (50 µg/l, 5 µg)
Glass Column	493.63 µg	499.95 µg	0.37 µg	0.17 µg
Florisil trap	0.17 µg	12.33 µg	2.22 µg	2.12 µg
Water trap	N/A	N/A	0	0
Glass tubing	6.35 µg	4.05 µg	0.40 µg	0.44 µg
Viton tubing	0	0	0	0
Steel tubing	12.82 µg	3.42 µg	0.226 µg	0.225 µg
PCB recovery	512.80 µg 102.56%	519.75 µg 103.95%	3.216 µg 64.32%	2.995 µg 59.1%

Table A2 presents the results of the first set of experiment of determining the DCB distribution within the system. Every part of the experimental apparatus was extracted separately. Mass balance was attempted to close at the end of the experiment, however, the PCB recovery was not so good due to the undetected leakage of the system by then. Results indicated that florisil was capable of adsorbing almost all of the volatilized DCB; only small portion of DCB stayed in the water trap or got stuck on the tubing. As shown in Figure 3-1, there are two parts of the stainless steel tubing that connects the entire system. One is ahead of the water trap and another is after the PCB trap. Data showed that PCB might be absorbed on the stainless steel

tubing before the water trap, but after the PCB trap, no volatilized PCB would be circulating in the system.

Table A2 Results of Preliminary Experiments

	100rpm	100rpm (D)	20rpm	20rpm (D)
Glass column	1.183	1.008	2.028	1.009
PCB trap	1.592	1.454	0.371	0.858
Water trap	0	0	0	0
Glass tubing	0	0	0	0
Viton tubing	0	0	0	0
SSB tubing	0	0.197	0.323	0.290
SSA tubing	0	0	0	0
Trap tube	0	0.140	0	0.073
PCB recovery (%)	64.91	66.64	64.65	52.96

Note:

1. SS-stainless steel; SSB-stainless steel tubing before the water trap; SSA- SSB-stainless steel tubing after the florisol trap
2. The mass is in  $\mu\text{g}$ ; initial amount of DCB loaded to the glass column was 4.21  $\mu\text{g}$
3. D-duplicate

The following Table A3 summarizes the preliminary experimental results of the second set on selection of optimum operational parameters for the system; that is effect of airflow rate. Three different speed pump heads that controlled the airflow rate of the system were tested in the experiments in duplicate sets. The experiments were run for one day on volatilization of solid DCB. DCB recovery improved quite a bit. Data showed no volatilization of DCB for the 20rpm pump head in one day. The discrepancy of volatilization rate caused by using 100rpm and

300rpm pump heads was not significant, in other words, the 100rpm pump head was able to provide sufficient flow rate. Hence the 100rpm pump head was selected to use in the future experiments. Another florasil trap was connected following the first one in the experiments to prevent DCB breakthrough. Null of DCB was extracted from it. So in the following experiments, one PCB and one water trap were used.

Table A3. Experimental results of selection of optimum operational parameters

	300rpm	300rpm (D)	100rpm	100rpm (D)	20rpm	20rpm (D)
Glass column	1.528	1.851	1.531	1.601	2.719	2.4
PCB trap	0.241	0.27	0.433	0.29	0	0
Water trap	0	0	0	0	0	0.207
Glass tubing	0	0	0	0	0	0
Viton tubing	0	0	0	0	0	0
SS tubing	0.111	0	0	0	0.253	0.138
Trap tube	0	0	0	0	0	0
PCB recovery (%)	82.89	93.52	86.6	83.38	92.01	84.98

Note:

1. SS-stainless steel;
2. The mass is in  $\mu\text{g}$ ; initial amount of DCB loaded to the glass column for 100 rpm and 300 rpm was 2.27  $\mu\text{g}$  and 3.23  $\mu\text{g}$  for 20 rpm
3. D-duplicate

## Appendix 2 Silylation

Silylation is a technique that applies to treat chromatography columns, glass injection port liners, reaction vessels, sample storage containers and other glassware to minimize nonspecific binding and sample loss. It chemically binds a thin water-repellent film to glass, quartz, silica, and ceramics. Coated surfaces are neutral, hydrophobic and non-oily; it offers increased electrical resistivity, so the glass surface are not affected by solvents nor readily hydrolyzed. It also reduces adsorption of polar compounds, including proteins and trace metals, onto glass surface; protects delicate samples against the possible reactive effects of –OH sites present on all types of glassware.

Reagent used in this study was 5% DMDCS (dimethyldichlorosilane) in toluene (**Supelco**). Procedures of silylation are summarized as the following steps:

1. Coat the glass surface by rinsing with the reagent for 10 to 15 seconds, then discard the reagent.
2. Rinse the surface two times with toluene.
3. Rinse the surface three times with methanol.
4. Dry the surface, using clean nitrogen, not air. Since airlines can contain oils and rust particles.

### **Appendix 3 Preparation of the PCB contaminated substrates**

The PCB contaminated substrates used for the PCB volatilization study were prepared in advance so that the substrates had enough time to age. For example, The moisture content of the wet sediment was experimentally determined to be 49.84%, so the dry weight was 50.16% of the original weight. Therefore, to obtain an initial target concentration of 70 µg of PCB per g of dry sediment, 35µg of PCB were applied to 1g of wet sediment. DCB and HCB were spiked into PCB-free sediments according to the following procedures:

1. Glass jars were silylated and baked;
2. Each jar was filled with approximately 570g wet clean sediments, 250 ml of water and 15 ml of biocide. The jars were put in the tumbler for one day to inhibit bioactivity in the sediment.
3. 20 mg of either DCB or HCB in acetone was introduced into each jar, the caps were tightened, and the jars were put again in the tumbler to mix the sediment/PCB mixture.
4. Jars were tumbled for at least three months.

The other two contamination levels were be obtained by adding 10 mg and 5 mg PCB to the jar respectively.

The contaminated silica sand and bentonite clay were prepared in the similar way. Approximately 250g dry silica sand and bentonite clay were spiked with 10mg of DCB and

10mg of HCB, tumbled with 600ml water for over three months. The spiked and aged substrates were used in the volatilization experiments.

## Appendix 4 Establishment of Sediment Extraction Method

Preliminary experiments were conducted to determine the optimum extraction method. The following variables needed to be specified: proportion of the solvents acetone and hexane; mixing method; and mixing period.

**Solvent Proportion Test.** Three 10g sediment samples were extracted using different proportions of acetone and hexane in the solvent. 70% hexane and 30% acetone was used in the first experiment and 75% acetone and 25% hexane was used in the second one. In both cases the total amount of solvent used was 100 ml. The results are shown in tables A4 and A5, respectively.

**Table A4.** Experiment 1. 70% Acetone and 30% Hexane

Sample #	DCB 1	DCB 2	DCB 3	HCB 1	HCB 2	HCB 3
PCBs recovered (µg)	269.6	260.6	267.9	223.7	185.6	195.0
Average (µg)	266.0			201.4		
Surrogate recovery rate (%)	92.7	90.4	93.0	90.7	88.0	92.2

**Table A5.** Experiment 2. 25% Acetone and 75% Hexane

Sample #	DCB 1	DCB 2	DCB 3	HCB 1	HCB 2	HCB 3
PCBs recovered (µg)	237.5	267.4	253.5	223.8	269.6	216.0
Average (µg)	252.8			236.5		
Surrogate recovery rate (%)	90.2	84.8	87.2	84.8	87.9	85.2

These experimental data showed that the higher proportion of hexane (75% in Table A5) increases the recovery of HCB by 17% while the recovery of DCB is only reduced by 5%. The solvent proportion of 25% acetone and 75% hexane was chosen to be used in sediment extraction.

Two different mixing methods and time lengths were investigated: sample tumbling for 2 days and sample shaking for 1 day. Experiments were conducted using three 10g sediment samples. The results of these experiments are shown in table A6 and A7.

**Table A6.** Experiment 3. Tumbling for 2 days.

Sample #	DCB 1	DCB 2	DCB 3	HCB 1	HCB 2	HCB 3
PCBs recovered (µg)	267.4	273.8	275.6	239.4	228.7	236.1
Average (µg)	272.3			234.7		
Surrogate recovery rate (%)	90.9	97.8	98.1	95.4	90.4	92.9

**Table A7.** Experiment 4. Shaking at constant 35EC for 1 day.

Sample #	DCB 1	DCB 2	DCB 3	HCB 1	HCB 2
PCBs recovered (µg)	236.6	251.8	264.2	183.0	173.4
Average (µg)	250.9			178.2	
Surrogate recovery rate (%)	81.0	84.8	81.5	83.3	73.6

From the results in Table A6 and Table A7 it can be concluded that the mixing method of tumbling for 2 days achieves better PCB and surrogate recovery. Tumbling at high temperature



didn't really enhance extraction efficiency. Therefore, the solvent proportion of 75% hexane and 25% acetone with 2 days of tumbling was selected to be used in the future sediment extraction.

In summary, a solvent proportion of 75% hexane and 25% acetone with 2 days of tumbling at room temperature were decided to be used in sediment extraction in this research.

## **Appendix 5 Moisture Content Analysis**

The soil moisture content of each soil sample was determined during analytical extraction using a modified version of American Society for Testing and Materials (ASTM) Method D2216. The method was modified as follows: about 4 g of soil sample were placed in a pre-weighed aluminum-weighing pan (W0). The weight was recorded (W1), and the pan was then placed in a drying oven at  $110\pm 5^{\circ}\text{C}$ . The sample was dried to constant weight for 24 hours, cooled in a desiccator for 2 to 4 hours, and weighed again (W2). The soil moisture content (moisture mass relative to total soil mass) was calculated as  $[(W1-W2)/(W1-W0)] \times 100\%$ .

## **Appendix 6 Volatile Organic Matter Content Analysis**

The volatile organic matter content of each soil sample was calculated from gravimetric changes resulting from heating to 500°C after initially drying at 110°C. The method is described in the following details: about 4 g of soil sample were placed in a pre-weighed aluminum-weighing pan (W1). The pan was placed in a drying oven at 110±5°C for 2 hours, cooled in a desiccator and the weight was recorded (W2). The pan was then placed in the furnace at 550°C for 4 hours and weighed (W3) after cooling down. The organic matter content was calculated as  $[(W2-W3)/(W2-W1)] \times 100\%$ .

## Appendix 7 PCB Analysis by GC-ECD

PCB was analyzed using an HP 5890 gas chromatograph (Hewlett-Packard Co. Palo Alto, C.A) equipped with an electron capture detector. The method is summarized as follows.

Instrument:	Hewlett Packard 5890 Series II GC
Detector:	ECD
Column:	Capillary, DB-5 (30m×0.53mm ID), 1.5 µm film thickness
Carrier Gas:	Helium
Make-up Gas:	P5 mix (argon 95% / methane 5%)
Inlet Temperature:	250 °C
Detector Temperature:	300 °C
Temperature Program:	150°C for 8.00 min to 250°C at 10 °C /min
Column Flow rate:	30ml/min
Injection Volume:	1 µl

## Appendix 8 <sup>14</sup>C-labeled PCB Analysis by LSC

Cycles: 1

Count Time: 4.00 min

2 Sigma Coincidence: yes

# Counts/Vial: 1

# Vials/Standard: 1

# Vials/Sample: 1

Radionuclide: <sup>14</sup>C

Data Mode: CPM

	LL	UL	Bkg	2 Sigma%	LCR
Region A:	0.0	156.0	0.00	.50	0
Region B:	4.0	156.0	0.00	.50	0
Region C:	0.0	0.0	0.00	.00	0

## Appendix 9 Measurement of System Flow Rate

The flow rate of the experimental system (see Figure 3-1) was measured using a flowrate meter, bubble soap and a timer. One end of the flowrate meter was connected to the experimental apparatus; the other end was open to air. The time was recorded for passing through 90ml air. The measurement was performed 10 times and the data are shown in Table A9.

Table A9. System flowrate measurement

	1	2	3	4	5	6	7	8	9	10	Ave.
Time (s)	55.87	56.46	55.84	56.25	56.44	56.63	56.44	56.56	56.59	55.81	56.29

The flowrate of the system was calculated to be  $90\text{ml}/56.29\text{s}=5.76\text{l/h}=96\text{ml/min}$ .

## Appendix 10 Original Data for Figures in Chapter 4

**Table A4-1** Results of Exp. 1: 50 ml of water ( $\mu\text{g}$ ).

Time, hours	8		16		24		48		72		96	
	A	A'	B	B'	C	C'	D	D'	E	E'	F	F'
Glass Column	0.671	0.686	0.168	0.153	0.080	0.108	0.043	0.038	0	0	0	0
PCB Trap	0.363	0.249	0.873	0.936	0.983	0.981	1.161	1.192	1.209	1.231	1.173	1.249
Water Trap	0	0	0	0	0	0	0	0	0	0	0	0
Tubing	0	0	0	0	0	0	0	0	0	0	0	0
PCB Recovery (%)	79.59	71.98	80.16	86.65	81.83	83.83	92.68	94.69	93.07	94.75	90.28	96.17

**Table A4-2** Results of Exp. 1': 50 ml of water ( $\mu\text{g}$ ).

Time, hours	8		16		24		48		72		96	
	A	A'	B	B'	C	C'	D	D'	E	E'	F	F'
Glass Column	0.564	0.553	0.236	0.254	0.158	0.097	0	0	0	0	0	0
PCB Trap	0.288	0.310	0.614	0.663	0.408	0.868	0.947	0.983	0.984	0.905	0.980	1.015
Water Trap	0	0	0	0	0	0	0	0	0	0	0	0
Tubing	0.169	0.088	0.070	0.138	0.426	0.031	0.026	0.054	0.028	0.059	0.033	0
PCB Recovery (%)	95.13	88.60	85.80	98.30	92.50	92.80	90.70	96.70	85.90	89.80	87.70	94.36

**Table A4-3** Results of Exp. 2: 100 ml of water ( $\mu\text{g}$ ).

Time, hours	12		24		48		72		96		120	
	A	A'	B	B'	C	C'	D	D'	E	E'	F	F'
Glass Column	1.177	1.146	0.654	0.701	0.283	0.298	0.046	0.082	0.030	0.036	0	0.153
PCB Trap	0.388	0.479	1.067	0.936	1.539	1.466	1.727	1.727	1.800	1.805	1.901	1.836
Water Trap	0	0	0	0	0	0	0	0	0	0	0	0
Tubing	0.119	0.078	0.064	0.115	0	0	0	0	0	0	0	0
PCB Recovery (%)	83.28	84.22	88.28	86.65	90.11	87.26	87.69	89.47	90.50	91.05	94.01	98.36

**Table A4-4** Results of Exp. 2': 100 ml of water ( $\mu\text{g}$ ).

Time, hours	12		24		48		72		96		120	
	A	A'	B	B'	C	C'	D	D'	E	E'	F	F'
Glass Column	2.093	1.976	1.016	2.681	0.403	0.522	0.236	0.132	0.169	0.181	0.080	0.113
PCB Trap	0.423	0.425	1.924	0.726	2.706	2.536	2.625	3.413	2.887	3.271	3.368	2.937
Water Trap	0	0	0	0	0	0	0	0	0	0	0	0
Tubing	0.731	1.079	0.356	0	0	0	0	0	0.205	0.106	0.081	0.123
PCB Recovery (%)	88.37	94.72	89.71	92.73	84.62	83.23	77.87*	96.48	88.76	96.84	96.05	86.36

\*Note: The low recovery rate in system D was due to a leakage from the viton tubing connecting the pump.



**Table A4-5** Results of Exp. 3: 150 ml water ( $\mu\text{g}$ ).

Time, hours	12		24		48		72		96		120	
	A	A'	B	B'	C	C'	D	D'	E	E'	F	F'
Glass Column	1.776	2.532	1.166	1.094	0.662	0.666	0.395	0.435	0	0.734	0	0
PCB Trap	0.925	0	1.558	1.338	1.920	1.839	2.294	2.179	2.551	1.767	2.382	2.574
Water Trap	0	0	0	0	0	0	0	0	0	0	0	0
Tubing	0.059	0.257	0.075	0.133	0.026	0.061	0.02	0.04	0	0.01	0.038	0
PCB Recovery (%)	98.34	99.36	99.71	91.38	92.90	91.40	96.50	94.55	90.88	89.45	86.20	91.70

**Table A4-6** Results of Exp 3': 150 ml water ( $\mu\text{g}$ ).

Time, hours	12		24		48		72		96		120	
	A	A'	B	B'	C	C'	D	D'	E	E'	F	F'
Glass Column	2.205	1.950	1.197	1.293	0.678	0.572	0.420	0.783	0.640	0.296	0	0.315
PCB Trap	0.955	0.707	1.513	1.400	2.085	2.141	2.403	2.429	2.112	2.426	2.633	2.366
Water Trap	0	0	0	0	0	0	0	0	0	0	0	0
Tubing	0.188	0.189	0.399	0.221	0.259	0.173	0.243	0.267	0.427	0.210	0.218	0.176
PCB Recovery (%)	98.2	88.2	96.4	90.4	93.7	89.5	95.1	107.9	98.6	90.9	88.4	88.6

**Table A4-7** Results of Completely Mixed Water Phase Experiments ( $\mu\text{g}$ )

Time, hours	4		8		12		24		36		48	
	A	A'	B*	B'	C	C'	D	D'	E	E'	F	F'
Glass Column	1.126	1.163		0.54	0.11	0.089	0	0	0	0	0	0
PCB Trap	0.938	0.873		1.302	2.14	2.169	2.196	2.11	2.262	2.13	2.289	2.327
Water Trap	0	0		0	0	0	0	0	0	0	0	0
Tubing	0.09	0.127		0.207	0	0	0	0	0	0	0	0
PCB Recovery (%)	89.16	89.53		84.8	93.12	93.27	90.9	87.32	93.62	88.17	94.75	96.32

Note: \* Sample was broken by accident.

**Table A4-8** PCB volatilization from sediments without overlaying water layer ( $\mu\text{g}$ )

Time, days		2		4		6		8		10		12	
		A	A'	B	B'	C	C'	D	D'	E	E'	F	F'
Glass Column	DCB	63.71	62.58	58.8	61.79	58.3	55.9	54.1	55.67	59.7	58.1	55.9	47.17
	HCB	47.31	61.3	67.74	62.58	58	66.27	44.5	53.26	57.22	57.46	64.04	61.13
	TCB (%)	98.9	87.7	106	91	100.9	87.3	87.2	90.2	99.6	100	87.4	91.6
PCB Trap	DCB	3.32	3.21	5.61	4.65	8.47	8.03	9.85	8.17	6.76	7.68	10.93	11.54
	HCB	0	0	0.05	0	0.22	0.1	0.2	0.11	0	0	0	0.19
Water trap		0	0	0	0	0	0	0	0	0	0	0	0
Tubing	DCB	0	0	0	0	0	0	0	0	0	0	0	0
	HCB	0	0	0.02	0.02	0.04	0.05	0.01	0.03	0.04	0.07	0.1	0
PCB Recovery (%)	DCB	103.8	101.9	99.79	102.9	103.5	99.1	99.1	98.9	102.9	101.9	103.5	91
	HCB	72.7	91.1	100.7	93	86.6	98.7	66.4	79.3	85.1	85.4	95.3	91.1

**Table A4-9** PCB volatilization from sediments with a thin overlaying water layer ( $\mu\text{g}$ )

Time, days		2		4		6		8		10		12	
		A	A'	B	B'	C	C'	D	D'	E	E'	F	F'
Glass Column	DCB	59.47	56.52	56.16	57.49	54.46	54.50	60.62	55.10	54.41	55.10	55.50	58.59
	HCB	53.79	51.23	52.91	53.31	52.39	48.59	50.92	51.80	49.64	52.39	48.89	49.76
	TCB (%)	95.5	82.4	90.9	90.5	96.2	90.4	97.3	99.6	97.8	91.8	95.0	95.7
PCB Trap	DCB	0.93	1.19	2.17	2.06	2.76	2.51	3.19	3.26	2.96	2.49	4.23	2.96
	HCB	0	0	0	0	0	0	0	0	0	0	0	0
Water trap		0	0	0	0	0	0	0	0	0	0	0	0
Tubing	DCB	0	0	0	0	0	0	0	0	0	0	0	0
	HCB	0	0	0.04	0.03	0	0	0	0	0	0	0	0
PCB Recovery (%)	DCB	101.6	97.1	98.1	102.2	96.3	95.9	107.4	98.2	96.5	96.9	100.5	103.5
	HCB	98.9	94.2	97.4	98.1	96.3	89.3	93.6	95.2	91.3	96.3	90.6	92.3

**Table A4-10** DCB Volatilization from sediments for 55 days ( $\mu\text{g}$ )

Time, days		2		6		13		26		40		55	
		A	A'	B	B'	C	C'	D	D'	E	E'	F	F'
Glass Column	DCB	57.15	57.18	55.20	54.33	54.56	55.55	50.50	46.93	47.00	49.21	42.27	44.09
	TCB (%)	90.2	91.1	91.0	90.4	86.6	92.4	91.6	92.5	90.2	84.4	90.2	89.7
PCB Trap		1.13	1.37	2.54	2.92	3.94	4.02	9.88	11.82	13.79	10.80	17.12	18.68
Water trap		0	0	0	0	0	0	0	0	0	0	0	0
Tubing		0	0	0.14	0	0	0	0	0	0	0	0	0
PCB Recovery (%)		98.8	99.2	98.1	97.0	99.1	100.9	102.3	99.5	103.0	101.7	100.6	106.4

**Table A4-11** PCB Volatilization from sediments for 80 days ( $\mu\text{g}$ )

Time, days		5		20		35		50		65		80	
		A	A'	B	B'	C	C'	D	D'	E	E'	F	F'
Glass Column	DCB	55.43	52.43	51.92	51.32	48.99	50.73	45.63	43.98	40.19	42.54	40.66	41.35
	HCB	53.76	50.90	53.60	54.23	51.23	51.31	51.57	53.53	51.09	54.10	52.24	51.85
	TCB (%)	91.5	87.8	98.3	98.6	94.5	91.3	92.7	90.7	105.8	106.5	96.3	107.0
PCB Trap	DCB	1.67	1.85	5.31	4.47	8.18	7.00	10.43	10.72	14.73	11.49	16.87	13.09
	HCB	0	0	0.31	0.24	0.52	0.38	0.83	1.15	0.58	0.59	0.87	0.63
Water trap		0	0	0	0	0	0	0	0	0	0	0	0
Tubing	DCB	0	0	0	0	0	0	0	0	0	0	0	0
	HCB	0	0	0	0	0	0	0	0	0	0	0	0
PCB Recovery (%)	DCB	100.6	95.6	100.8	98.3	100.7	101.7	98.8	96.4	96.8	95.2	101.5	95.9
	HCB	100.8	95.4	101.1	102.1	97.0	97.0	98.2	102.5	96.8	102.5	99.6	98.4

**Table A4-12** PCB Volatilization from low and middle contamination-level sediments ( $\mu\text{g}$ )

Time, days		1		3		10		20		40		60		80	
		A	A'	A	A'	A	A'	A	A'	A	A'	A	A'	A	A'
High	DCB	0	0.19	1.13	0.88	2.41	2.2	1.83	1.98	2.27	1.76	1.85	2.23	2.18	2.72
	HCB	0	0	0	0.09	0.09	0.07	0	0.14	0.13	0.07	0.08	0.08	0.14	0
Low	DCB	0.16	0	0.39	0.2	0.83	0.88	1.1	1.16	1.07	1.11	0.67	0.85	1.21	1
	HCB	0	0	0.16	0	0	0.1	0.18	0.11	0.25	0.12	0	0.07	0.13	0.07

**Table A4-13 PCB Volatilization from Silica Sand (µg)**

Time, days		4		8		12		16		20	
		A	A'	B	B'	C	C'	D	D'	E	E'
Glass Column	DCB	44.65	41.53	40.96	41.75	37.95	36.15	33.23	32.03	28.9	29.81
	HCB	49.2	49	48.97	50.14	48.49	49.03	49.01	49.35	47.45	47.25
	TCB (%)	95.3	90.1	94.1	91.7	98.5	93.8	95.3	94	98	97.9
PCB Trap	DCB	4.37	5.17	9.15	8.65	15.11	13.78	19.14	18.22	22.43	23.07
	HCB	0.31	0.37	1.45	0.93	1.27	1.68	1.81	1.29	2.75	2.72
Water trap		0	0	0	0	0	0	0	0	0	0
Tubing	DCB	0	0	0	0	0	0	0	0	0	0
	HCB	0.14	0.15	0.15	0	0	0	0	0	0	0.06
PCB Recovery (%)	DCB	99.4	94.7	101.6	102.2	106.8	101.2	106.2	101.9	104.1	107.2
	HCB	95.6	95.3	97.5	98.2	95.8	97.5	97.8	96.7	96.7	96.2

**Table A4-14 PCB Volatilization from Bentonite Clay (µg)**

Time, days		4		8		12		16		20		24	
		A	A'	B	B'	C	C'	D	D'	E	E'	F'	F'
Glass Column	DCB	18.49	18.14	16.33	16.27	14.33	14.42	13.86	13	12.45	12.98	10.86	10.17
	HCB	19.9	20.11	20.41	20.34	20.24	19.13	21.38	19.85	20.52	19.96	21.64	20.41
	TCB (%)	91.4	93.2	101.4	91.9	96.1	91.1	91.4	89.6	97.5	91.8	102.4	102
PCB Trap	DCB	1.57	1.79	3.46	3.48	5.34	5.35	6.57	6.93	7.76	7.45	9.03	9.45
	HCB	0	0	0.26	0.23	0.34	0.33	0.34	0.26	0.53	0.53	0.47	0.49
Water trap		0	0	0	0	0	0	0	0	0	0	0	0
Tubing	DCB	0	0	0	0	0	0	0	0	0	0	0	0
	HCB	0	0	0	0	0	0	0	0	0	0	0	0
PCB Recovery (%)	DCB	97.4	96.7	96.1	95.9	95.5	96	99.2	96.7	98.1	98.2	96.6	95.2
	HCB	96	96.7	99.4	98.9	98.9	93.6	104.4	96.7	101.2	98.5	106.3	100.5

## Appendix 11 Original Data for Chapter 5

**Table A5-1** Equilibrium Data for Sediment

DCB quantity introduced (× solubility)	q <sub>0</sub> (μg)	C <sub>e</sub> (μg/l)		q <sub>e</sub> (mg/kg)	
		A	A'	A	A'
20×	144	3.63	3.63	35.89	35.89
60×	432	6.5	6.71	107.81	107.8
100×	720	7.18	7.37	179.78	179.78
150×	1080	9.54	9.45	269.71	269.72
200×	1440	11.59	12.36	359.65	359.63
250×	1800	12.36	12.8	449.63	449.62
300×	2160	14.25	14.58	539.57	539.56

**Table A5-2** Equilibrium Data for Sand and Clay

DCB quantity introduced (× solubility)	q <sub>0</sub> (μg)	Silica Sand				Bentonite Clay			
		C <sub>e</sub> (μg/l)		q <sub>e</sub> (mg/kg)		C <sub>e</sub> (μg/l)		q <sub>e</sub> (mg/kg)	
		A	A'	A	A'	A	A'	A	A'
10×	72	4.04	4.26	17.88	17.87	3.38	3.24	17.9	17.9
20×	144	6.43	6.6	35.81	35.8	4.76	4.7	35.86	35.86
60×	432	8.21	8.52	107.75	107.74	6.92	7.19	107.79	107.78
100×	720	9.62	9.44	179.71	179.72	8.31	8.74	179.75	179.74
150×	1080	10.62	10.79	269.68	269.68	9.73	9.74	269.71	269.71
200×	1440	12.73	12.51	359.62	359.62	11.3	11.07	359.66	359.67

## Appendix 12 Original Data for Figures in Chapter 7

**Table A7-1 PCB volatilization from top layer sediments\***

PCB (ng)	S0	A1	A3	A10	A20	A40	A60	A80	S80	% of Rec.	% Of Vol.
PCB8/5	76.59	ND	ND	0.56	0.94	1.71	1.58	5.26	60.81	0.93	13.13
PCB18	39.21	ND	ND	ND	ND	ND	ND	2.70	27.80	0.78	6.88
PCB28	119.60	ND	ND	ND	0.42	0.99	1.68	3.72	81.84	0.74	5.70
PCB31	70.63	ND	ND	ND	0.32	0.77	0.84	2.63	44.62	0.70	6.45
PCB33/20	27.94	ND	ND	ND	ND	ND	ND	1.06	19.50	0.74	3.79
PCB41/64/71	130.19	ND	ND	ND	ND	0.64	1.51	3.13	76.95	0.63	4.06
PCB42	53.13	ND	ND	ND	ND	ND	ND	1.15	34.23	0.67	2.17
PCB44	109.70	ND	ND	ND	ND	0.65	1.40	2.24	67.82	0.66	3.91
PCB49	187.89	ND	ND	ND	0.52	1.43	2.01	4.74	112.65	0.65	4.63
PCB52	205.66	ND	ND	ND	1.03	1.76	3.79	5.55	123.72	0.66	5.90
PCB56/60	108.02	ND	ND	ND	ND	0.29	0.62	1.09	63.08	0.60	1.85
PCB66	198.66	ND	ND	ND	0.25	0.75	1.42	2.86	119.71	0.63	2.65
PCB70/76	133.17	ND	ND	ND	ND	0.41	0.87	2.08	78.89	0.62	2.53
PCB74	119.64	ND	ND	ND	ND	0.25	0.88	1.64	71.08	0.62	2.31
PCB84	45.28	ND	ND	ND	ND	ND	ND	0.74	26.37	0.60	1.63
PCB85	36.61	ND	ND	ND	ND	ND	ND	ND	19.53	0.53	0.00
PCB87/115	75.07	ND	ND	ND	ND	0.18	ND	ND	42.70	0.57	0.24
PCB92	43.50	ND	ND	ND	ND	ND	ND	ND	24.06	0.55	0.00
PCB95	147.45	ND	ND	ND	ND	0.53	1.33	2.34	85.20	0.61	2.85
PCB97	55.64	ND	ND	ND	ND	ND	ND	ND	30.75	0.55	0.00
PCB99	116.29	ND	ND	ND	ND	0.23	0.53	0.98	64.44	0.57	1.50
PCB101/90	187.14	ND	ND	ND	ND	0.24	0.99	1.97	105.28	0.58	1.71
PCB105	65.24	ND	ND	ND	ND	ND	ND	ND	36.35	0.56	0.00
PCB110	270.80	ND	ND	ND	ND	0.62	1.12	2.41	150.04	0.57	1.53
PCB118	187.46	ND	ND	ND	ND	ND	0.54	0.98	103.39	0.56	0.81
PCB128	33.33	ND	ND	ND	ND	ND	ND	ND	18.70	0.56	0.00
PCB132	54.56	ND	ND	ND	ND	ND	ND	1.16	26.43	0.51	2.13
PCB135/144	27.25	ND	ND	ND	ND	ND	ND	ND	15.02	0.55	0.00
PCB136	20.57	ND	ND	ND	ND	ND	ND	ND	11.57	0.56	0.00
PCB137	9.03	ND	ND	ND	ND	ND	ND	ND	5.01	0.55	0.00
PCB138/160/163	197.46	ND	ND	ND	ND	ND	ND	ND	104.74	0.53	0.00
PCB141	17.96	ND	ND	ND	ND	ND	ND	ND	9.71	0.54	0.00
PCB146	31.35	ND	ND	ND	ND	ND	ND	ND	16.69	0.53	0.00
PCB149	121.83	ND	ND	ND	ND	ND	ND	1.23	64.82	0.54	1.01
PCB151	28.08	ND	ND	ND	ND	ND	ND	ND	15.21	0.54	0.00
PCB156	15.74	ND	ND	ND	ND	ND	ND	ND	8.54	0.54	0.00
PCB158	13.85	ND	ND	ND	ND	ND	ND	ND	7.57	0.55	0.00
PCB167	5.99	ND	ND	ND	ND	ND	ND	ND	3.61	0.60	0.00
PCB170/190	23.95	ND	ND	ND	ND	ND	ND	ND	12.26	0.51	0.00
PCB174	15.78	ND	ND	ND	ND	ND	ND	ND	8.60	0.55	0.00
PCB177	12.74	ND	ND	ND	ND	ND	ND	ND	6.85	0.54	0.00
PCB180	26.10	ND	ND	ND	ND	ND	ND	ND	14.20	0.54	0.00
PCB183	7.59	ND	ND	ND	ND	ND	ND	ND	3.89	0.51	0.00
PCB184	ND	ND	ND	ND	ND	ND	ND	ND	ND	0.00	0.00
PCB187/182	19.29	ND	ND	ND	ND	ND	ND	ND	10.34	0.54	0.00
PCB194	4.44	ND	ND	ND	ND	ND	ND	ND	2.90	0.65	0.00
PCB195	2.01	ND	ND	ND	ND	ND	ND	ND	0.46	0.23	0.00
PCB203/196	4.25	ND	ND	ND	ND	ND	ND	ND	2.78	0.65	0.00
PCB206	2.46	ND	ND	ND	ND	ND	ND	ND	1.14	0.46	0.00
PCB209	0.61	ND	ND	ND	ND	ND	ND	ND	0.23	0.37	0.00
Total	3506.71	0.00	0.00	0.56	3.48	11.45	21.11	51.64	2042.08	0.61	2.52

\* S–sediment sample; A–air sample; Rec.–recovery; Vol.–volatilization;

**Table A7- 2 PCB volatilization from deep layer sediments\***

PCB (ng)	S0	A1	A3	A10	A20	A40	A60	A80	S80	% of Rec.	% Of Vol.
PCB8/5	2660.04	14.87	33.15	45.09	51.63	100.52	116.68	87.74	1425.56	70.50	16.90
PCB18	741.80	2.61	5.57	8.26	9.43	21.59	22.15	20.61	427.95	69.85	12.16
PCB28	234.28	0.65	1.10	1.33	1.69	4.36	3.93	4.27	182.41	85.25	7.39
PCB31	1012.99	2.17	4.28	6.84	8.28	20.38	18.67	18.78	706.77	77.61	7.84
PCB33/20	136.66	ND	ND	0.34	0.40	0.67	ND	1.54	27.20	22.06	2.15
PCB41/64/71	1041.29	ND	1.54	4.44	4.69	12.48	11.14	12.95	841.24	85.32	4.54
PCB42	190.28	ND	0.57	0.79	0.86	2.48	2.00	2.23	172.35	95.27	4.69
PCB44	276.59	ND	0.92	1.20	1.65	3.90	3.20	3.87	215.26	83.16	5.33
PCB49	2876.06	4.69	8.68	13.53	15.46	48.31	39.69	47.34	2929.32	108.03	6.18
PCB52	2978.28	5.74	10.36	15.26	18.01	51.33	43.85	48.77	2758.52	99.11	6.49
PCB56/60	27.47	ND	ND	ND	ND	ND	ND	ND	30.25	110.12	0.00
PCB66	93.85	ND	ND	0.48	0.33	1.39	1.04	1.48	109.56	121.77	5.02
PCB70/76	78.49	ND	ND	0.10	0.19	0.80	0.52	0.59	79.67	104.32	2.81
PCB74	146.94	ND	ND	0.38	0.45	1.42	1.05	1.36	152.78	107.15	3.17
PCB84	228.45	ND	ND	0.59	0.39	1.97	1.32	1.87	233.15	104.74	2.68
PCB85	21.89	ND	ND	ND	ND	ND	ND	ND	25.69	117.39	0.00
PCB87/115	29.18	ND	ND	ND	ND	ND	0.72	0.58	36.80	130.53	4.43
PCB92	128.20	ND	ND	ND	ND	1.22	0.74	0.96	142.19	113.20	2.28
PCB95	1025.22	1.47	2.60	3.39	3.70	12.12	8.38	11.50	1012.96	103.01	4.21
PCB97	39.47	ND	ND	ND	ND	ND	ND	ND	47.79	121.07	0.00
PCB99	276.79	ND	ND	0.49	0.35	2.01	0.95	2.31	335.65	123.47	2.21
PCB101/90	301.09	ND	ND	0.79	0.53	2.39	1.37	2.68	360.78	122.40	2.58
PCB105	19.90	ND	ND	ND	ND	ND	ND	ND	29.42	147.87	0.00
PCB110	1172.63	ND	0.68	2.56	1.67	6.82	2.58	6.19	1756.39	151.53	1.75
PCB118	171.92	ND	ND	ND	ND	0.62	ND	0.61	252.84	147.78	0.71
PCB128	44.28	ND	ND	ND	ND	ND	ND	ND	65.40	147.69	0.00
PCB132	146.95	ND	ND	ND	ND	ND	ND	52.09	214.47	181.39	35.45
PCB135/144	132.60	ND	ND	ND	ND	0.70	ND	0.72	174.03	132.32	1.07
PCB136	122.64	ND	ND	ND	ND	1.07	0.51	1.08	165.69	137.26	2.17
PCB137	8.96	ND	ND	ND	ND	ND	ND	ND	12.04	134.35	0.00
PCB138/160/163	457.73	ND	ND	ND	ND	1.04	ND	0.81	678.01	148.53	0.40
PCB141	12.09	ND	ND	ND	ND	ND	ND	ND	18.94	156.70	0.00
PCB146	116.16	ND	ND	ND	ND	ND	ND	ND	175.03	150.68	0.00
PCB149	654.95	ND	0.53	1.17	0.47	3.37	0.92	3.14	1001.69	154.41	1.47
PCB151	121.68	ND	ND	ND	ND	0.82	ND	0.62	157.57	130.68	1.18
PCB156	18.92	ND	ND	ND	ND	ND	ND	ND	32.44	171.41	0.00
PCB158	21.95	ND	ND	ND	ND	ND	ND	ND	31.95	145.56	0.00
PCB167	10.17	ND	ND	ND	ND	ND	ND	ND	14.47	142.27	0.00
PCB170/190	51.83	ND	ND	ND	ND	ND	ND	ND	113.69	219.33	0.00
PCB174	37.60	ND	ND	ND	ND	ND	ND	ND	65.55	174.35	0.00
PCB177	67.95	ND	ND	ND	ND	ND	ND	ND	112.00	164.83	0.00
PCB180	84.71	ND	ND	ND	ND	ND	ND	ND	139.48	164.66	0.00
PCB183	30.93	ND	ND	ND	ND	ND	ND	ND	48.40	156.48	0.00
PCB184	ND	ND	ND	ND	ND	ND	ND	ND	ND	0.00	ND
PCB187/182	133.60	ND	ND	ND	ND	0.30	ND	0.34	209.84	157.55	0.48
PCB194	19.43	ND	ND	ND	ND	ND	ND	ND	29.41	151.35	0.00
PCB195	8.42	ND	ND	ND	ND	ND	ND	ND	12.85	152.48	0.00
PCB203/196	21.21	ND	ND	ND	ND	ND	ND	ND	33.79	159.30	0.00
PCB206	12.10	ND	ND	ND	ND	ND	ND	ND	17.33	143.21	0.00
PCB209	3.22	ND	ND	ND	ND	ND	ND	ND	3.85	119.39	0.00
Total	18249.8	32.21	69.97	107.0	62.69	304.0	281.4	336.9	17820.4	104.19	6.54

\* S–sediment sample; A–air sample; Rec.–recovery; Vol.–volatilization



**Table A4-15** Volatilization of solid PCB from glass surfaces ( $\mu\text{g}$ )

Time, days	4		8		12		16		20		24		Glass column		Tubing & Trap		Recovery (%)	
	A	A'	A	A'	A	A'	A	A'	A	A'	A	A'	A	A'	A	A'	A	A'
HCB (0)	0	0	0.3	0.17	0.29	0.63	0.41	0.38	0.39	0.39	0.47	0.43	19.25	16.02	0.14	0.86	106.3	94.4
HCB (10)	1.48	1.81	2.32	1.16	1.04	0.94	0.8	0.79	1.91	1.5	1.1	1.12	10.04	10.35	0.14	1.7	94.2	96.9
DCB (0)	1.37	1.74	1.2	1.07	1.25	1.09	1.28	1.24	1.19	1.09	1.09	0.92	4.3	3.99	0	0	97.3	92.8
DCB (10)	2.66	2.77	2.33	2.24	2.25	2.15	2.09	2.04	1.46	1.42	--	--	1.29	1.22	0	0	100.7	98.7
DCB (75)	0.34	0.28	2.08	2.31	2.88	2.68	2.26	2.5	2.56	2.44	1.97	2	3.4	3.46	0	0	91.3	92.3
DCB (150)	0.3	0.34	1.71	1.5	1.59	1.5	1.92	2	1.46	1.3	1.35	1.36	6.6	6.48	0	0	87.9	85.3
HCB (75)	0	0	2.44	2.5	2.83	2.87	2.26	2.3	1.37	1.43	1.35	1.32	9.41	9.88	0	0	98.3	101.5
HCB (150)	0	0	1.8	1.48	2.22	2.44	1.54	1.73	0.97	1.05	0.8	1.18	11.87	12.23	0	0	96	100.6
HCB (0, u)	0	0	0.15	0.14	0.15	0.17	0.15	0.15	0.17	0.21	0.16	0.15	0.78	0.82	0	0	92.7	91.8
HCB (10, u)	1.81	1.62	1.73	1.92	2.01	1.97	1.38	1.26	0.77	0.88	1	0.82	9.29	9.98	0	0	90.5	92.8
DCB (0,u)	1.46	1.62	1.34	1.39	0.97	1.05	1	1.11	1.09	0.99	0.91	1.01	10.1	9.67	0	0	97.9	97.8
DCB (10,u)	2.58	2.37	2.17	1.91	1.79	1.83	1.55	1.59	1.35	1.43	1.45	1.43	6.1	5.58	0	0	98.7	93.7